

Elastic Systems for Compliant Shading Enclosures

By: Brent D. Vander Werf

A Master's Report Submitted to the Faculty of the Department of
Architecture In Partial Fulfillment of the Requirements for the Degree of
Master of Architecture in the Graduate College of The University of Arizona.



The University of Arizona
College of Architecture and Landscape Architecture
Emerging Material Technologies (EMT) Laboratory

Spring 2009

**The University of Arizona Electronic Theses and Dissertations
Reproduction and Distribution Rights Form**

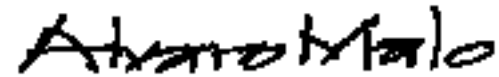
Name (Last, First, Middle) (please print) Vander Werf, Brent, Daniel	
Degree (Ph.D., ED.D., MS, MA, etc): MArch	
Major: Architecture	
Date you defended: May 12th, 2009	
Title of Dissertation (please print) Elastic Systems for Compliant Shading Enclosures	
The University of Arizona Library Release	<p>I hereby grant to the University of Arizona Library the non-exclusive worldwide right to reproduce and distribute my dissertation or thesis and abstract (herein, the "licensed materials"), in whole or in part, in any and all media of distribution and in any format in existence now or developed in the future. I represent and warrant to the University of Arizona that the licensed materials are my original work, that I am the sole owner of all rights in and to the licensed materials, and that none of the licensed materials infringe or violate the rights of others. I further represent that I have obtained all necessary rights to permit the University of Arizona Library to reproduce and distribute any nonpublic third party software necessary to access, display, run or print my dissertation or thesis. I acknowledge that University of Arizona Library may elect not to distribute my dissertation or thesis in digital format if, in its reasonable judgment, it believes all such rights have not been secured.</p> <p>Signed: _____</p> <p>Date: <u>May 15th, 2009</u></p>

Elastic Systems for Compliant Shading Enclosures

By: Brent D. Vander Werf

A Master's Report Submitted to the Faculty of the Department of Architecture In Partial Fulfillment of the Requirements for the Degree of Master of Architecture in the Graduate College of The University of Arizona.

Approval by Master's Report Thesis Committee Members:



Álvaro Malo, Chair
Professor & Director of Architecture: Emerging Material Technologies Date

Larry Medlin
Professor of Architecture Date

Dr. William Bickel
Professor Emeritus of Physics Date

TABLE OF CONTENTS

1.0	ABSTRACT	07
2.0	INTRODUCTION	09
3.0	PERFORMANCE CRITERIA	13
4.0	MATERIAL PROPERTIES	16
	4.1 Mechanical Properties	
	4.2 Thermal Properties	
5.0	PRECEDENT STUDIES	22
	5.1 Architectural Precedents	
	5.2 Material Precedents	
	5.3 Biological Precedents	
	5.4 Industrial Precedents	
6.0	EMPIRICAL INVESTIGATIONS	30
	6.1 Light Shade and Shadows	
	6.2 Dynamic Frames	
	6.3 Membranes	
7.0	IDEAL SYSTEM DEVELOPMENT	42
	7.1 Bistable Mechanisms	
	7.2 Thermostat Bimetal Coils	
8.0	PROTOTYPE SYNTHESIS	58
	8.1 Prototype 01	
	8.2 Prototype 02	
	8.3 Node Development	
	8.4 Aperture Layout Development	
	8.5 Membrane Development	
	8.6 Prototype 03	
	8.7 Final Prototype	
	8.8 Light Reflection Properties	
	8.9 Thermal Heat Properties	
9.0	POTENTIAL APPLICATIONS	70
	9.1 University of Arizona, Solar Decathlon - Seed POD	
	9.2 Ideal Frame	
	9.3 SHGC / U - Value / R-Value	
	9.4 Other Applications	
	9.5 Final Thoughts	
10.0	APPENDIX	78
	10.1 Location - Tucson, AZ	
	10.2 Location - Washington D.C.	
	10.3 Existing Shading / Thermal Techniques	
	10.4 Overview of Existing Light - Deflecting Systems	
	10.5 Bibliography	
	10.6 Glossary	
	10.7 Company Profiles	
	Thank You	

1.0 ABSTRACT

Forces are everywhere, in and on every object. They even act in 'empty space'. Forces form objects, hold them together or destroy them. Forces act within atoms, molecules, and gases, in liquids and in solid bodies.

Frei Otto. *Krafte, die Objekte bilden.*

This study investigates elastic structures and materials in terms of mechanical and physical properties for the design of a bistable (capacitor) mechanism which is programmed to deform an aperture, complying to variable thermal loads and light to provide shade and thermal comfort regulation between an exterior and interior space.

Elastic properties, precedents and materials are studied and modeled to identify the maximum stress and strain force by which materials and structures are capable of deforming and returning to an original size and shape without permanent deformation. Bistable structural mechanisms, organized with elastic spring steel strips and pin connections, in the form of an aperture, are then investigated as a capacitor. The capacitor utilizes prestressed structural strips which deform an aperture with activated thermostat coils through diurnal thermal loads from the sun. The increasing storage of elastic strain energy is programmed to rotate and close the aperture at a maximum stressed position, at which point, it is capable of releasing the stored kinetic energy with a decrease in heat input, triggering the mechanism to open the aperture instantly.

The arrangement of the self adjusting shade system is organized and manipulated spatially through a variety of prototype developments as a passive glass enclosure for the east and west facades of buildings. The University of Arizona's entry for the Department of Energy's Solar Decathlon Competition is used as a testing platform for the final prototype, validating its performance, function and value as a potential building component.

2.0 INTRODUCTION

Give me a place to stand and I shall move the earth.

Archimedes, *On Balancing Planes*

To comply, means to adapt, based on a requirement or direct request. In buildings and structures, architects and engineers often ask their designs to comply to specific environmental performance factors: providing light, shade and shadows, protecting the structure and inhabitants from rain, sun, and extreme temperatures, just to name a few, and controlling the interior environment for human comfort.

These principles are required or requested by the user of the building, but the ability of a principle to adapt to external environmental conditions is often non-existent. In the desert, shade is of the utmost importance for cooling, and the current design trends of shade structures comply only to unidirectional, seasonal azimuth movement of the earth in relationship the sun, but are ignorant to the sun's diurnal movement and the interrelated thermal radiation exposure.

This project considers the question, 'how can an enclosure be designed and organized structurally to comply to the earth's rotation around the sun both diurnally and annually, to produce shade, when required, in the desert and elsewhere'?

Structurally, the enclosure is imagined to be arranged of elastic materials in the form of an aperture which acts as a capacitor, aiding in the storage and release of energy, while deforming an aperture in response to changes in diurnal light and thermal radiation. The geometric tessellation of an aperture then forms a skin and produces variable levels of shade, shadow and light based on the enclosure location and the intensity of the sun.

The sun's light rays are truly electromagnetic wavelengths with variable frequencies from which a constant level of thermal radiation is transmitted. The amount of radiation which reaches a surface is dependent on the angle of incidence against a particular planes placement. Throughout the day, the amount of thermal radiation on a given surface varies based on its orientation to the sun, giving the ability to track the sun can by quantifying the amount of radiation reaching a particular surface or material at a known time.

Given that the sun's incident energy acts on all objects each and every day, thermal expansion and contraction properties will occur at variable scales, dependent on internal properties, and quantifying the exposure force through a thermal expansion reaction force.

This led to the formulation of the initial hypothesis for the research.

2.1 Hypothesis

If the thermal expansion properties of smart materials can be programmed to store and release varying amounts of elastic strain energy in the structural form of an aperture, then the exposure of the system to heat, in the form of sunlight, will passively deform the system between its stable and unstable states, opening and closing an aperture based on solar exposure.

An itemized list of performance criteria is identified in the next section to try and answer this proposal in terms of how, why and where the hypothesis can be justified and tested.

1.0 ABSTRACT

2.0 INTRODUCTION

3.0 PERFORMANCE CRITERIA

4.0 MATERIAL PROPERTIES

5.0 PRECEDENT STUDIES

6.0 PRELIMINARY EMPIRICAL INVESTIGATIONS

7.0 SYSTEM DEVELOPMENT

8.0 PROTOTYPE SYNTHESIS

9.0 POTENTIAL APPLICATIONS

10.0 APPENDIX

3.0 PERFORMANCE CRITERIA

Goal:

To design an enclosure system which adapts to exposure from the sun.

How:

With direct exposure to sunlight, the enclosure experience a “miosis” function, or the constriction of light, based on thermal expansion properties of smart materials and programmatic structural arrangement.

With no direct exposure to sunlight, the enclosure experiences a “mydriasis” or dilation function, allowing for indirect light to penetrate into interior spaces based on the orientation and materials ability to recoil with lack of heat input.

Why:

Functionally, to minimize heat gain, glare, and undesired reflection of sunlight in and on an enclosure while optimizing visual contact to the exterior.

Physiologically, the interior space is intended to be a place to reside, wether one’s is working, studying, reading or praying. A place where time is expressed by the movement of the sun with a direct expression of life based on the diurnal and seasonal display of light and shadow.

The design of an enclosure system is evaluated based on a Solar Heat Gain Coefficient (SHGC), which provides a value of measure based on the systems material and design characteristics.

Solar radiation is constantly absorbed through an enclosures material and transferred to heat. The amount of heat dissipated is dependent on the material design and properties, i.e. reflectivity, atomic elements and structure, thickness, surface area, etc.

The optimization of a low SHGC is constantly contrasted by the amount of visual connection from interior to exterior and vice versa, a high SHGC allows maximum visual contact but minimal thermal properties. This thesis aims at adapting these performance values to maximize functional properties.

Where:

East and West building facades in hot and arid climates.

The alternating exposure from intense direct light to indirect diffused light and finally to no light for east and west facades is a programmatic phenomena which yields possibility for design creativity with the sun’s energy as a power source. This thesis is intended to provide a design answer to this phenomenon through built forms.

The North building facade was not used for this study given the sitting location was in the northern hemisphere, upon which, minimal direct light penetrates

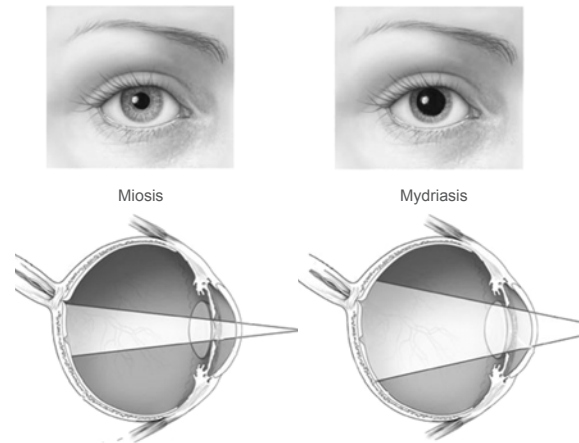


Figure 3.1, Eye Adaptation, National Eye Institute

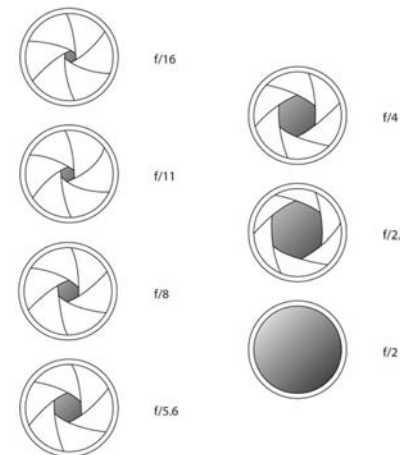


Figure 3.2, Camera Lens, Digital Photography For Dummies, 5th Edition

into the building throughout the year. In the same manner, the South building facade was not used due to the existing shading techniques developed for passive solar shading.

1.0 ABSTRACT

2.0 INTRODUCTION

3.0 PERFORMANCE CRITERIA

4.0 MATERIAL PROPERTIES

5.0 PRECEDENT STUDIES

6.0 PRELIMINARY EMPIRICAL INVESTIGATIONS

7.0 SYSTEM DEVELOPMENT

8.0 PROTOTYPE SYNTHESIS

9.0 POTENTIAL APPLICATIONS

10.0 APPENDIX

4.0 MATERIAL PROPERTIES

4.1 Mechanical Properties

Ut tensio, sic vis (As the Extension, So the Force).

Robert Hooke, 1678

Elasticity is the property and testing of a materials tensile strength and its ability to recoil to the original dimension or form. The atomic bonding and cell unit structure inherent to materials defines its specific elastic strain limit and is directly correlated to the applied stress. This relationship between stress and strain is known as the Modulus of Elasticity and can be expressed by (Robert) Hooke's Law, which states:

For an elastic body, the ratio of stress present on an element to the strain produced is constant.

$$\frac{\text{Stress}}{\text{Strain}} = \text{Constant for Material}$$

$$= \text{Modulus of Elasticity}$$

$$\text{Strain} = \frac{\text{Increase in Length}}{\text{Original Length}}$$

The modulus of elasticity for a given material is linearly constant until the strain force reaches a transition point, known as the limit of proportionality. At this point the material begins to experience elastic as well as plastic deformation until the maximum load (yield limit) is reached. Plastic deformation is not to be confused with a polymeric signification but rather is defined as a strain force which slips the atomic bonding of a material and permanently deforms the molecular structure (Figure 4.1).

For most structural applications the modulus of elasticity of a material remains linear as the applied stress is below the elastic limit and Hooke's Law remains constant. However, it is possible for a structural material to be subject to eccentric loads which cause structural nonlinearity to occur and the known constants are no longer valid (Howell, Compliant Mechanisms).

Structural nonlinearity for a system can be defined by two functions, material and geometry. Material nonlinearity occurs when the stress to strain is not proportional resulting in plasticity, nonlinear elasticity, hyper-elasticity, and creep. Geometric nonlinearity results in large deflections, stress stiffening and large strains based on the deflection of a structural system which alters the intended load distribution (Howell, Compliant Mechanism).

For this study, structural nonlinearity principles are identified as design related problems which are to be considered in evaluating the deformation of elastic components; however, the nonlinearity equations and assumptions are beyond the scope of this work.

In addition to Hooke's Law for determining materials elasticity, (Simeon) Poisson's Ratio, defines the lateral deformation of materials in the elastic range. The ratio is based on the fact that the lateral dimension will decrease when subjected to a tensile force and the lateral dimension will increase when subjected to a compressive force. The ratio is such:

Poisson Ratio (ν)

$$\nu = \frac{\text{Transverse Strain}}{\text{Axial Strain}}$$

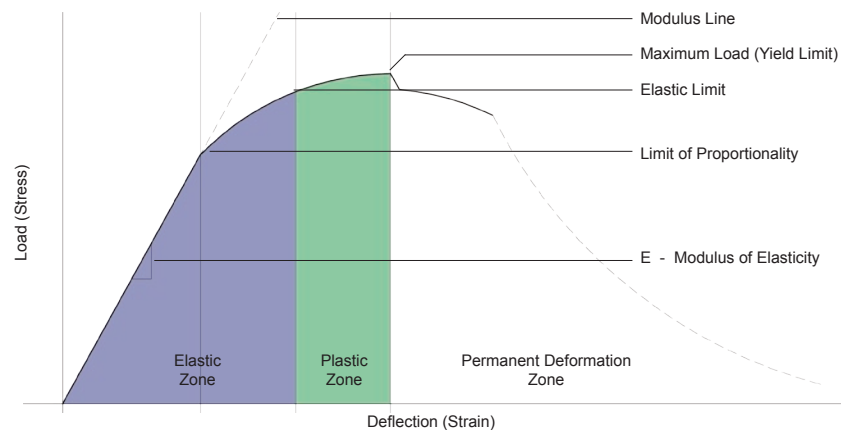


Figure 4.1, Static Bending Test / Stress & Strain Diagram

The shape and length of elastic materials also affects the deformation of assemblies based on the slenderness ratio, which is directly related to the stiffness of the material. The slenderness ratio is commonly applied to columns which buckle under compressive forces. The overall shape, whether it be a column, bar, ellipse, etc., needs to be considered in relationship to the applied stress and length of member (Figure 4.2 & 4.3). Mathematician Leonhard Euler devised the formula that gives the maximum axial load that a long slender column can carry without buckling in 1757. The equation is identified below:

$$F = \frac{3.1416^2(EI)}{(KI)^2}$$

Where:

- F = Max. Force
- E = Modulus of Elasticity
- I = Area Moment of Inertia
- l = Length of Column
- K = Column effective Length Factor
 - Both Pinned, K=1
 - Both Fixed, K=.5
 - 1 Fixed / 1 Pin K=1/ 2
 - 1 Fixed / 1 Free K = 2

Other design considerations of elastic components are fatigue and corrosion. Fatigue is the lowering of strength or failure of a material due to repetitive stress in the form of tension, compression, bending, vibration, thermal expansion, contraction and other stresses which may be above or below the yield strength (Askeland, 241). Fatigue failure is often based on flaws within materials by which cyclical loads cause the flaws to propagate to the surface

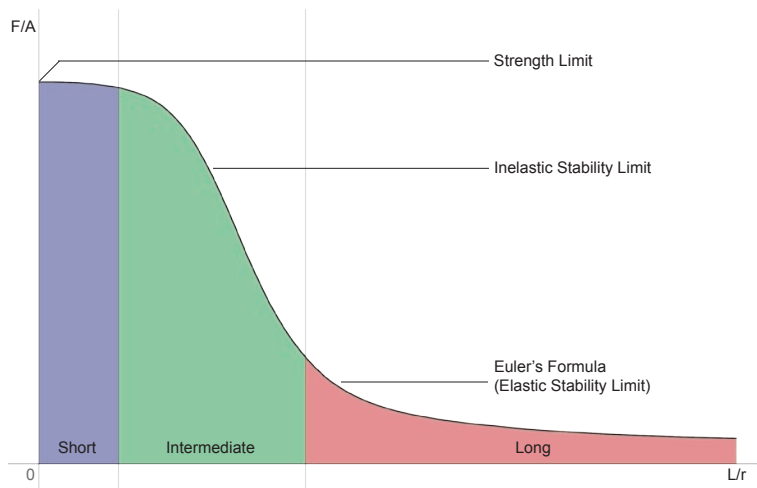


Figure 4.2, Slenderness Diagram

and throughout the cross-section continually, eventually failing the material when the flaws create a minimal cross-section of connected molecules. For fatigue to play a role in the design of a material, at least part of the stress in the material has to be tensile. Fatigue will also tend to lower the overall elastic modulus of composite materials, as fibers or other reinforcing phases begin to degrade over time.

The fatigue life of a component can be evaluated by knowing the time associated with each cycle and the maximum applied load which the component is subject to. Thus, an endurance ratio can be evaluated as such:

$$\text{Endurance Ratio} = \frac{\text{Endurance Limit}}{\text{Tensile Strength}}$$

Corrosion becomes apparent in elastic materials when they directly act with corrosive chemical in the environment, i.e. oxygen, gases, liquids, etc. The amount of corrosion a material is subject to is based on the atomic properties of the material or the anti-corrosive agents applied to the surface. Rubber and polymers are given additives to resist corrosion, such as introducing carbon black filler to effectively protect against ultraviolet radiation. Swelling of rubbers is also of concern when subject to liquids as it influences the mechanical properties and fatigue stress. Ultimately when a material begins to corrode, the abrasive chemicals cause additional flaws to form and the fracture mechanics specific to the material are of concern.

The selection, design and organization of elastic components involves a complex understanding of multiple forces and the function for the component. This study will identify the specific mechanical properties associated with elastic components from an architectural viewpoint and evolve a prototype towards a realistic design solution.

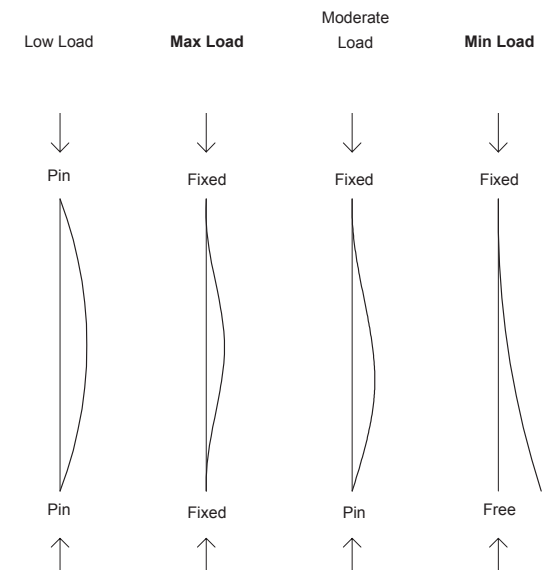


Figure 4.3, Euler Buckling Modes Diagram

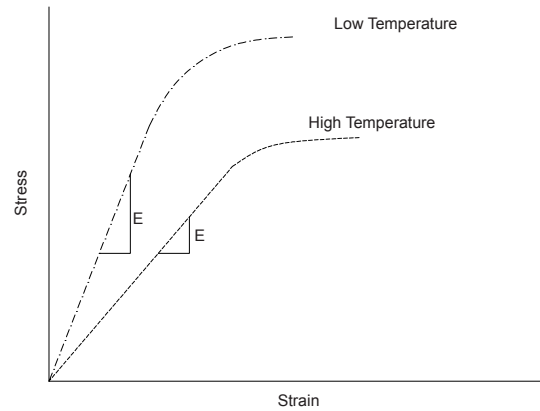
4.2 Thermal Properties

Thermal expansion is a mechanical property, in which, all materials either increase or decrease in volume or length based on a response to temperature change. As a material is heated, particles move based on the structure and strength of atomic bonding. Generally, a higher bond energy results in lower thermal expansion and a lower bond energy results in higher thermal expansion. Bond strength is linked to the hardness of a material, therefore harder materials often exhibit lower thermal expansion and vice versa. The Coefficient of Thermal Expansion (CTE) is the numerical designation for thermal material properties and is equated as a fractional expansion per degree: $F \times 10^{-6}$ or $C \times 10^{-6}$.

Figure 4.4, identifies the tensile test of materials based on the difference in temperature and the related mechanical properties: elastic modulus, tensile strength, yield strength and ductility. Of significance is the change in a materials elastic modulus and yield strength, as both decrease significantly with highly elevated temperatures.

For this study, thermal expansion properties of materials are investigated in regards to their ability to perform work as the temperature fluctuates diurnally. Thermal expansion materials (TEM), expansion materials (EM), thermo-bimetals (TB), and shape memory alloys (SMA) are typical thermostrictive smart materials used in engineering today.

Other materials excited by effect of temperature, include: thermo-bi-composites, shape memory polymers (SMP), shape memory foams, shape memory ceramics, and biological systems with shape memory effects. These materials were researched but eventually phased out for more in depth focus on thermo-bimetals.



Property	Temperature Change	
	Increase	Decrease
Elastic Modulus	Decrease	Increase
Tensile Strength	Decrease	Increase
Yield Strength	Decrease	Increase
Ductility	Increase	Decrease

Figure 4.4, Temperature Effects on Mechanical Properties, Askeland/Phulé

4.2.1 Thermo-bimetals (TB)

Thermostat metals are the most common TB materials and are composites which consist of two or more metallic layers having different coefficients of thermal expansion. When the layers are permanently bonded together, the different coefficients of expansion between the metals cause the resultant shape to curve or deform when subject to change in temperature. The bending of the material, in response to temperature change, is known as the Flexivity of the material, and is an inherent principle to all thermostat metals. Flexivity is resultant of an alloys composition and is non-linear; altering the metals ability to deform as temperature increases or decreases significantly (See Appendix 10.7.2).

In mathematical terms, the bending of the metal is directly proportional to the difference in the coefficient of expansion and the temperature change of the component, and inversely proportional to the thickness of the composite. The bending is also affected by the ratio of the moduli of elasticity of the metallic layers and their thickness ratio (Figure 4.6).

The adjacent diagrams and equations identify the variables present in the design and the resultant outputs achievable. Thermostat metals will be discussed in more detail in section 7.2.

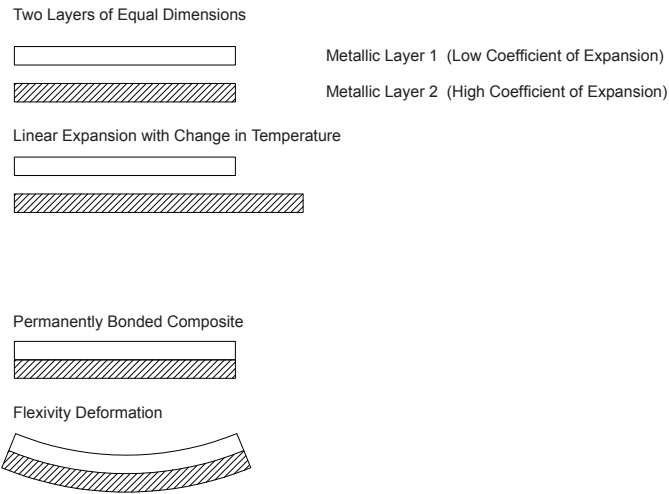


Figure 4.5, Thermal Expansion Diagrams for Bi-laminates, Engineered Material Solutions

Spiral Coil Formulas

Thermal Deflection:

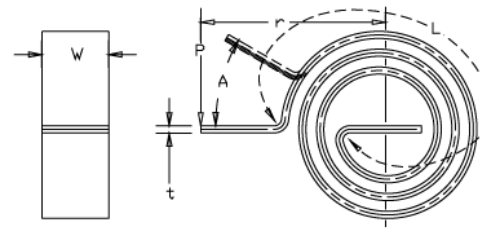
$$A = \frac{67F (T_2 - T_1) L}{t}$$

Mechanical Force

$$P = \frac{0.0232E Aw t^3}{Lr}$$

Thermal Force

$$P = \frac{1.55EF (T_2 - T_1) wt^2}{r}$$



Formula Symbol Key

Variable	Definition	Units
t	Material Thickness	Inches
w	Material Width	Inches
L	Active Length	Inches
E	Elastic Modulus	Lbs/Inch ² (psi)
F	Flexivity	Inch/Inch/°F
A	Angular Rotation (Coils)	Degrees
B	Linear Deflection	Inches
P	Force	Ounces
r	Radius At Point of Load (Coils)	Inches
D	Outside Diameter (Disc)	Inches
d	Inside Diameter (Disc)	Inches
(T ₂ - T ₁)	Temperature Change	°F

Simple Supported Beam Formulas

Thermal Deflection:

$$B = \frac{0.133F (T_2 - T_1) L^2}{t}$$

Mechanical Force

$$P = \frac{64EBwt^3}{L^3}$$

Thermal Force

$$P = \frac{8.51EF (T_2 - T_1) wt^2}{L}$$

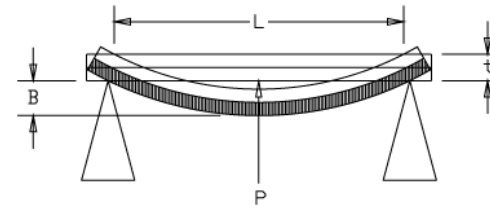


Figure 4.6, Bimetal Equations for Coils and Beams, Engineered Material Solutions

1.0 ABSTRACT

2.0 INTRODUCTION

3.0 PERFORMANCE CRITERIA

4.0 MATERIAL PROPERTIES

5.0 PRECEDENT STUDIES

6.0 PRELIMINARY EMPIRICAL INVESTIGATIONS

7.0 SYSTEM DEVELOPMENT

8.0 PROTOTYPE SYNTHESIS

9.0 POTENTIAL APPLICATIONS

10.0 APPENDIX

5.0 PRECEDENT STUDIES

5.1 Architectural Precedents

5.1.1 Structure

Frei Otto - Vertebrae, Temporary Installation

In 1963, Frei Otto developed a tensegrity column system which utilized post-tensioned cable elements stranded through compressive strut members which narrowed in width as the column was elevated. The purpose of the model was to investigate the structural components of tensegrity columns as well as the ability to straighten, or curve the system with precise tension placed on individual cables. This structure is of interest as it exemplifies the adjustable movement of the system which is reliant on the stress applied to a particular component. Stressed applied to one component effects the entire placement of the structure. Otto's vision for the structure was for adaptable surfaces or structures and advanced devices for medical industries and handling of hazardous materials.



Figure 5.1, Vertebrae

Shigeru Ban - Japanese Pavilion

The essence of this precedent is in the simplicity of the details. The latticed assembly of paper tubes and PVC membrane with fabric and metal straps creates a redundant structure which equally distributes forces to the foundation. Shigeru Ban's collaboration with Frei Otto assisted in designing the deployment, stabilization and disassembly of the pavilion to maximize and reduce waste to provide a sustainable and modern pavilion.



Figure 5.2, Japanese Pavilion - Expo 2000 Hanover, Germany

Nickolas Grimshaw - Eden Project

Grimshaw's Eden Project has been researched in terms of material designation and structural efficiency. The enclosure of the Eden Pavilion is wrapped in a material named ethylenetetrafluoroethylene (ETFE). This thermoplastic polymer is Ultra-Violet resistant and does not discolor, it has a high impact resistance and is 99% translucent. The triangulated structure is organized into modules of hexagons which are tensioned into a domed vaulted enclosure.



Figure 5.3, Eden Project - St.Austell, Cornwall, UK, 2001

5.1.2 Enclosure

Jean Nouvel, Arab World Institute

Nouvel's enclosure design is a complex mechanical based element which utilizes photosensitive sensors to actively adjust the amount of light and thermal radiation based on the intensity of light which reaches the sensors. The mechanics which drove the system eventually failed and the enclosure is now static. The vision and engineering of the system is quite ingenious and directly related to my personal goals for this thesis. By translating the same vision from an active to a passive system presents particular design problems but hopefully ensures the longevity of its function.

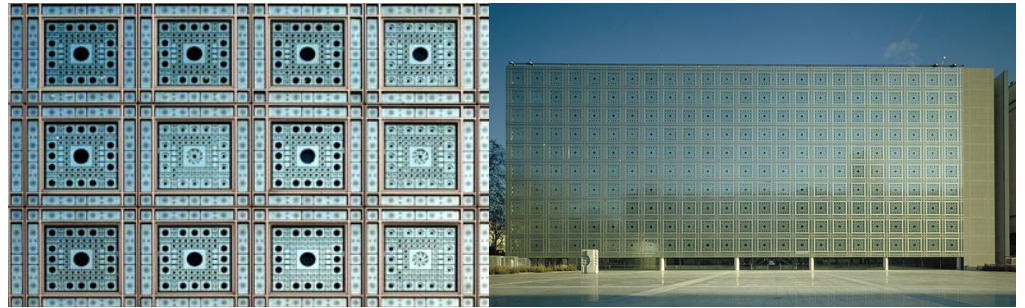


Figure 5.4, Arab World Institute - Paris, France, 1987

Will Bruder, Phoenix Central Library

This is another study of an enclosure system which actively adjust the amount of light entering the building based on programmable solar angles for Phoenix determined by sophisticated software. Once again, the active system in this building has failed and has yet to be replaced. The louvers along the south facade of this structure are acting as horizontal light captures and redirecting the light to the ceiling. Additionally, the louvers are not the enclosure system but rather a secondary external system which protect the structural glazing system within and further aid in SHGC.



Figure 5.5, Phoenix Central Library - Phoenix, AZ, 1995

Werner Sobek - Rothenbaum Stadium

A membrane canopy structure covers this stadium and was designed to deploy and provide compliance to the environment for the users. Compression members and tensile cables are arrayed from the center of the stadium and allow membrane to be controlled by the manipulation of the tensile forces along the surface. Maximum tension deploys the membrane and relaxed tension pleats the membrane to the center.

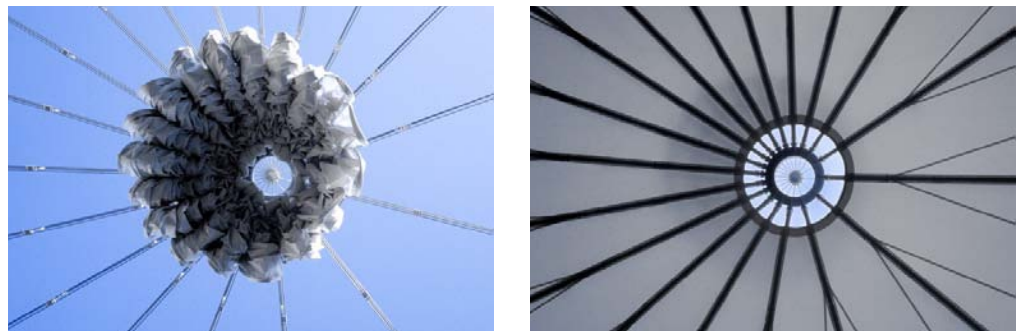


Figure 5.6, Rothenbaum Stadium - Hamburg/Germany, 1997

5.2 Material Precedents

Wayne Jenski, Architecture Master's Thesis - University of Arizona

Mr. Jenski studied and documented adaptable skins for his architectural thesis as a means for providing a "breathable" skin with pores which activate based on heat. The studies depicted to the right utilize the lamination of polymeric materials and engineered bimetal strips to passively open and close a pore for an enclosure system. Jenski, later connected with Mr. Blonder (below) and his "c-motion" material and assembled a final model that consisted of modular unit with integrated adaptable pores.



Figure 5.7, Wayne Jenski Studies (Left to Right): Silicon & HDPE; Manganese & Invar Bimetal Strips within Silicon

Figure 5.8, Wayne Jenski, Assembled Model

Greg Blonder, Genuine Ideas, LLC, New Jersey

Mr. Blonder invented a thermosetting polymer film which deforms through heat based on the lamination of specific materials with different expansion rates or Coefficient of Thermal Expansion (CTE). The materials is assembled by laminating a 1 millimeter layer of Polyethylene film with a 1 millimeter layer of Mylar film. These polymers are then coated with 100 angstroms of aluminum on one side and the other side is printed with a thin layer of black ink. The final product is a 2.5 millimeter film, which when restricted to a substrate, allows the deformation to occur when placed in sunlight.



Figure 5.9, Greg Blonder - Genuine Ideas, LLC, New Jersey / "C-Motion" Closed & Open

Dietrich Schwarz, Senior Citizens' Apartments - GLASSXcrystal

In Switzerland, Dietrich Schwarz utilized the Phase Change Material (PCM), GLASSXcrystal, within polycarbonate enclosure panels and an external light directing prism panel. The polycarbonate panels are filled with a salt hydrate mixture, which stores heat between 26°C to 28°C. The function of the facade is to vary the opacity of the triple insulated glazing unit based on the phase change properties of the salt hydrate when heated. Above 28°C the salt hydrate is in a liquid state allowing light to diffuse to inside and below 26°C the salt hydrate crystallizes into a solid state and stores the heat from sunlight for latent heat transfer. While the enclosure passively alters the opacity and thermal heat transfer from outside to inside, the overall effect or change in opacity is visually hindered due to the prismatic panel. The system as an integrated building system is however softly refined and displays the technology material science has developed for architectural systems.



Figure 5.10, Senior Citizen Apartments - Domat/Ems, 2004

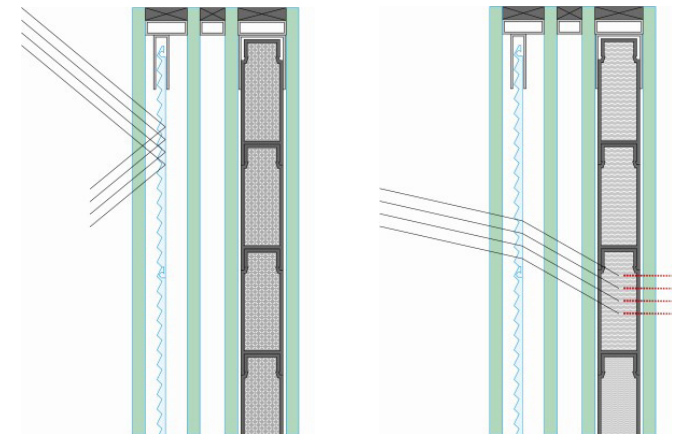


Figure 5.11, Glassx - PCM: Liquid Crystal Enclosures

Priva-Lite, SGG - Electrooptic Material: Liquid Crystals

Saint Gobain Glass (SGG), developed an Electrooptic Material (EO) which utilizes thin films of liquid crystal polymer composites between glass substrates and electrically conductive coatings. Without an applied Alternating Current (AC), the molecules in the films are excited and form irregular orientation, reflecting and absorbing the spectrum of visual light causing a white, opaque, diffused surface. With a current, the film remains in a translucent state with regularly aligned molecules. Because this system requires constant energy to remain in a translucent state and the mechanical properties of light and heat are not affected by the realignment, this product does not provide adequate energy savings (<http://www.consumerenergycenter.org>).

The function and properties of the EO material defines the influence which material science technology has on architectural products and the future which advanced materials and technologies can bring to provide dynamic systems for alternating spaces.



Figure 5.12, Glass Crystals Demonstration, SGG

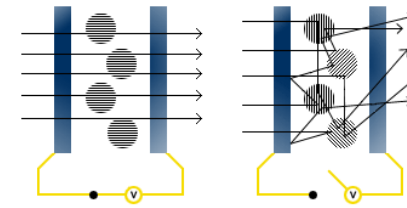


Figure 5.13, Diagrams of Crystal Orientation, SGG

5.3 Biological Precedents

5.3.1 Insects

Click Mechanism, Boettiger & Furshpan, 1952

Based on experiments with sedated flesh flies, this study identifies a 'click mechanism' which suddenly drops or raises the wing based on the amount of tension placed on the flies thorax. Of interest in this phenomena is the bi-stable function of geometric arrangements in accordance with specific energies, kinetic potential or gravitational. The diagrams to the right of the image identify the three possible assemblies to model the phenomena: compression spring, tension springs, and compression and tension springs. The elastic deformed strain force of the springs varies the amount of displacement present in the system between stable and unstable states.



Figure 5.14, Flesh Fly

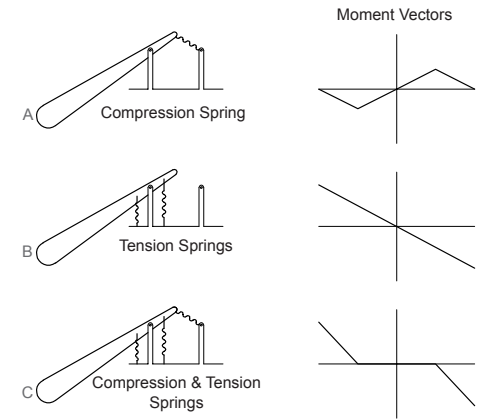


Figure 5.15, Click Mechanism Diagram - Boettiger & Furshpan, 1952

5.3.2 Plants

Dionaea Muscipula, Venus Fly Trap

Often learned of in early education as an appealing carnivorous plant, the Venus Fly Trap exhibits interesting movements directly associated with the propagation of fluids through the blades of the plant. Although it is not entirely understood, scientist believe it is the generation and degradation of calcium in the blades which expand or contract and alter the shape from a convex to concave form, digesting the insect captured within. Of interest, is the growth, form and geometry particular to this species.



Figure 5.16, *Dionaea Muscipula*, Venus Fly Trap

Mimosa Pudica Plant

This plant is also know as a sensitive plant, in that, when heat or pressure is applied to the blades or stems of the plant the affective areas deform or close for a temporary period. An external stimulus will cause the entire plant to close it blades and drop its stems as if it instantly dies. The response is thought to be related to the Venus Fly Trap phenomena in that, as the plant secretes chemicals within its leaves, the fluids propagate through the plant causing the response. The setting of the sun or the touch of a finger will cause the blades to deform.



Figure 5.17, Mimosa Pudica

5.4 Industrial Precedents

Binder Clip

The two metal clip ends of the binder clip office tool demonstrate a dynamic bistable structure very closely related to the click mechanism of the flesh fly. The metal clips are inserted into the black plastic clamp, locking the clip in the system. This “lock” within the system causes a strain force to be distributed throughout the material and upon an external force the metal clips experience a shift between a stable and unstable state based on the form of the black plastic clamp. When the metal clips are rotated, the rounded corners of the black clamp allow the metal clips to deform slightly, increasing strain and storing maximum potential energy at the point of instability. Once this point is reached, the clip converts the potential energy to kinetic energy and rotates one of two ways, whichever path is of least resistance.



Figure 5.18, Binder Clip (Open and Closed)

Light Switch

Another simple product of everyday use that demonstrates bistability is the light switch. We know that the switch can be either in the up or down position and that the switch creates a designed connection to a live circuit to extend electricity to a light source, but how this happens is hidden, yet quite simple.

A compression spring is the source for the bistability and is fitted between the plastic molded switch and the back metal casing of the assembly. The spring stores the energy through elastic strain and at the midpoint, the potential energy is the greatest and thus at the point of greatest instability, similar to Figure 5.15, diagram A of flesh fly. It is almost impossible to withstand the light switch at the midpoint position as the springs compression ratio is quite high, however, through decades of use the spring may experience fatigue and the overall Young's Modulus will decrease allowing the switch to potentially stick in the unstable state.



Figure 5.19, Light Switch

1.0 ABSTRACT

2.0 INTRODUCTION

3.0 PERFORMANCE CRITERIA

4.0 MATERIAL PROPERTIES

5.0 PRECEDENT STUDIES

6.0 PRELIMINARY EMPIRICAL INVESTIGATIONS

7.0 SYSTEM DEVELOPMENT

8.0 PROTOTYPE SYNTHESIS

9.0 POTENTIAL APPLICATIONS

10.0 APPENDIX

6.0 PRELIMINARY EMPIRICAL STUDIES

The following studies delimited the thesis and created sets of learning from which the resultant prototypes were realized. These studies included:

- Light, Shade and Shadows
- Rigid Body Frames for Collapsible Systems
- Membranes as Enclosures with Functional Pores

6.1 Light, Shade and Shadows Introduced

The selection of a prototype system to provide shade in the desert was a natural response to the properties of composites and geometric systems. An introduction to shadow theory is briefly explained and followed by focused research into how variable intensities of shadows can be produced to regulate heat gain.

The creation of shadows is based on three principles: 1) a light source, 2) a surface, and 3) an object between the source and surface.

A light source never contains shadows.

An object captures the light through absorption, reflection, etc.

A surface captures the shadow or anti-light.

And, a resultant variable inherent to shadows can be defined: the proximity of an object to a surface, assuming that the light source is static.

The light source then has two forms, a true point source (infinitely extended source) or an extended source with a specified diameter. A point source produces only linear, one-type umbra shadows, while a source of a given diameter produces linear, two type shadows, umbra (totality) and penumbra (partial). The diameter of the extended source thus has infinite point sources along its surface, each extending out its maximum tangency (Figure 6.2).

With these variables combined, a linear relationship between the source, object, surface and relative distance becomes directly correlated to each other based on principles of geometry and light.

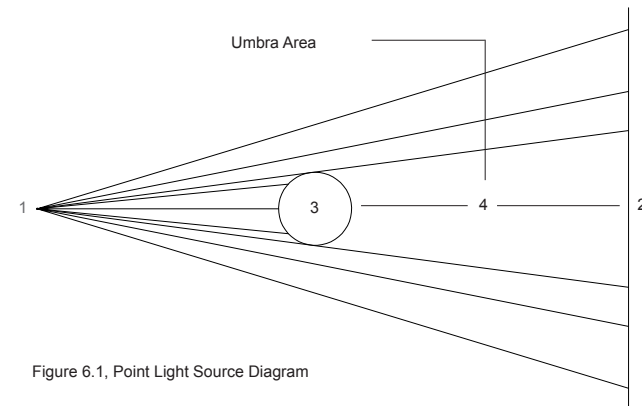


Figure 6.1, Point Light Source Diagram

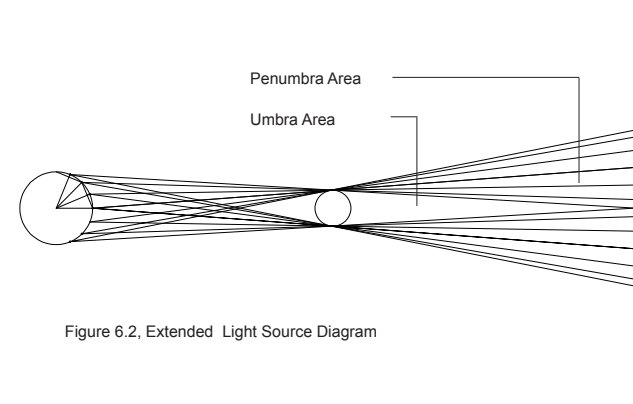


Figure 6.2, Extended Light Source Diagram

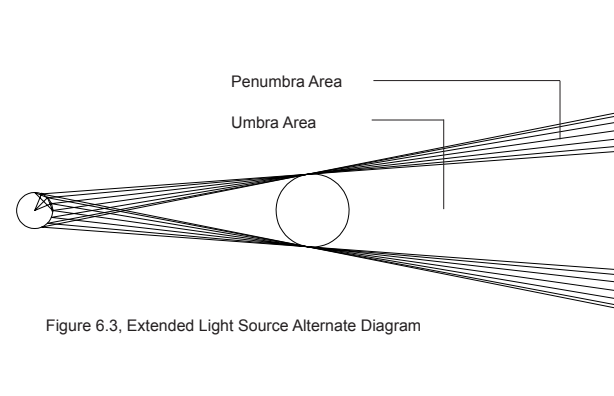


Figure 6.3, Extended Light Source Alternate Diagram

6.1.1 Empirical Shadow Studies

The initial investigation of light and shadow properties was executed empirically by recording shadows through photos of an emptied plastic water bottle with varying distances between the bottle and a surface. Given the shadow diagrams produced by an extended source, the sun in this case, a coordination of light qualities was estimated by slicing planes (Figure 6.4) in the approximate locations of umbra and penumbra levels which were observed.

The following pages will further explain the inherent principles behind the system of shade, shadows and light in a more in depth analysis and a proposal for shading membranes will be evaluated in relationship to independent variables.

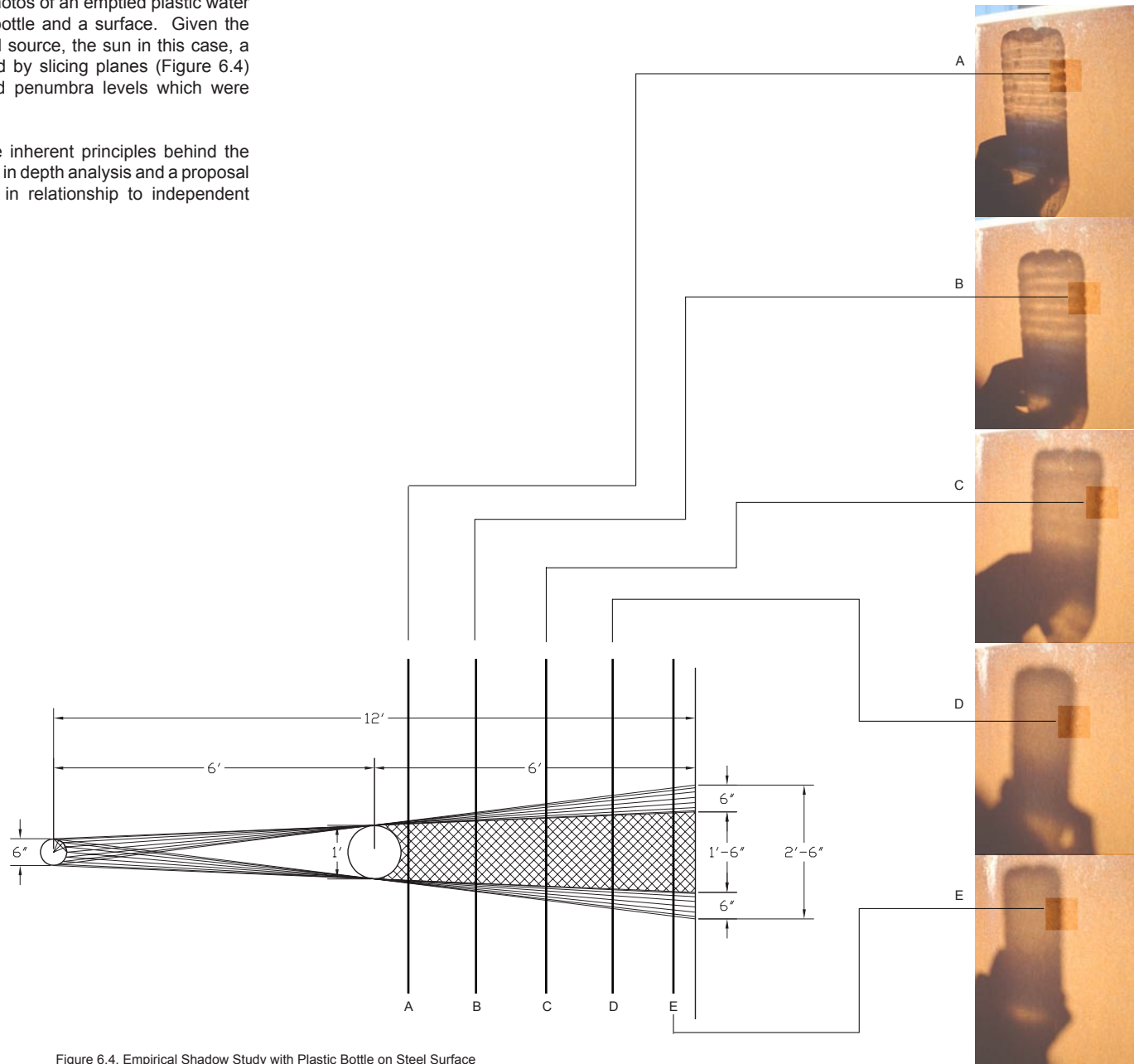


Figure 6.4, Empirical Shadow Study with Plastic Bottle on Steel Surface

6.1.2 Light Spot Model

The most efficient and accurate way to view and record shadows is based on the perpendicular placement of the object (which cast the shadow) and surface (which the shadow is cast on) in relationship to the source, for this instance the sun's rays.

To record the azimuth and altitude angles of the sun's diurnally and annually variability, a parametric model was modeled to pivot across the altitude angle and rotate about the azimuth angle by means of hinges and ball bearings. 3'-0" parallel guides placed perpendicular to the sun's rays accepted several pinhole frames for a linear range of motion and measurement.

The resultant equipment allowed for the testing and recording of shadows and light qualities throughout the day with measurable results in terms of brightness and clarity. However, slight color distortion were observed while testing, of which it was determined to be based on the sun's location in the sky and the interrelated refractive color of the sky being diffused around the equipment.

The model was finished with two paint colors. The recording surface was applied with a matte white coating to allow high contrast between shadow and light and the surrounding materials were coated flat black to absorb as much light as possible, minimizing spectral reflectance.

The model was then tested with aperture sizes ranging from 1/16" to 5/16", at 1/16" increments and a distance to surface at 6", 1'-6" and 2'-6". The resultant data was recorded with imperial measurement devices and also photographed for further analysis. Once the data was organized and compared between apertures and distance, a consistent linear relationship was discovered between size of aperture and size of light spot based on distance to surface.

Coordinating with a University of Arizona's Optics Professor, Mike Nofziger, an equation was derived based on the solar arc of the sun, circumference of the light spot and length between surface and aperture to determine the resultant size of any given light spot based on a known aperture size. The equation follows as:

$$k = d + (1/2(\text{deg}) \times 3.14/180(\text{deg})) \times L$$

Where: k = diameter of light spot
 d = diameter of aperture
 L = length between surface and aperture

Figure 6.7, identifies the testing of equation based on recorded data and shows the direct relationship between light spot diameter and distance for a particular aperture. Given this information, porous shading membranes which increase and decrease aperture size based on external forces can be analyzed to determine the effect the pores have on shading principles. The umbra and penumbra shadows can then be identified and the amount of light radiation which penetrates through the surface can be accurately estimated.



Figure 6.5, Light Spot Model - Photographs

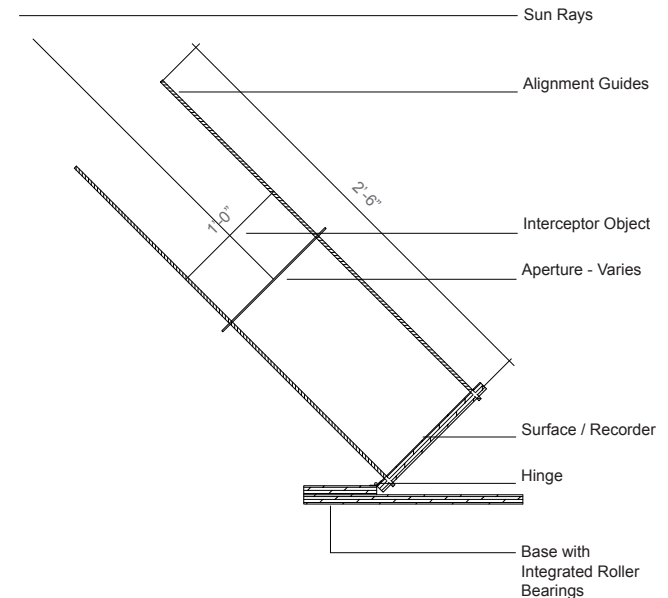


Figure 6.6, Light Spot Model - Section

6.1.3 Light Spots

These examples (Figure 6.7 & 6.8) identify the empirical testing and analysis of varying the aperture and distance and in turn, affect the resultant light spot.

It was determined that there was a programmatic direct linear relationship between the sun, aperture and resultant light spot based on the developed equation, allowing for the approximation of umbra and penumbra regions of shadows based on particular aperture size.

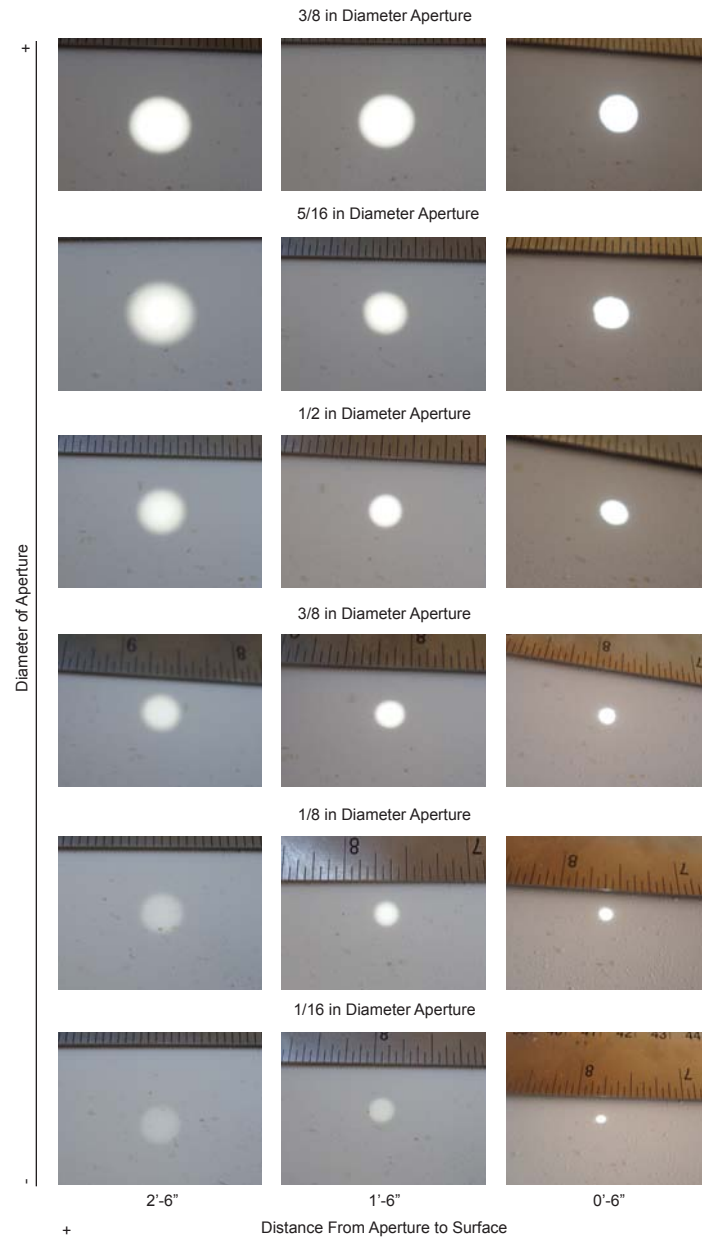


Figure 6.7, Light Spot Documentation

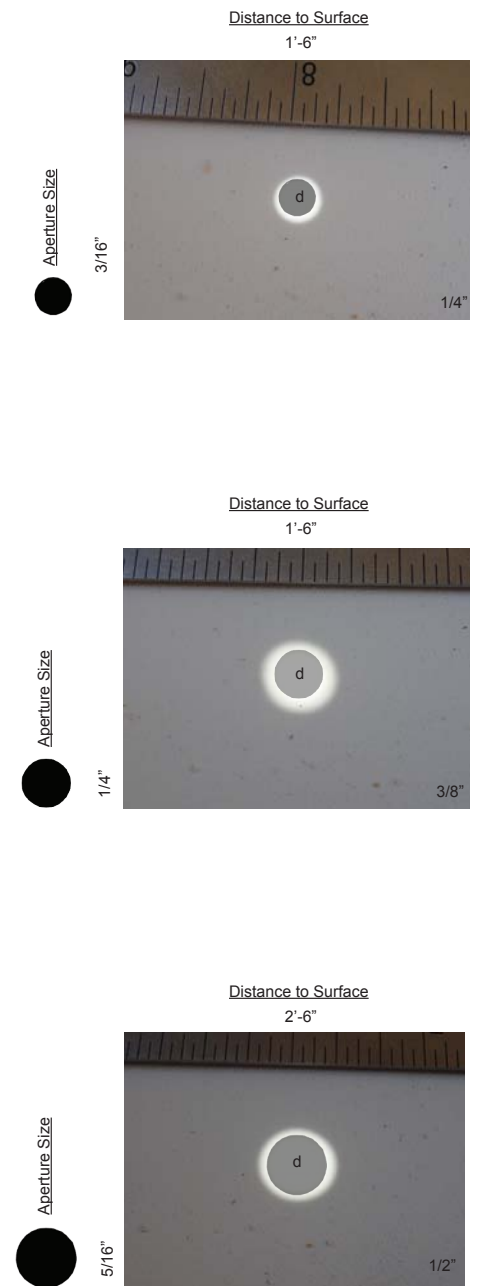


Figure 6.8, Light Spot Analysis

6.1.4 Shade Meshes

A tightly woven mesh in regards to shadows and light is nothing more than a large number of pinhole lenses which refract a certain amount of light. Based on the size of the opening the “lens”, has a particular focal length upon which the clarity of light is observed. The following photographs identify this phenomenon.

Furthermore, the location of the woven mesh to the source and lens is critical. If the lens is closer to the source than the mesh, the visibility factor is greatly reduced. If the lens is farther from the source and the mesh is in between, the visibility factor is greatest (at an oblique angle to the source).

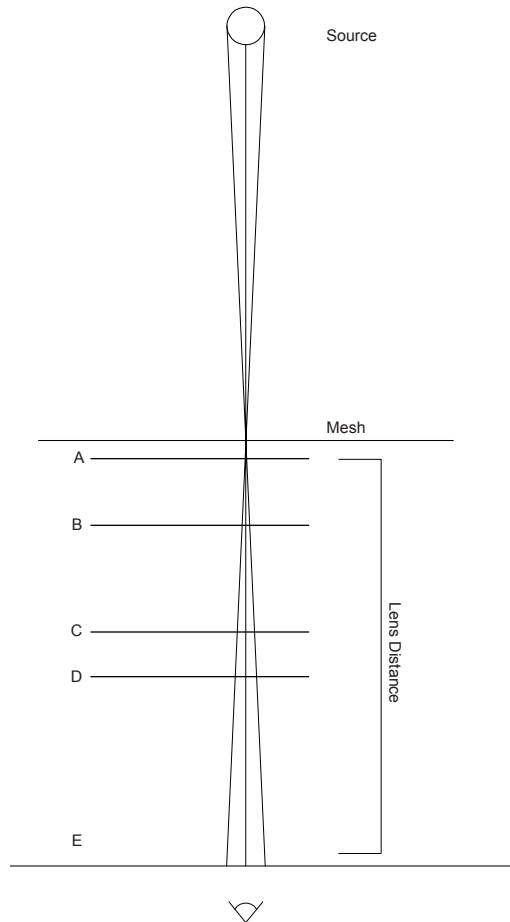


Figure 6.9, Diagram Identifying Location of Mesh to Camera

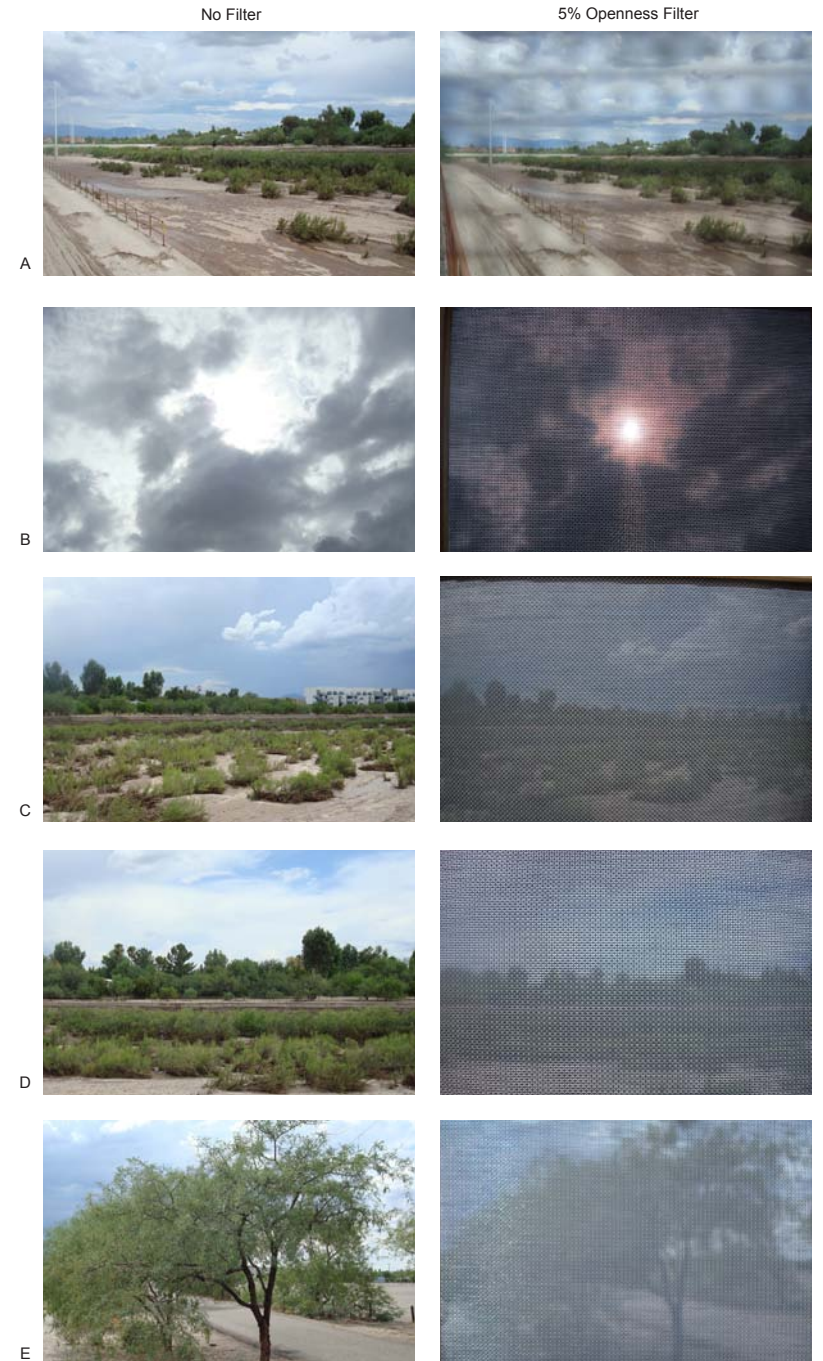


Figure 6.10, Empirical Photographs with Shade Meshes

6.2 Rigid Body Frames

The understanding of structural frames can be best explained through mathematical relationships and the deduction of empirical modeling. The structural triangulation of system in general regulates the stability of all frames as the systematic parametric methodology. Other methods of controlling shear forces and overall stability include: rigid connections and shear planes.

All structural systems incorporate both tensile and compressive forces based on inherent gravitational loads, ie. live, dead, dynamic and environmental. Forces are required to be transferred through materials and equalized against the opposing loads to establish a stable structural system.

In architecture, materials are either utilized for a particular resistant of force, such as concrete for compression or woven fabrics for tension, or as a multi-functional resistant of forces, such as steel. The study of material science defines the mechanical properties of all materials through the molecular composition of elements, atom structure, inherent dislocations and fracture mechanics. Given this explicit knowledge, along with specific architectural design and performance criteria, the form and function of each structural element is defined.

6.2.1 Static Structural Frames

Two dimensional and three dimensional frames were investigated in the first half of the thesis program for an organized database of structural frames in regards to specific loads, joinery, and geometry (Figure 6.11). The following represents the methodologies for determining the structural stability of planar and spatial frames.

6.2.2 Simple Planar Frame Analysis

From Santiago Calatrava's "Creative Process", he describes how he utilized "F. Stussi's Baustatik 1" numerical relationship for a dimensionally stable planar frame between compression bars and nodal connections. The equation is such:

$$2g = n + 3$$

where:

g = # of nodal connections

n = # of bars

Elements / Energy:	
1) Force	Tension Compression Torsion Bending Buckling
2) Loads	Live Dead Dynamic Environmental
3) Joinery	Pin Sliding pin Spherical Roller Rigid
4) Equilibrium	Force = Load

Figure 6.11, List of Variables for Rigid Body Frames

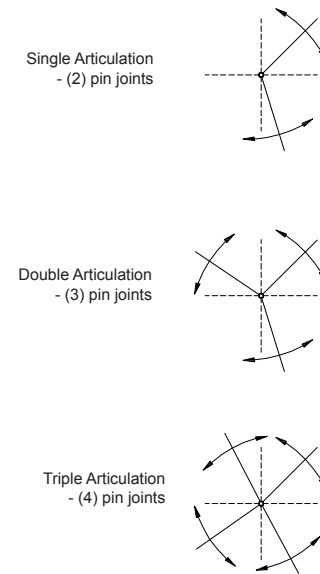


Figure 6.12, Typical Joint Articulation

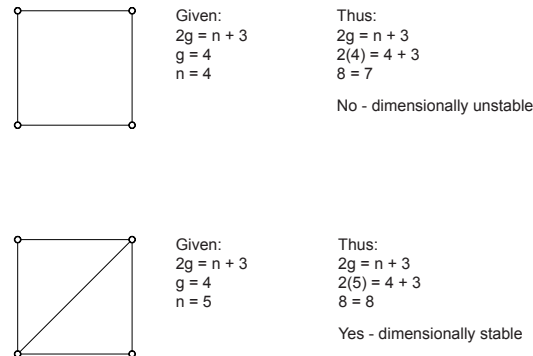


Figure 6.13, Simple Planar Frame Example

6.2.3 Space Frame Mechanism

The same method of analyzing planar frames can be modified for space frames or three dimensional networks of compressive bars and joints. Triangulation of both planar and space frames dominates the structural stability or degrees of freedom which the system possess. In general, the degree of freedom can be described as the number of bars that must be integrated into the structure in order for the system to be dimensionally stable. The following examples identify the mathematical and diagrammatic understanding of space frames.

Equation for evaluating space frames:

$$f = 3g - n - 6$$

n = # of bar

f = degrees of freedom

Example / Octahedron -
Given:

$$f = 3g - n - 6$$

$$g = 6$$

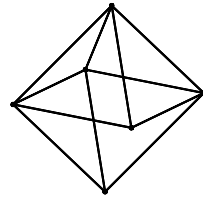
$$n = 11$$

Solution:

$$f = 3(6) - 11 - 6$$

$$f = 18 - 17$$

$$f = 1 = \text{degrees of freedom}$$



Example / Icosahedron -
Given:

$$f = 3g - n - 6$$

$$g = 12$$

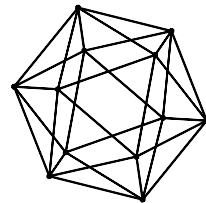
$$n = 30$$

Solution:

$$f = 3(12) - 30 - 6$$

$$f = 36 - 30 - 6$$

$$f = 0$$



Result:

The frame is inherently dimensionally stable, the degree of freedom = 0. If bars or nodes were added or subtracted the resultant space frame would require action to stabilize.

g = # of nodal connections



Figure 6.14, Dynamic Frame System Modeled - Santiago Calatrava Precedent Study

6.2.4 Preliminary Modeling

Modeling with compression members and pin joints was initiated to develop an empirical understanding of form and forces. Replicating the design of an expandable planar hexagonal pattern from Santiago Calatrava, the ability to collapse and deploy a planar frame was built (Figure 6.14). Special interest was focused on the placement of pin joints in relationship to one another and deployment properties along a vertical member.

6.2.5 Post-Tensioned Collapsible Shade Cantilever

The final research on collapsible systems within the thesis focused on the ability to provide a dynamic relationship within an applied landscape, allowing for adaptations to future environments and use. The methodology and empirical understanding for the organization of planar and spatial elements was researched through case studies, as seen in the previous example. These basic ideas were manipulated and re-constructed to understand how the equilibrium of compressive and tensile forces are transferred through specific joints and elements.

The final product of this research was a post-tensioned shade cantilever which utilized a three dimensional space frame which collapses based on the organization of elements. The resultant modeled materials included: polyester elastic membrane, carbon fiber compression rods, silicon - flexible joints and steel tensile cables (Figure 6.15).

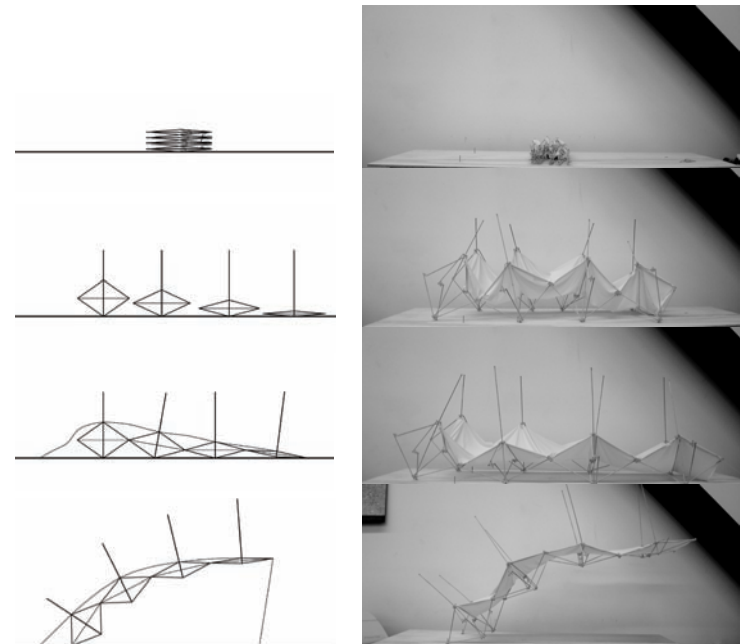


Figure 6.15, Post-Tensioned Collapsible Shade Cantilever - Digital and Physical Modeling

6.3 Membranes

In its purest form, a membrane performs as a 'tautly stretched skin' within a structural assembly of tensile and compressive forces in equilibrium. The physical properties which determine the design considerations of membranes include: dominant orientation, isotropic or anisotropic, and material molecular characteristics, crystalline or amorphous.

Elastomers, steel matrices, plastics, reinforced fibers (glass and carbon), woods, cotton fibers and glass fibers are the primary elements used in membrane assemblies.

Textile fabrics are manufactured through a weaving of warp and weft fibers leading to a directional or anisotropic orthogonal orientation. Often the warp direction is more tautly assembled than the weft direction leading to variable stretch of the fabric when loaded. The fabric is then subject to angular distortion under load and is unable to resist a shear force. To alleviate this strain, textile fabrics are typically coated with a bonding material such as Urethane or PVC to provide a composite matrix material which is an intermediate of isotropic and anisotropic orientation.

To compare, plastic fabrics alone possess isotropic orientation through amorphous molecular orientations. Plastics, such as Polyethylene, are often translucent and bond easily to other plastics and fabrics through heat welding. The fatigue strength of plastics is very low, but can be increased by introducing a secondary matrix material with high modulus of elasticity.

Elastomers have high fatigue strength due to its inherent interlocking of molecular chains, but with high ductility come lower yield strength. Rubbers thus show extreme elasticity when loaded, and based on the capability for large deformation, greater than 1000% elongation, its use as a structural material is limited.

The following membrane studies focus primarily on isotropic membranes including: plastic sheets, rubber membranes and plastic coated fabrics; and the post-production technologies which isolate the membranes to create new layers of enclosures. The elasticity of the chosen membranes is important as it controls the programmable deformation of the membrane and stores or releases inherent strain energy associated with deformation.



Figure 6.16, Translucent Grade I Silicon Membrane

6.3.1 Isotropic Membranes

The hypothesis for the membrane research was aimed at utilizing a fabric as a primary enclosure material which could stretch and strain by means of an adjustable frame, which, in turn would open and close pores that were cut into the membrane. The pores would then act as a functional performance property, allowing for air and or light to penetrate through the enclosure.

The initial tests were limited by fabric availability, size and purchase price, however by knowing the material properties for the first tests, assumptions as to the unobtainable materials was capable of being estimated. The primary membrane materials researched included:

- 1) Rubber membranes
 - Silicone Rubber
 - EDPM (Ethylene-Propylene)
 - SBS (Styrene Butadiene Styrene)
- 2) Plastic sheets
 - ETFE (Ethylene-Tetrafluorethylene)
- 3) Fabric Membranes
 - Plastic Fabrics
 - PVC Coated Polyester
 - PTFE Coated Glass Fiber
 - Urethane Coated Nylon
 - Silicon Coated Fiberglass



Figure 6.17, Bi-laminate Elastomeric Studies.



Figure 6.18, Bi-laminate Membrane With Different Coefficient of Thermal Expansion - Greg Blonder, Blonder Inventions, LLC, New Jersey

6.3.1 Pore Development

Once a variety of fabrics were obtained, the design and placement of pore patterns were investigated. The pattern and design of the pore was initially investigated as a stochastic study with random patterns, hole sizes and cut line curvature. These test were then examined through a parametric deductive method, by which, the pore function was analyzed in terms of: load, force direction, adjacencies, and openness. New sets of pore patterns were then developed and tested with silicon rubbers, polyester fabrics, nylon fabrics, and silicon coated fiberglass.

The resultant tests held unique characteristics. It was first determined that to produce an open pore, the cut line was to be perpendicular to the applied force direction, allowing the material to stretch around the cut and expand the pore. Second, the size of one cut line was determined to be relative to its proximity to adjacent cuts and relative to the tear strength of the membrane. Third, the direction of cut line segment, straight, curved, s-shaped, bent, etc, held different distribution of forces when strained, altering the function of the pore.

In the end, the performance of a membranes ability to strain, open pores, and recoil back to its original shape was determined to be successful, however, the appropriate dynamic frame and force required to strain the membrane and produce the open pore was unsuccessful. It was assumed that the mechanism to deform the membrane was non-mechanical and thus there was a design struggle to achieve the required forces passively without large loading.

These studies were not completely lost in the prototype synthesis, but rather reconsidered and rearranged as a shading material which moves from a negative strained position (slack) to zero strain (taut). See section 8.5 for more information.

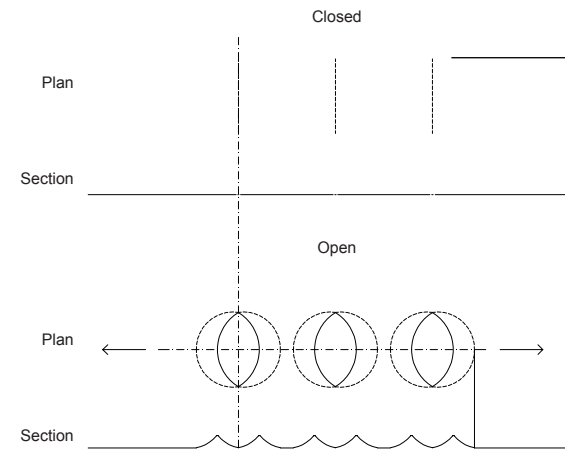


Figure 6.19, Pore Analysis 01

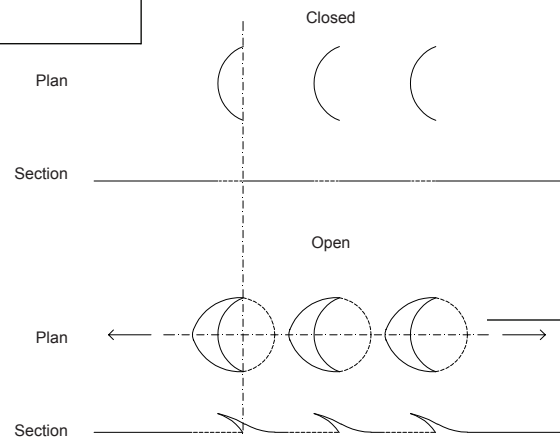


Figure 6.20, Pore Analysis 02

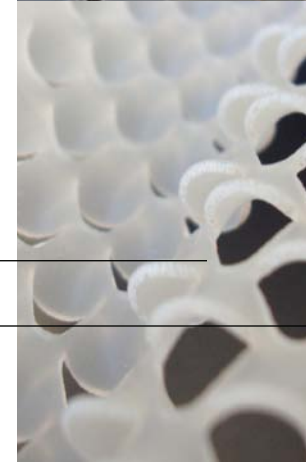
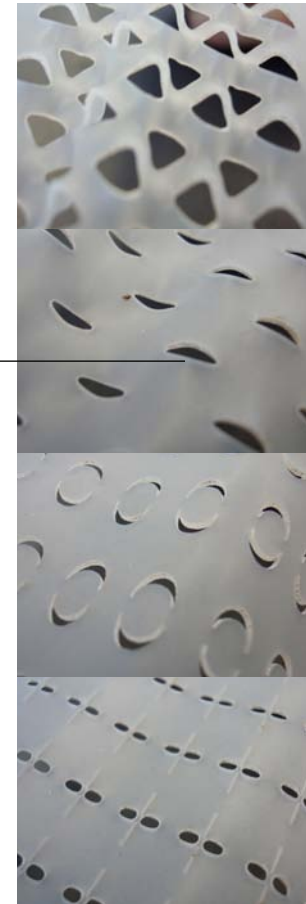


Figure 6.21, Silicon - Laser Cut



Figure 6.22, Polyester/Nylon - Laser Cut

1.0 ABSTRACT

2.0 INTRODUCTION

3.0 PERFORMANCE CRITERIA

4.0 MATERIAL PROPERTIES

5.0 PRECEDENT STUDIES

6.0 PRELIMINARY EMPIRICAL INVESTIGATIONS

7.0 SYSTEM DEVELOPMENT

8.0 PROTOTYPE SYNTHESIS

9.0 POTENTIAL APPLICATIONS

10.0 APPENDIX

7.0 SYSTEM DEVELOPMENT

7.1 Bistable Mechanisms

Two local minimum enclose a local maximum, two stable equilibrium positions will have an unstable position between them.

Larry Howell, *Compliant Mechanisms*

While modeling dynamic frames a unique characteristic of one particular model was observed (Figure 7.1).

The model was built from numerous wood dowels with rubber bands connecting each intersection between two dowels. Each dowel was a straight segment, intersected by five additional dowels. In principal, the form was a regular polygon of twenty-five dowels with four congruent sides and four congruent angles, or a square.

The square, however, was not observed. The wrapping of the dowels with the elastic rubber bands caused a tensile force to be biased within the system, pulling and deforming the square into a quadrilateral rhombus, demonstrated not only planar deformation but also three-dimensional deformation. The farthest points of the rhombus tended to bend into each other, resulting in a hyperboloid form.

In general, the model was pre-stressed due to the elastic joints, and displayed unique flexural characteristics. When a torsion force was exerted on the far points of the model and the middle was free, the hyperboloid form slowly elongated and flattened out, forming an apparent planar rhombus. Then, instantaneously, the model snapped, in the direction of torsion force, into a stable position inverse of the original state. This position was rigid due to the geometry and friction force of the wood dowels. The sequence can be repeated until the elastic joints fatigue and need to be retightened.

The mechanical engineering signification for this behavior in a system is known as a bistable mechanism. Bistable mechanisms exhibit two stable equilibrium positions with an unstable position between them (Compliant Mechanisms).

7.1.1 Bistable Development

Once the bistable phenomena of the initial model was investigated further, it was determined that the function of the mechanism to act as a capacitor, which stores and releases inherent strain energy as a dynamic frame, held numerous possibilities for producing the required force to deform a membrane and create an adjustable enclosure.

The first step was to simplify the original model and create a new model that required only the minimal parts for the same function (Figure 7.2). The simplification of the system was not only a reduction in parts but a holistic analysis of the forces inherent to the system. At this point, a unit was created from which identical sub-units could be organized around or within to create a surface or enclosure. The modeling of a surface identified numerous geometric restrictions however, and was later found to be due to the three-dimensionality of the first unit, thus a two-dimensional frame of the same function was sought after.

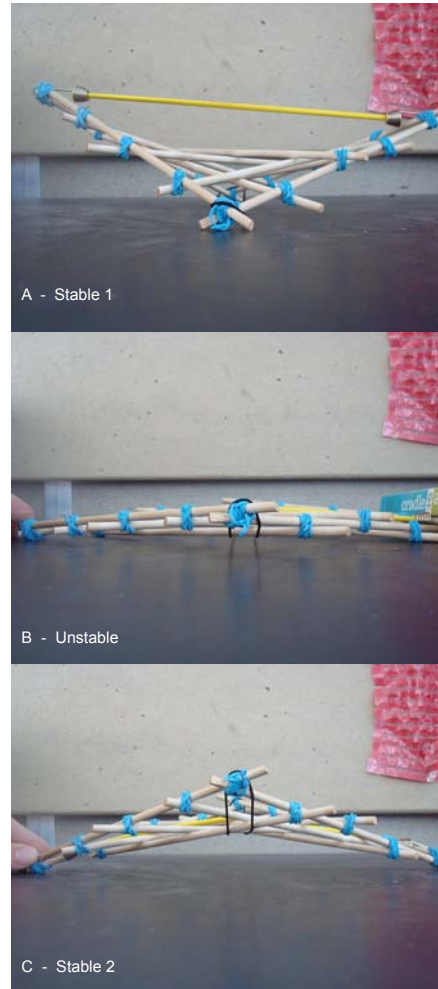


Figure 7.1, Initial Bistable Model - Wood Dowel / Rubber Band / Bungee Cord

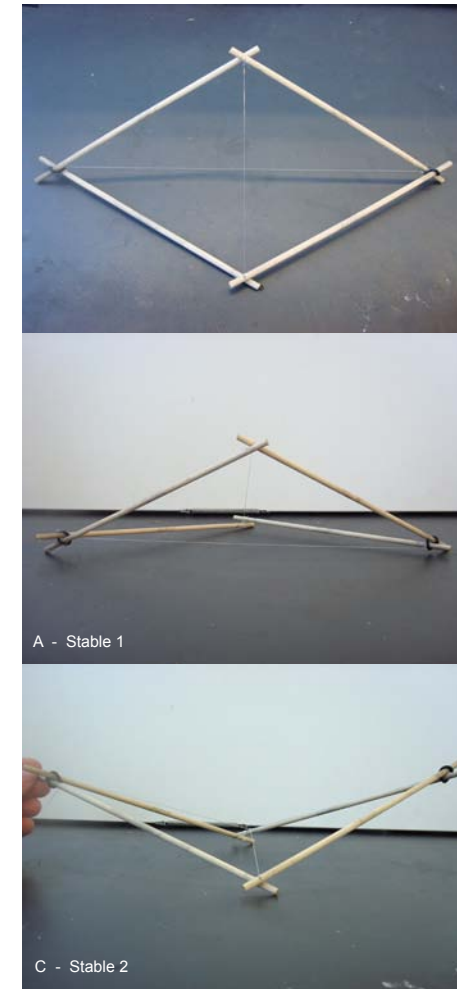


Figure 7.2, Refined Initial Bistable Model - Wood Dowel / Elastomer O-Ring / Tension Line

7.1.2 Two-Dimensional Bistable Development

The movement from a 3-D to 2-D bistable frame was a move of efficiency and realized through sectional analysis of the original model. In section, the model identified a tensile spring line segment which restricted the (2) wood dowel beams in 3-D. It was assumed that if the beams were joined to form a continuous planar strip and the tensile spring line pre-stressed the strip a 2-D bistable frame with pin joints, it could then be modeled and allow for the desired movement.

This assumption proved to be correct and the bistable movement and capacity of storage and release of strain energy of the system was much more pronounced (Figure 7.6).

The frame was now in its most efficient form, but the material designation however was not. The move from the 3-D to 2-D frame yielded a change in material from wood dowels to longitudinal Carbon Fiber Reinforced Plastic (CFRP) strips. The carbon fiber's high modulus of elasticity allowed the strip to recoil without permanent deformation, but it also yielded a higher strain force to deform the strip between the stable and unstable states.

At first, the slenderness ratio of the strip was analyzed to determine the appropriate length and cross-sectional area required to minimize the buckling force of the system while maintaining frame stability. This proved to be a good study, however, the available manufacturing sizes of carbon fiber strips were limited in both width and thickness. In addition, the aesthetic function of the frame in relationship to the human body and perception played a part in the length and was determined to not exceed 1'-6". These parametric variables pushed the frame material to be reconsidered.

Various plastic strips and spring steel strips were chosen as alternates for the carbon fiber and wood strips and the pin joint yielded research into 3-D printed nodes and anti-friction bearings for smooth rotation. Results for these tests will be revealed later in the document.

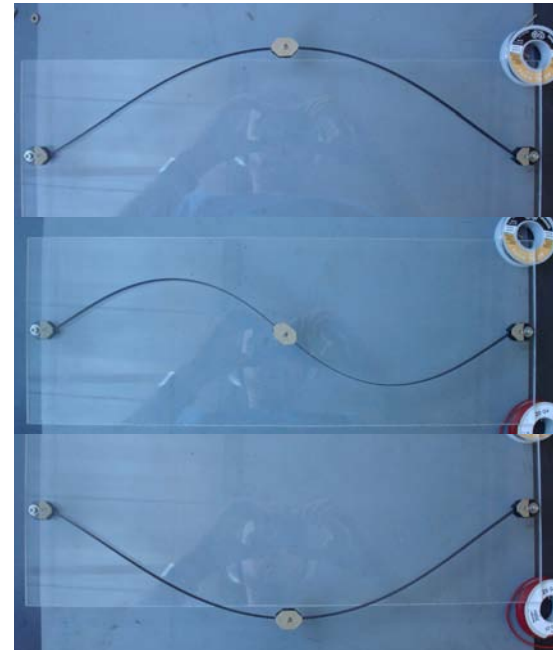


Figure 7.6, Bistable Model - CFRP Strips / Elastomer Pin Connection

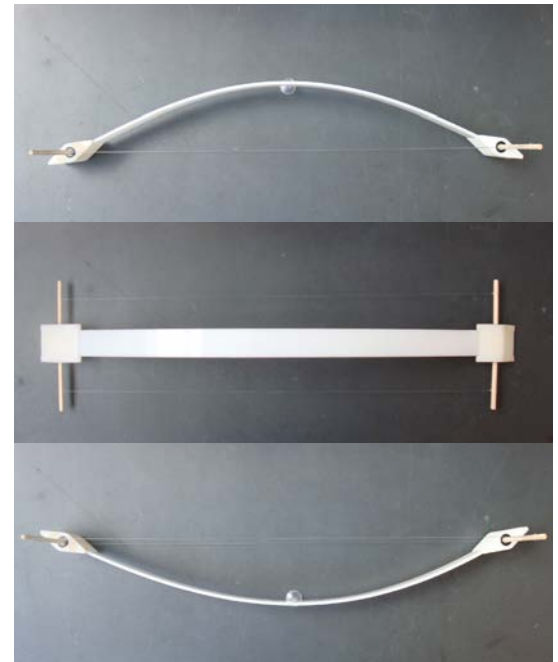


Figure 7.7, Refined Bistable Model - HDPE Strips / Sterolithography Pin Connections / S.S. Ball Bearings

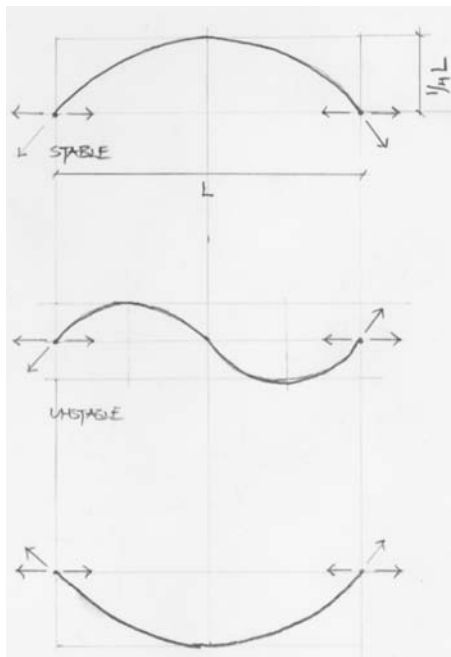


Figure 7.3, Bistable Vector Diagram

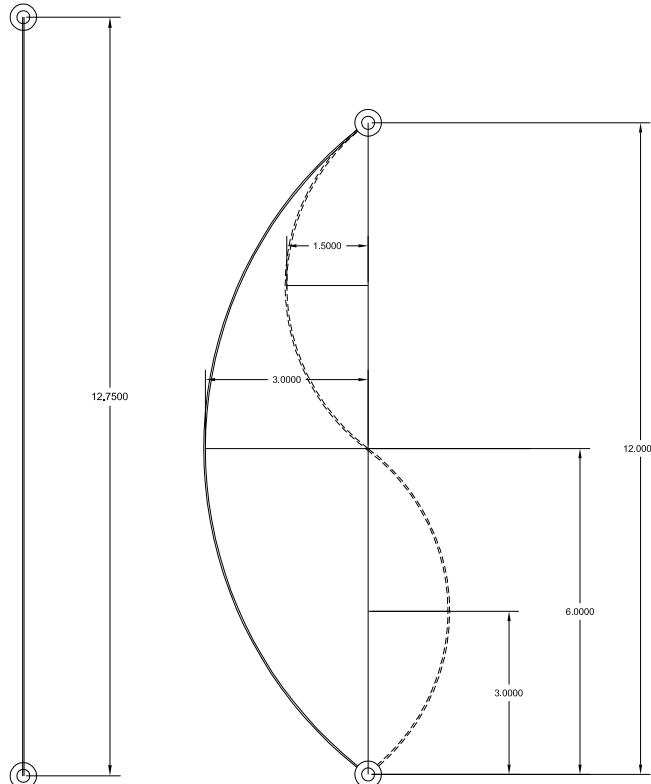


Figure 7.4, Spring Steel Strip - No Stress

Figure 7.5, Spring Steel Strip in Bistable Arrangement - Postensioned

7.1.3 Computational & Parametric Modeling

Until this point in the research, the bistable mechanism was investigated independently as its own system with less awareness to its final orientation or function. This was primarily done to focus the development of the system to its maximum potential, knowing that the movement and capacitor function inherent could be tuned later for adaptable systems.

The research from this point on takes on a multidisciplinary approach to the set of original performance goals (Page 13) with investigations relating the bistable frame between: membrane materials, mechanical properties, optical properties, form, and function.

The first move was to determine the orientation, placement and organization of the bistable frame unit to be used as a mechanism which adjusts an enclosure for light and heat regulation.

After numerous models failed in trying to organize the bistable frame into an enclosure, it was finally realized that if single bistable unit could be offset and mirrored, it could produce an aperture, or large scale pore with two bistable strips, that then could open and close as the strips were rotated (Figure 7.8). This was first modeled and rendered in the computer and later physically modeled (Figure 7.9 and 7.10).

The aperture was thought of much like a camera lens or iris which could adjust to the exposure of the sun based on its orientation. Thus, as the sun was to be exposed to the mechanism, the strips would deform and overlap each other, providing a surface of continuous shade. Once the sun was no longer on the surface, the mechanism would then release its stored energy and return or recoil to an open aperture.

A sequence of actuators for the system was then revealed:

- The sun heats and expands a passive actuator.
- The actuator expands and rotates the bistable strips.
- Strips store the increased strain energy.
- An aperture system closes

- Sequence reverses once heat input ceases.

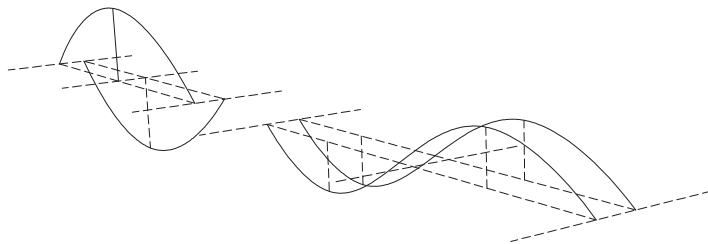


Figure 7.8, Offset Strip Diagram (Open and Closed)

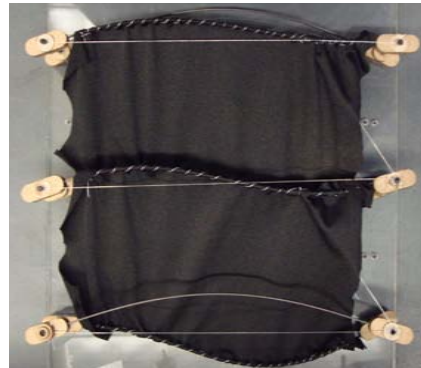


Figure 7.9, Bistable Assembly 03 Model - CFRP Strip & Rod / Polyester - Nylon Fabric / Tension Line / Composite Pin Connection

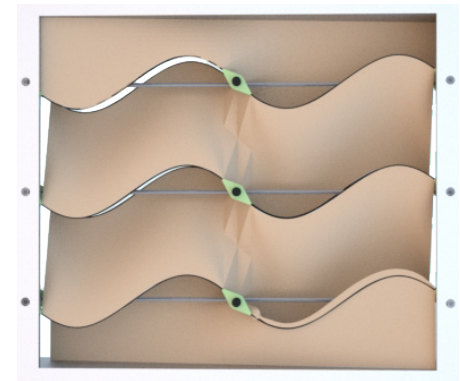
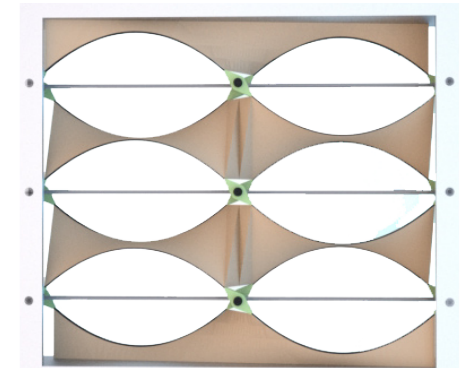


Figure 7.10, Elevation - Open (Top) / Closed (Bottom)

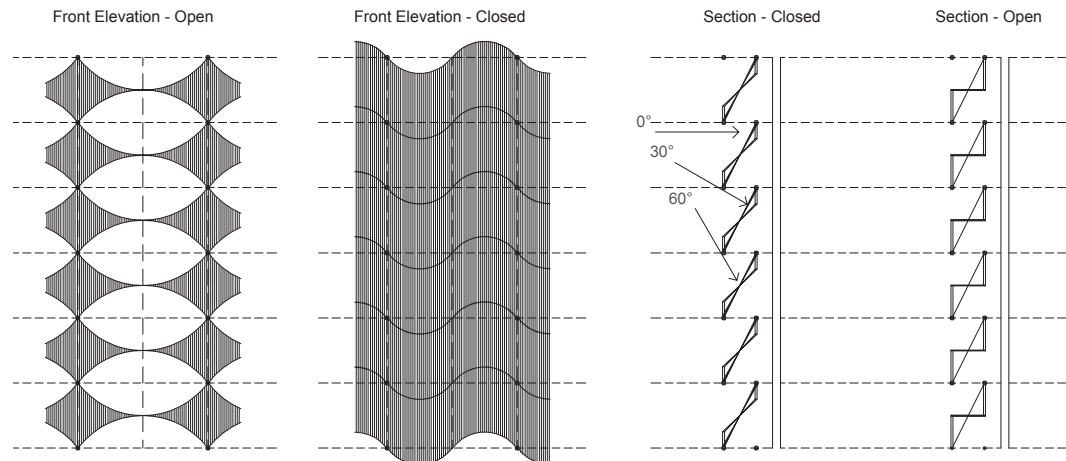


Figure 7.11, Elevation & Section Diagrams

7.1.4 Enclosure Model 01

Before the sequence of passive heating, actuating and movement could be accurately tested, additional modeling of the system was required to qualify and quantify the method of the system. The next four pages identify the system in terms of:

- Large-scale modeling and array patterning.
- Membrane and enclosure connections.
- Required force to rotate strips.

These steps in modeling and testing of the system further delimited and focused the enclosure to validate its existence and performance as a system which could be passively actuated and functional.

The larger scale model depicted in Figure 7.12 and 7.13 held a dimension of 3'-0" x 1'-6", with 18 carbon fiber strips, 32 pinned nodes made of carbon fiber rods and layered wood elements, a tensile string and 1 membrane pattern repeated 3 times.

The model visually identified the movement of the surface from an open state to close state and back to open, but the tolerances for the node and membrane were not considered holistically within the assembly, resulting in a system which is hard to close completely as it reacts sporadically to the transfer of forces through the movement of strain energy. The adjacent photo showing the system close was one of the few times it remained close long enough for a photo.



Figure 7.12, Elevation - Closed



Figure 7.13, Elevation - Open

7.1.5 Membrane Studies & Suction Cups

After the large scale model was investigated empirically for errors and problem areas, smaller subunits were modeled to investigate more intimately the membranes relationship to the frame and the reconsideration of the all material designation was researched.

A cut pattern for the membrane was developed for the maximum closed state, creating a membrane that exhibits zero tautness when fully deployed. The pore studies for the membrane was reinstated but the expansion of the membrane was so minimal that the force required to activate the pores appropriately was lost (Figure 7.16). A pleated paper membrane was then investigated to anticipate the folding of the fabric within itself as the frame opened completely (Figure 7.17).

The connection to a new or existing enclosure was then anticipated by designing a suction cup connection, within the node, to attach the system securely and permanently to glass or other non-porous substrates.



Figure 7.14, Node Detail With Suction

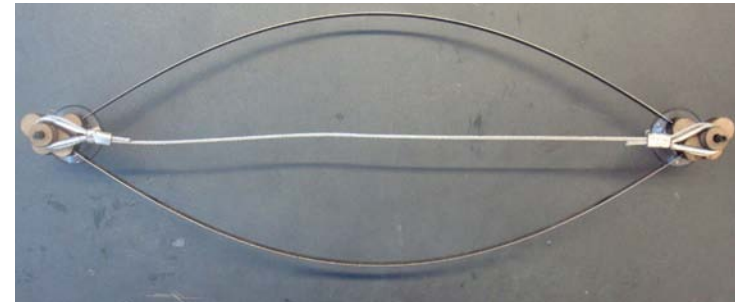


Figure 7.15, Single Bay Bistable Model Plan - Spring Steel Strips, S.S. Tensile Cable



Figure 7.16, Silicone Coated Fiberglass Membrane



Figure 7.17, Pleated Paper Membrane

7.1.6 Empirical Force Test

Empirical tests were conducted to determine the force required to deform the bistable strip system (two bays) based on three locations with varying distances to the pin connection. Two materials were tested: longitudinal Carbon Fiber Reinforced Plastic (CFRP) strips, and 1095 Spring Steel.

The hypothesis for the test was set that as the load was placed at a farther distance from the pin, a lower force would be required to rotate the strip due to the utilization of a moment arm.

The test was conducted by attaching a separate loading string to three strip locations and then connecting the string to a container and filling it with water. The rotation of the pin was attempted to be recorded at 25%, 50%, 75% and 100% rotation, or its stable state. The water container was measured at each interval and the results are shown in Table 7.1.

In the end, the test identified that the position of the load to the pin did have a direct affect on the weight; however, there were unexpected results of the test in measuring the percentage of rotation - the lower the weight, the more instantaneously the strip snapped to 100%. The bi-stability of the strip was in effect.

The two materials, CFRP and Spring Steel, also identified a large contrast in force based on the individual material properties. The CFRP strip resulted in a much higher stress to deform as its cross-sectional area and modulus of elastic were greater than the Spring Steel.

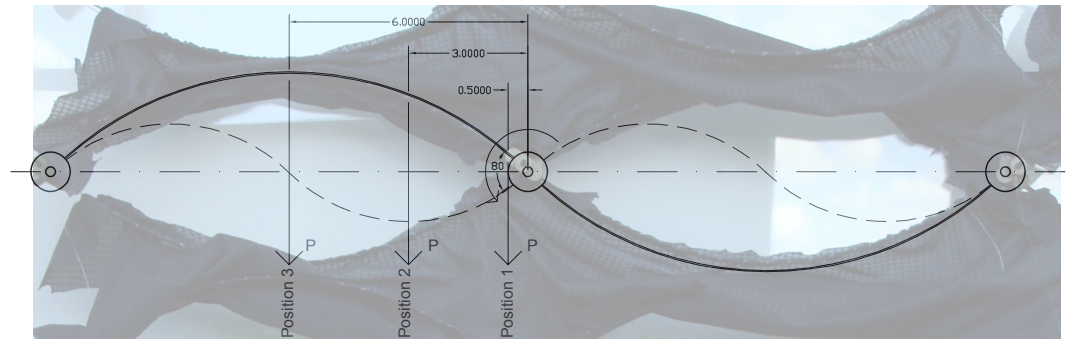


Figure 7.18, Force Analysis Diagram

CFRP Strips - 1/64" x 3/8" x 12"

Position	% Rotation (Open - Closed)	Weight / Force (Ounces)	Notes
1	100	52	Strip unstable at 75% rotation - immediately snaps to 100%
1	50	43	Horizontal placement of pin
1	25	24	Little deflection noticeable
2	100	12	Strip unstable at 50% rotation - immediately snaps to 100%
2	25	6-5/8	Visible deflection with only 25% rotation
3	100	14	Strip unstable at 50% rotation - immediately snaps to 100%
3	25	6	Visible deflection with only 25% rotation

1095 Spring Steel Strips - 1/64" x 1/4" x 12"

Position	% Rotation (Open - Closed)	vWeight / Force (ounces)	Notes
1	100	32	Similar to CFRP Strips - noticeably less weight required
2	100	6	Hard to measure % rotation - minute weight deflects to snap 100
3	100	6	Hard to measure % rotation - minute weight deflects to snap 100

Table 7.1, Force Charts - Carbon Fiber & Spring Steel

7.1.7 Flexure Material Test

Beyond the empirical testing, computer aided testing devices were utilized to determine more accurately the strain force between the carbon fiber and spring steel strips. A three point flexural test was conducted to deform the flat strip to its programmed deflection within the system. The results of these tests quantified the stress force of the strip at its prestressed state and through additional computer aid in the mechanical engineering program Ansys (Ansys Inc.), it was determined the stress required to deform to the S-shape yielded an increase of four times the initial stress. The charts below identify the prestressed state and with the multiplication of four, the final stress was determined (not shown).

The spring steel strips yielded the lowest stress but still remain geometrically stable. Spring steel can also be formed in sizes ranging from 0.005" to 0.25" thickness and widths from 0.125" to 12". Various sizes of strips were obtained and tested, and proved to be the most appropriate material for the strip in the bistable system.



Figure 7.19, Test Photos - Spring Steel Strip

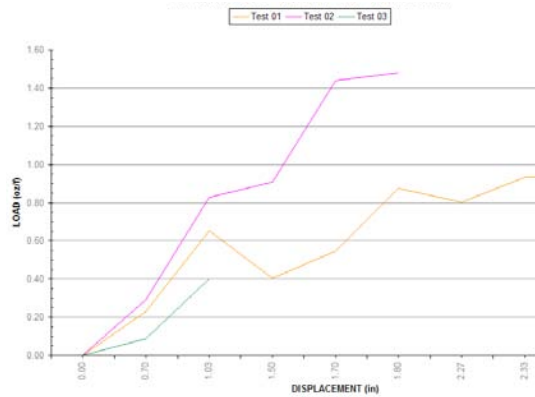


Figure 7.20, Flexural Test - 1/64" x 1/4" x 12" Spring Steel Strip

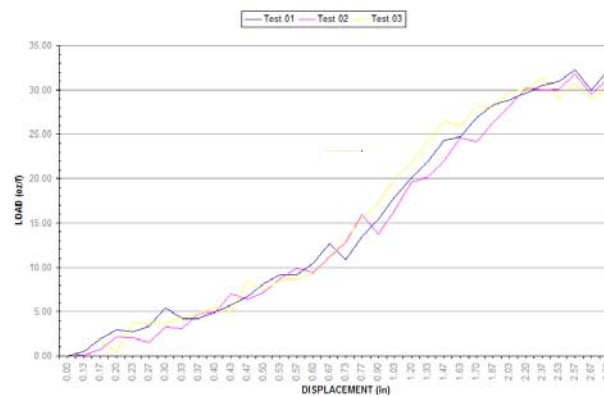


Figure 7.21, Flexural Test - 1/32" x 3/8" x 12" Spring Steel Strip

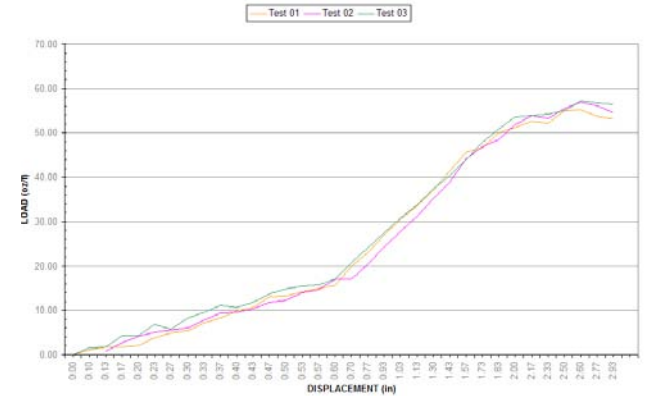


Figure 7.22, Flexural Test - 1/32" x 1/2" x 12" Spring Steel Strip

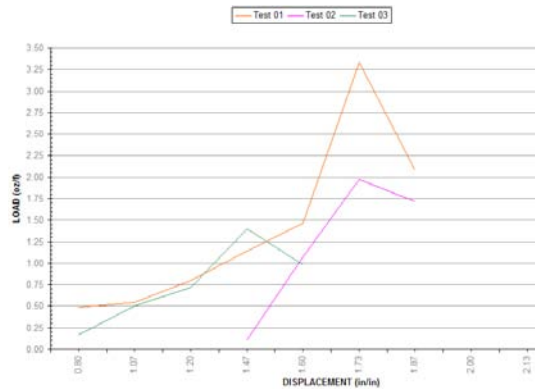


Figure 7.23, Flexural Test - 1/64" x 3/8" x 12" CFRP Strip

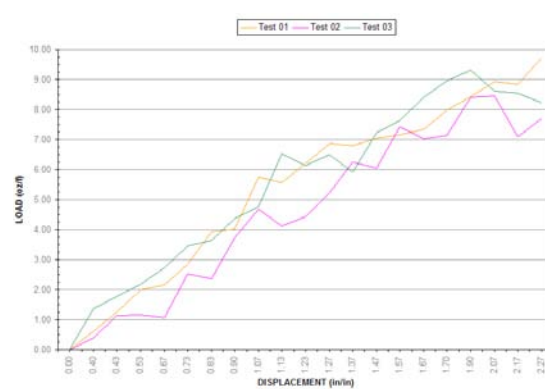


Figure 7.24, Flexural Test - 1/32" x 1/8" x 12" CFRP Strip

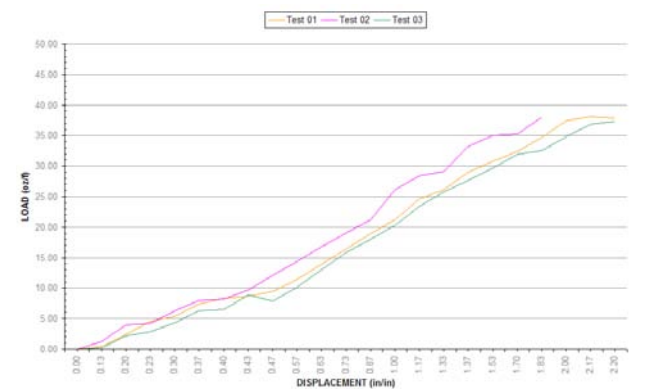


Figure 7.25, Flexural Test - 1/64" x 1" x 12" CFRP Strip

7.1.8 Bistable Mechanism Conclusion

After numerous iterations of models, sketches and testing of the bistable mechanism, the research concluded with yet a few missing variables for the system to adjust to solar exposure passively. These variables included:

- What is the actuator that rotates the strip?
- Given the new actuator, what is the design of the node?
- How does the membrane fit appropriately within the mechanism?

With the bistable mechanism research complete, the focus of work shifted to finding the appropriate actuator, one which responds to the force required to deform the spring steel strips and one that rotates the required 60 angular degrees over an appropriate change in temperature.

7.2 Thermostat Metal

The actuator for the system involved in depth research and analysis of passive reactive smart materials with appropriate thermal expansion properties (page 18). Numerous materials and composites were quickly eliminated from the research as they did not provide: 1) adequate force when heated; 2) rotational deformation; and 3) response to change in temperature. In the end, Thermo-bimetals, in the form of Thermostat metals were determined to be the best venture given the required goals for the system.

Thermostat metals are composite materials which consist of two or more metallic layers having different coefficients of thermal expansion. When the layers are permanently bonded together, the different coefficients of expansion between the metals cause the resultant shape to curve or deform when subject to change in temperature. The bending of the material, in response to temperature change, is known as the Flexivity of the material and is an inherent principle to all thermostat metals.

In mathematical terms, the bending of the thermostat metal is directly proportional to the difference in the coefficient of expansion and the temperature change of the component, and inversely proportional to the thickness of the composite. Furthermore, the bending is also affected by the ratio of the moduli of elasticity of the metallic layers and their thickness ratio (See Figure 7.27). The design of the thermostat metal is further defined by the form in which it is set.

The manufacturing process of bonding the metals consists of heating and rolling the thin metallic layers to a precise thickness by means of an intermediate annealing operation, followed by pickling, cleaning and brushing procedures. Each side of the composite is then etched to identify high and low expansion sides and finally set in a variety of forms, including: strips, spiral coils and helix, creep discs, u-shapes, and double u-shapes. Each resultant form has an individual equation to determine the thermal deflection (distance or angle), and the mechanical and thermal forces based on dimensions and materials mechanical properties.

For this study, thermostat coils are investigated as thermally responsive actuating devices to deform and set the shade enclosure. The adjacent diagrams and equations identify the variables present in the design and the resultant outputs achieved.

Formula Symbol Key		
Variable	Definition	Units
t	Material Thickness	Inches
w	Material Width	Inches
L	Active Length	Inches
E	Elastic Modulus	Lbs/Inch ² (psi)
F	Flexivity	Inch/Inch/°F
A	Angular Rotation (Coils)	Degrees
B	Linear Deflection	Inches
P	Force	Ounces
r	Radius At Point of Load (Coils)	Inches
D	Outside Diameter (Disc)	Inches
d	Inside Diameter (Disc)	Inches
(T2 - T1)	Temperature Change	°F

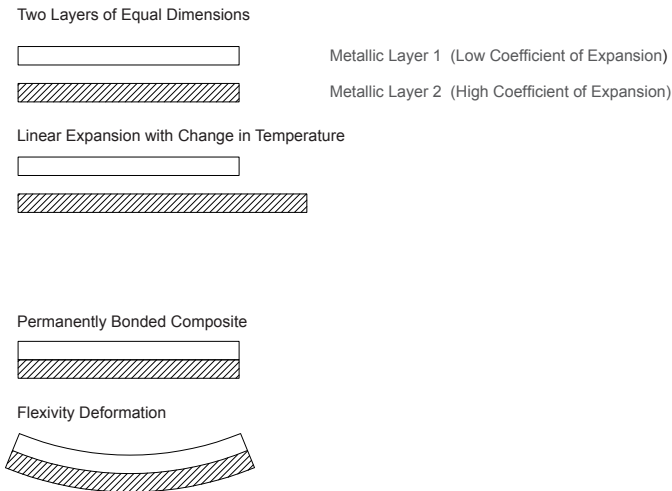


Figure 7.26, Thermal Expansion Diagrams for Bi-laminates, Engineered Material Solutions

Spiral Coil Formulas

Thermal Deflection:

$$A = \frac{67F (T2 - T1) L}{t}$$

Mechanical Force

$$P = \frac{0.0232E Awt^3}{Lr}$$

Thermal Force

$$P = \frac{1.55EF (T2 - T1) wt^2}{r}$$

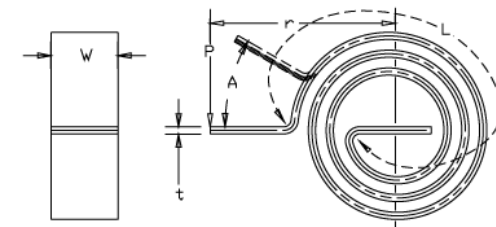


Figure 7.27, Bimetal Equations for Coils and Beams, Engineered Material Solutions

7.2.1 Thermostat Material Specifications

Based on actuation required by diurnal temperature change, a thermostat coil with a high Flexivity range, between 50 - 100 degrees Fahrenheit, was required. ASTM standards define thermostat metal mechanical properties and classifications, and the following composites were determined to be the most appropriate for the given application:

1) ASTM - TM2 / P675R

- **Most active and most widely produced thermostat metal.**
- High Expansion Alloy (72% Mn, 18% Cu, 10% Ni) 55% Overall
- Low Expansion Alloy (36% Ni, Bal. Fe (Invar)) 45% Overall
- Flexivity 50 to 100 Degrees F. = 215×10^{-7}
- Flexivity 100 to 300 Degrees F = 209×10^{-7}
- Modulus of Elasticity = 20×10^6 psi
- Maximum Temperature = 500 Degrees F

2) ASTM - TM1 / B1

- Best all purpose thermostat metal
- High Expansion Alloy (22% Ni, 3%Cr, Bal., Fe) 50% Overall
- Low Expansion Alloy (36% Ni, Bal. Fe) 50% Overall
- Flexivity 50 to 100 Degrees F. = 150×10^{-7}
- Flexivity 100 to 300 Degrees F = 146×10^{-7}
- Modulus of Elasticity = 25×10^6 psi
- Maximum Temperature = 1000 Degrees F

2) ASTM - TM21 / GB14

- High corrosion resistance
- High Expansion Alloy (18% Ni, 11.5%Cr, Bal., Fe) 50% Overall
- Low Expansion Alloy (42% Ni, Bal. Fe) 50% Overall
- Flexivity 50 to 100 Degrees F. = 101×10^{-7}
- Flexivity 100 to 300 Degrees F = 100×10^{-7}
- Modulus of Elasticity = 25×10^6 psi
- Maximum Temperature = 900 Degrees F

Due to the required force output determined by the empirical testing of the system, it was found that a spiral coiled thermostat metal with maximum thickness to angular rotation ratio was required due to the low change in temperature. The following spiral coil sizes were available for immediate use:

1) ASTM - TM2 / P675R

- a) Thickness = 0.0400" Width = 0.6250"
- b) Thickness = 0.0475" Width = 0.2810"
- c) Thickness = 0.0350" Width = 0.4375"
- d) Thickness = 0.0320" Width = 0.5000"

Thermostat Coil Calculations:

1) ASTM - TM2 / P675R - Thickness = 0.0350" Width = 0.4375"

Given: t = 0.0350"
w = 0.4375"
E = 20×10^6 psi
F = 215×10^{-7}
A = 30 degrees
P = 32 ounces
T2-T1 = 60 degrees fahrenheit



Thermal Deflection:

$$A = \frac{67F (T2 - T1) L}{t}$$

Thermal Deflection:

$$A = 30 ; \text{Thus } L = 12.1485"$$

Mechanical Force

$$P = \frac{0.0232E Aw^3}{Lr}$$

Mechanical Force

$$P = 32.09oz$$

Thermal Force

$$P = \frac{1.55EF (T2 - T1) wt^2}{r}$$

Thermal Force

$$P = 32oz ; \text{Thus } r = 0.6697"$$

2) ASTM - TM2 / P675R - Thickness = 0.0320" Width = 0.5000"

Given: t = 0.0320"
w = 0.5000"
E = 20×10^6 psi
F = 215×10^{-7}
A = 30 degrees
P = 32 ounces
T2-T1 = 60 degrees fahrenheit



Thermal Deflection:

$$A = \frac{67F (T2 - T1) L}{t}$$

Thermal Deflection:

$$A = 30 ; \text{Thus } L = 11.107"$$

Mechanical Force

$$P = \frac{0.0232E Aw^3}{Lr}$$

Mechanical Force

$$P = 32.09oz$$

Thermal Force

$$P = \frac{1.55EF (T2 - T1) wt^2}{r}$$

Thermal Force

$$P = 32oz ; \text{Thus } r = 0.6398"$$

Table 7.2, Thermostat Coil Calculations

7.2.2 Thermostat Metal Testing

Once the first sets of thermostat coils were received, initial empirical tests were devised to determine and validate the mechanical specification of the coil to determine appropriateness with the bistable system.

Utilizing a laboratory in the Physics Building at U of A, a testing platform was set up to perform calculations of angular rotation, change in temperature, and force exerted for the two obtained coils:

- 1) ASTM - TM2 / P675R - Thickness = 0.0350" Width = 0.4375
- 2) ASTM - TM2 / P675R - Thickness = 0.0320" Width = 0.5000

Figure 7.29 identifies the test setup. A heat gun was used to provide a laminar flow of heat onto the coil and a digital thermometer sensor recorded the room temperature and temperature of heat flow at the coils surface. A Plexiglas sheet with angular tick marks was placed behind the coil to measure rotation at specific change in temperature. The set up was completed by locking the inside tab of the coil, allowing the outside tab to rotate, while a string and weight device was connected to the outside tab to return the coil to a level plane, giving the force exerted by the coil at a specific change in temperature.

The two following sheets document the test procedure and results for the two coils. A conclusion for the thermostat coil testing then follows.

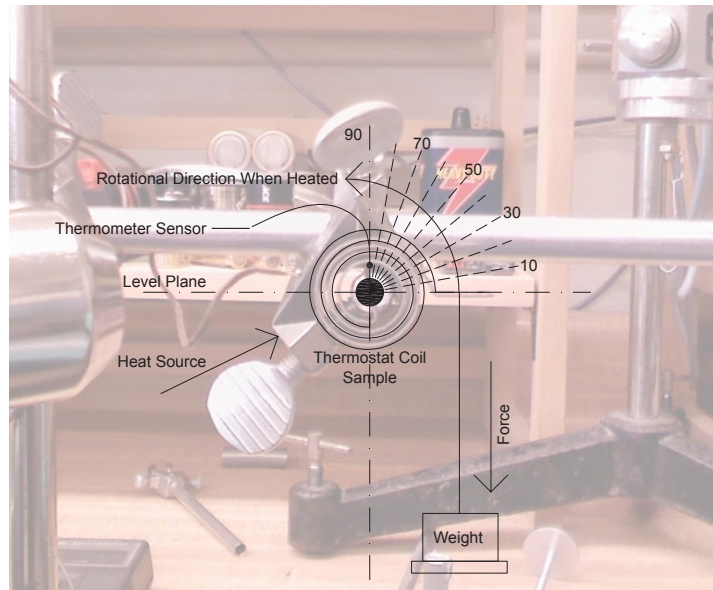


Figure 7.29, Diagram of Heat Coil Test Setup

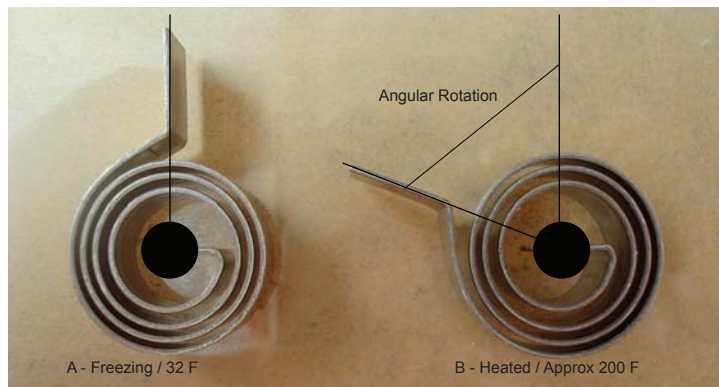


Figure 7.28, Empirical Testing of Thermostat Coil Deformation

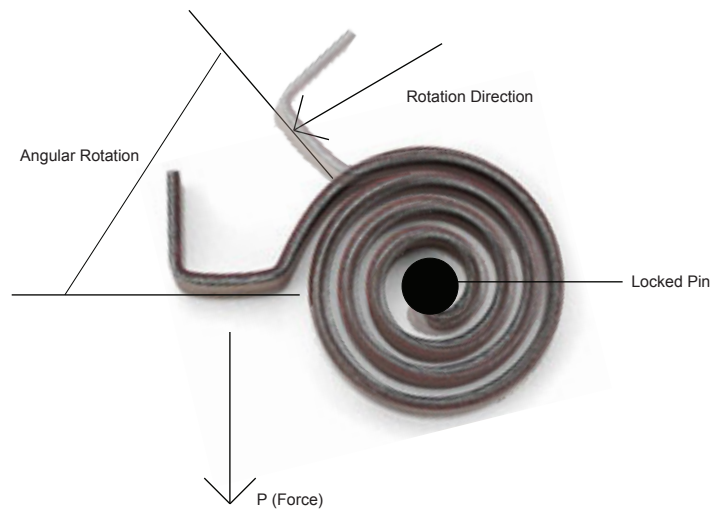


Figure 7.30, Theory of Thermostat Coil Deformation

7.2.3 Test 01

Coil Specification:

ASTM - TM2 / P675R - Thickness = 0.0350" Width = 0.4375

It was assumed that due to the thickness of this coil and its active length of approximately 9.7", it would yield a high force resistance when heated with a limited angular rotation.

The test results were such:

Table 7.3 - Coil Testing Results:

	ASTM - TM2 / P675R - Thickness = 0.0350" Width = 0.4375			
Point	Temp. (F) +/- 5	Weight (oz)	Rotation (Deg) +/- 3	Change in Temp. from freezing (F)
1	32.0	0.00	Level	0
2	72.8	9.80	15	40.8
3	191.0	40.00	50	159.0



Figure 7.31, Point 1 - Freezing (32.0 F / 0.0 oz)

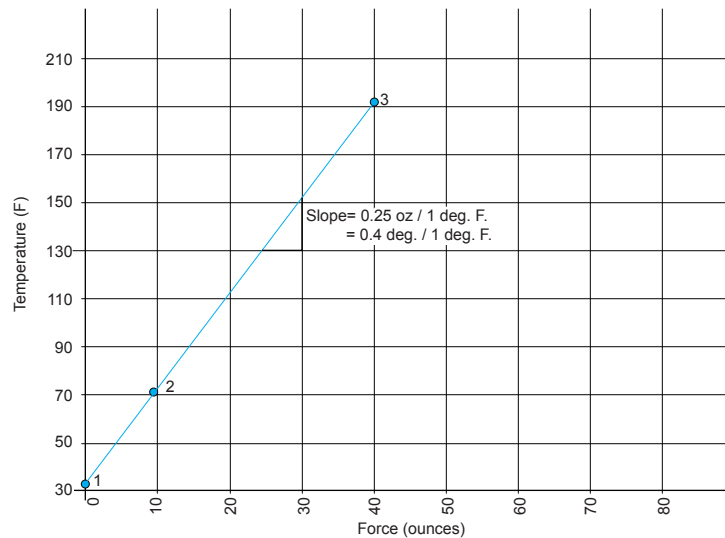


Figure 7.32, Point 2 - Room Temp. (72.8 F / 9.8 oz)



Figure 7.33, Point 3 - Heated (191.0 F / 40.0 oz)

Chart 7.1 - Graphical Representation of Coil Force With Temperature:



7.2.4 Test 02

Coil Specifications:

ASTM - TM2 / P675R - Thickness = 0.0320" Width = 0.5000

The second coil tested had a slightly smaller thickness than the first coil (0.032" versus 0.035"), but had an active length of 10.66", and width larger than Test 01. It was theorized then that this coil would yield a greater force at similar temperatures and thus have a lower slope.

The test results were such:

Table 7.4 - Coil Testing Results:

Point	Temp. (F) +/- 5	Weight (oz)	Rotation (Deg.) +/- 3	Change in Temp. from freezing (F)
1	32.0	0.00	Level	0
2	73.0	11.60	20	41.0 (from freezing)
3	190.0	59.35	65	158.0 (from freezing)



Figure 7.34, Point 1 - Freezing (32.0 F / 0.0 oz)

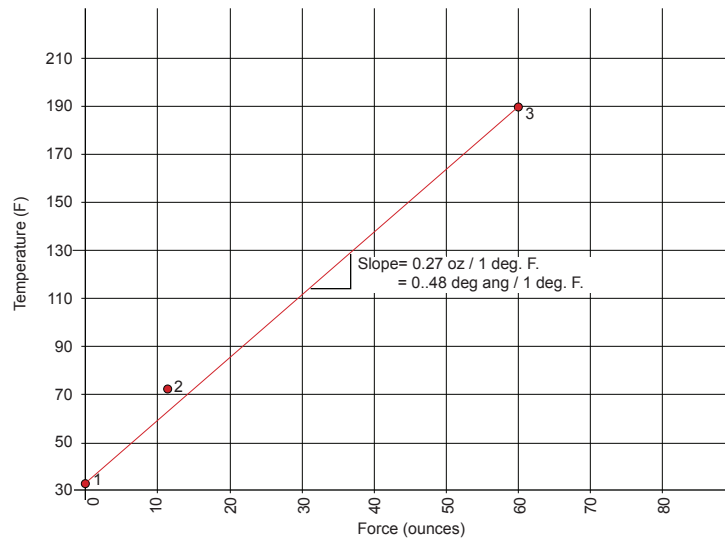


Figure 7.35, Point 2 - Room Temp. (73.0 F / 11.6 oz)



Figure 7.36, Point 3 - Heated (190.0 F / 59.3 oz)

Chart 7.2 - Graphical Representation of Coil Force With Temperature:



7.2.5 Force Test Conclusion - Extension

It was concluded from the tests and verified by the design equations that there was a partially linear correlation between temperature and force of the thermostat coils. It was only partially linear because the flexivity of the coils slightly changes as the temperature increases (See Appendix 10.7.2). An additional correlation was needed however between the relationship of the degree of angular rotation and change in temperature for a specific active length to accurately determine the specific coil required for the designed bistable system.

The test and results yielded assumptions as to defining specific correlations between the active length and thickness of coil related to change in temperature and angular rotation. For example, in Test 02, it was found that the ratio of force to temperature is 0.27 oz / 1 degree Fahrenheit and angular rotation to temperature is 0.48 degree angular / 1 degree Fahrenheit. This was achieved with a thickness of 0.032 inches and an active length of 10.7 inches. If the thickness is constant and active length is considered a variable, the resultant linear relationship yields a ratio of 0.045 angular degree rotation per inch of active length, see equation below for verification:

$$A = \frac{67F (T2 - T1) L}{t}$$

$$A = \frac{67 (215 \times 10^{-7})(10) 10.7}{0.032}$$

$$A = 4.816 \text{ degree angular}$$

$$\text{And, } 5.266 - 4.816 = 0.451$$

Thus, in Test 02, the 10.7" active length coil displayed a 0.48 degree angular / 1 degree Fahrenheit and if by increasing the active length to 11.7", 0.045 degree is added to the 10.7" ratio and now equals a 0.526 degree angular / 1 degree Fahrenheit.

This mathematical relationship allows for quick identification of a required angular rotation result based on the known thickness of material to find the change in temperature required to activate the coil. For example, the bistable system which is being investigated requires an angular rotation of 60 degrees. With the coil used in Test 02, at a thickness of 0.032 inches, we take the known rotation of 60 and divide by 0.48, and determine the change in temperature to be 125 degree Fahrenheit. This can be validated through testing by adding 125 from the starting point of 32 (freezing) to equal a temperature of 157 degree Fahrenheit.

Test 02 identifies a similar result through observation with a angular rotation of 20 degrees at a temperature change of 41 degree Fahrenheit. 20 divided by 0.48 equals 41.6 degrees Fahrenheit, which is within acceptable tolerance.

The ability to design the specific coil required to activate the bistable system was now feasible. For the examples listed adjacent, it dealt with a material thickness as a constant variable, thus each change in thickness has an independent ratio of temperature to angular rotation. Given this, we know the thickness is 0.032 inches and through reverse engineering the appropriate sized coil, given the coils required movement, can be determine.

So, if 60 degrees of angular rotation is desired with a change in temperature equal to 100 degrees Fahrenheit, then:

$$60 \text{ deg ang} / 100 \text{ deg F} = 0.60 \text{ deg ang} / 1 \text{ deg F}$$

For a 0.035 inch thickness coil at 10.7 inch active length, the ratio yields 0.48 degree angular / 1 degree Fahrenheit, and 0.045 is added to the ratio every 1" of active length addition. Thus, 0.60 - 0.48 = 0.12. And, 0.12 / .045 = 2.66" in addition to 10.66" coil = 13.33" final active length.

The final coil has an active length of 13.36 inches at a thickness of 0.032 inches and a width of 0.500 inches. See equation below for verification:

$$A = \frac{67F (T2 - T1) L}{t}$$

$$A = \frac{67 (215 \times 10^{-7})(100)13.33}{0.032}$$

$$A = 60.00$$

More importantly than knowing the exact active length required for the systems parameters, the developed system of analysis allows one to determine the angular position and force of the coil at any given temperature, ultimately allowing for design optimization to take place between the bistable system and the integrated thermostat coil.

These studies concluded the research for developing the system, and at once, began the synthesis of the work in forms of prototypes and instantiations for the search of a fine tuned operable component.

1.0 ABSTRACT

2.0 INTRODUCTION

3.0 PERFORMANCE CRITERIA

4.0 MATERIAL PROPERTIES

5.0 PRECEDENT STUDIES

6.0 PRELIMINARY EMPIRICAL INVESTIGATIONS

7.0 SYSTEM DEVELOPMENT

8.0 PROTOTYPE SYNTHESIS

9.0 POTENTIAL APPLICATIONS

10.0 APPENDIX

8.0 PROTOTYPE SYNTHESIS

With all the research objectives complete, the beginning of a working prototype was no longer a theory but a tangible objective focused on the specific organization of research elements: bistable mechanism, bistable strip, node design, membrane, actuator, and enclosure. The following pages identify the process and methods that led to the discovery of a passive self-adjusting shade system.

8.1 Prototype 01

The first prototype was a naive, stochastic approach to the system, with minimal examination of variables but yet a consideration for time and testing the of the coils which were purchased.

It was quickly determined that the coils which were being tested worked at high change in temperature, greater than 100 degrees Fahrenheit, however there was no physically explanation for how to obtain a temperature fluctuation of this amount. The average diurnal temperature change was determined to be less than 30 degrees Fahrenheit on an average day, thus, there began a search for increasing the change in temperature without the use of additional systems, i.e., heating units, etc.

It was then realized that the surface which connected the system, glass, could work as a sealed enclosure that takes advantage of heat gain by converting the sun's short wave radiation to long wave radiation, keeping the heat within an enclosure. A "heat box" was then built, utilizing a wood frame to seal two panes of 1/8" glass with dimensions of 26" by 14". A thermometer was placed within the enclosure to read the change in temperature from its starting point to extreme point.

Testing the box alone, it was found that the internal temperature could rise at a difference to ambient temperature at a rate of approximately 2:1, thus the diurnal temperature change of 30 degrees Fahrenheit could be increased to above 60 degrees Fahrenheit within the enclosure.

Prototype 01 was then situated within the enclosure and the box was sealed and placed in the sun. It was assumed that the 60 degrees Fahrenheit change was not high enough to fully deform the strips, but it was hoped that a certain amount of deformation was visible. The movement anticipated never occurred. The system experienced no visual deformation, while the thermometer within the enclosure rose to over 140 degrees Fahrenheit.

It was then determined that while the force output relationship to the system was maximized the change in temperature to achieve the output was not. New coils were then calculated and ordered, and Prototype 02 demonstrates the results.



Figure 8.1, Prototype Model 01 Within Test Box Enclosure

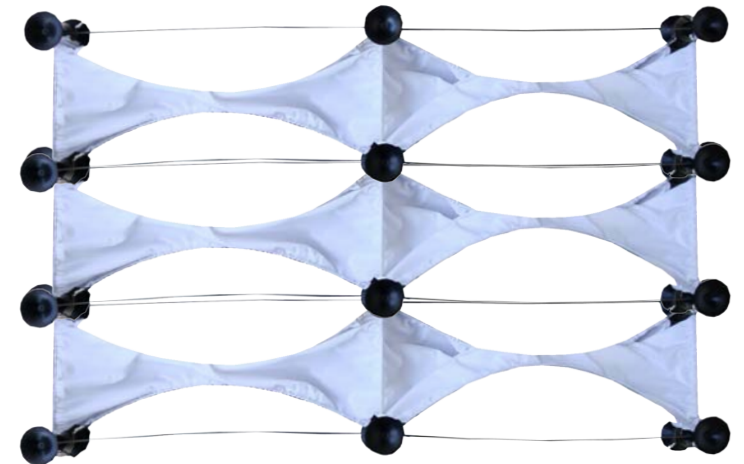


Figure 8.2, Representation of Model Array as Enclosure - Open



Figure 8.3, Representation of Model Array as Enclosure - Open

8.2 Prototype 02

Based on the previous research and tests, it was determined that the appropriate coil to deform the system required a minimum 1.5 angular degree rotation per 1.0 degree Fahrenheit change. This would allow for a 90 degree angular rotation with a change in temperature of 60 degrees Fahrenheit. Both the angular and temperature degrees were over estimated for the system, allowing for adequate design tolerances throughout.

The coil was purchased through the Polymetallurgical Corporation in North Attleboro, Massachusetts, and its final specifications were such:

- 1) ASTM - TM2 / P675R
 - Thickness = 0.018"
 - Width = 0.3125"
 - Active Length = 25"
 - 1.7 Angular Degree Rotation / 1.0 Degrees Fahrenheit

 - Most active and most widely produced thermostat metal.
 - High Expansion Alloy (72% Mn, 18% Cu, 10% Ni) 55% Overall
 - Low Expansion Alloy (36% Ni, Bal. Fe (Invar)) 45% Overall
 - Flexivity 50 to 100 Degrees F. = 215×10^{-7}
 - Flexivity 100 to 300 Degrees F = 209×10^{-7}
 - Modulus of Elasticity = 20×10^6 psi
 - Maximum Temperature = 500 Degrees F

The coil was immediately tested in a stripped down bistable system with the most lightweight strip and a lightweight membrane. This was an attempt to minimize the forces exerted on the system given the material available to produce a working prototype.

The test proved to be successful. As done with Prototype 01, Prototype 02 was placed within a sealed glass enclosure and placed facing cardinal direction east focusing the sun to heat the enclosure in the morning. Figure 8.4 , identifies the results of this test.

The test began in the middle of the morning, 9:30am, with an internal temperature of 80 degrees Fahrenheit and an outside ambient temperature of 70 degrees Fahrenheit. Within, fifteen minutes the actuator had rotated the strip almost 30 angular degrees. The expansion of the coil continued to rotate the strips until the maximum internal temperature of 120 degrees Fahrenheit was reached in the sealed enclosure, while the outside temperature was recorded at 80 degrees Fahrenheit. At this point, the heat stabilized and the coil actuator did as well, reducing the aperture to a sliver, but not yet 100% closed. It wasn't until the sun had passed Solar Noon that the box was now in shade and the internal temperature began to decrease (90 F) and in turn opened the aperture.

The test was repeated several times over the next few mornings and afternoons and yielded similar results. The adjacent photograph documentation was the clearest representation of the test.



9:30 am / Enclosure - 80 F



9:45 am / Enclosure - 95 F



10:00 am / Enclosure - 110 F



10:15 am / Enclosure - 120 F



12:30 pm / Enclosure - 90 F

Figure 8.4, Sequence of Movement - Prototype 02

8.3 Node Development

With a working prototype, it was now essential to develop and fine tune the node detail which attached to the glass enclosure, restricts the coil's inner tab from rotating and accepts the bistable strips from the adjacent offset coil.

The goal for the node was to design a universal joint of parts that could be manipulated and adjustable to conform to the different tolerances of materials within the system, while also being able to lock the parts in its final position. The solution was to design a set of male and female connection pieces that would allow for rotational movement and would lock by driving a set screw.

One large issue in the design of the node was its overall length, the distance from the suction cup connection to the adjacent piece of glass. With the coil width dimension at 0.3125" and set screws at 0.125", the length's minimum dimension was set at just under 2", allowing for appropriate manufacturing and assembly specifications. This dimension later set the size of the glass enclosure.

Given the offset orientation of the coils in the system, one coil was required to be outside while the other was inside (Figure 8.5 & 8.6). This created a set of seven individual pieces, three of which were identical and two sets of two pieces which were specific to an inside or outside nodal condition.

The custom nature of the node, complex configuration of locking pieces and need for quick and precise manufacturing led the structure pieces to be printed with a nylon, ABS material, in a stereolithography machine. A set of nodes could be printed in less than an hour and ready for assembly within two hours. The printability of the connection also allowed for several iterations to take place before the final design was accepted.

Node Material Specifications:

- Suction Cup -
01 All-Vac 138-MS-1 Rubber Suction Cup (See Appendix)
- Thermostat Coil -
02 PMC 675R - Thermostat Coil (See Appendix)
- Stereo-lithography Nylon Printed Parts -
03 Universal Nylon Rod With 1/8" Lock Set Screw & 8-32 Tapped Female Connection for Accepting Part 01
- 04a Nylon Insert - Accepts Coil and locks to Parts 03 & 05a
- 04b Nylon Insert - Accepts Coil and locks to Parts 03 & 05b
- 05a Nylon Spacer - Locks to Part 04a
- 05b Nylon Spacer - 8-32 Tapped Female Connection for Accepting Part 01 / Locks to Part 04b



Figure 8.5, Node_01 - Coil Outside

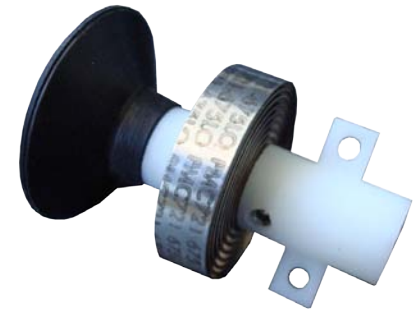


Figure 8.6, Node_02 - Coil Inside



Figure 8.7, Node_01 - Individual Parts



Figure 8.8, Node_01 - Individual Parts

8.4 Aperture Layout Development

In addition to the nodal development for the system, there was the understanding of how the one unit aperture could be arranged to form a surface of apertures. Previously iterations of the bistable system proved difficult to array or tessellate, however, the final aperture unit allowed the connection of various subunits, extending and arraying a surface of apertures.

The analysis of the aperture was first set to determine the number of nodes, coils, strips, etc. for one unit aperture, then two and three to allow an estimate for the total number of parts. One aperture was least efficient as it required two nodes, two coils and two strips to open one aperture. Two apertures however was more efficient in that it required three nodes, three coils, and four strips to open two apertures. The ratio continues for parts beyond two apertures saving one coil and one node detail for the total sum of apertures.

The unit and subunit investigation led to a layout of the units to form a surface of apertures. Figure 8.10, identifies a simple aligned array system which yields an openness factor of 57%. By nesting the linear units through a midpoint offset, the openness factor could be further increased 10% under a similar area (Figure 8.11)

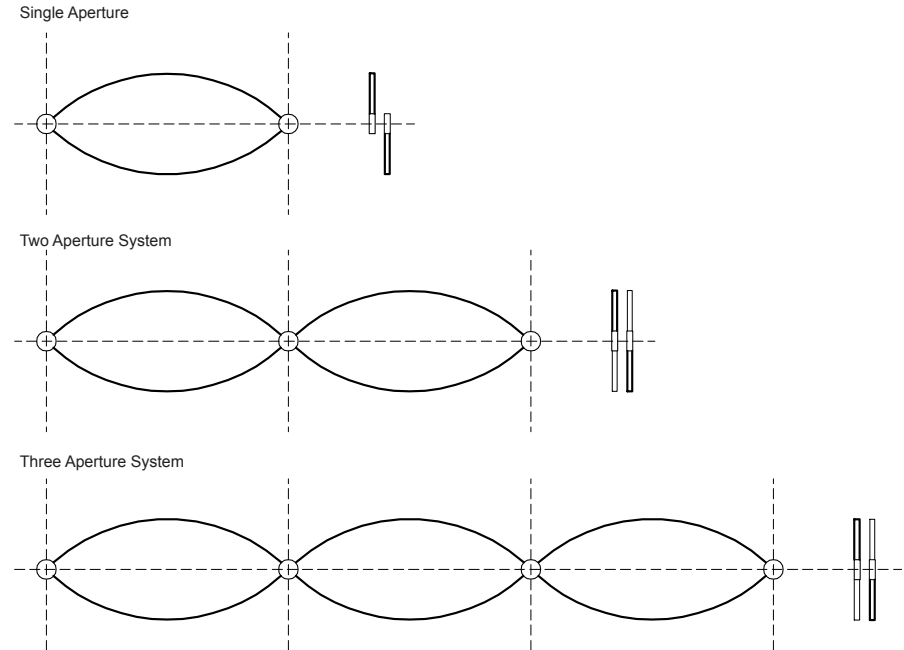


Figure 8.9, Analysis of Aperture System Unit and Subunits - Elevation and Section

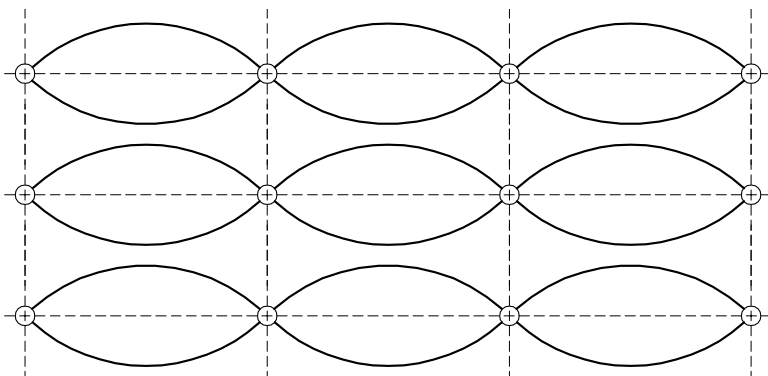


Figure 8.10, Aligned Array / Openness Factor = 57%

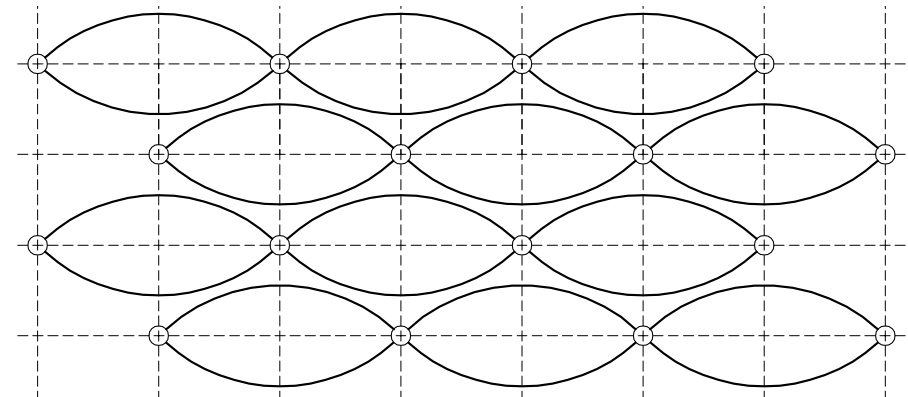


Figure 8.11, Nested Array / Openness Factor = 65%

8.5 Membrane Development

The attachment of the membrane to the bistable system posed a delicate and precise manufacturing and assembly tolerance as it was designed to be non-obtrusive to the forces within the system but yet provide the resultant surface to shade the interior.

Several iterations, cut patterns and seam designs were practiced and investigated before the assembly of the next prototype. Due to the offset design of the system, the membranes sheets had to be cut individual to each linear layer of apertures and then sewed together at the ends to form a continuous surface. Also, due to the minimal force relationship between the system and membrane, very thin and lightweight synthetic fabrics, such as polyester, were used for the models.

Figure 8.12, shows the initial two cut patterns for the specific prototype and the final assembly within the enclosure. The nodes were left open along the membrane surface to allow for light to contact the actuating coils directly. The edges of the membrane within the enclosure were restricted by 1/16" stainless steel tensile cables connected to the frame. A French seam was used to sew the edges of the fabric and lopped as necessary to accept and connect to the spring steel strips and tensile cables.

The color and finish of the membrane was considered an integral property throughout the system as it directly relates to the resultant light and heat characteristics. Dark fabrics were utilized in an attempt to increase heat gain in the enclosure while providing less light reflection and in turn light fabrics were modeled to reflect and redirect light while decreasing heat gain. Neutral colors were also investigated as a median fabric which could take advantage of both light and heat properties critical to the system.

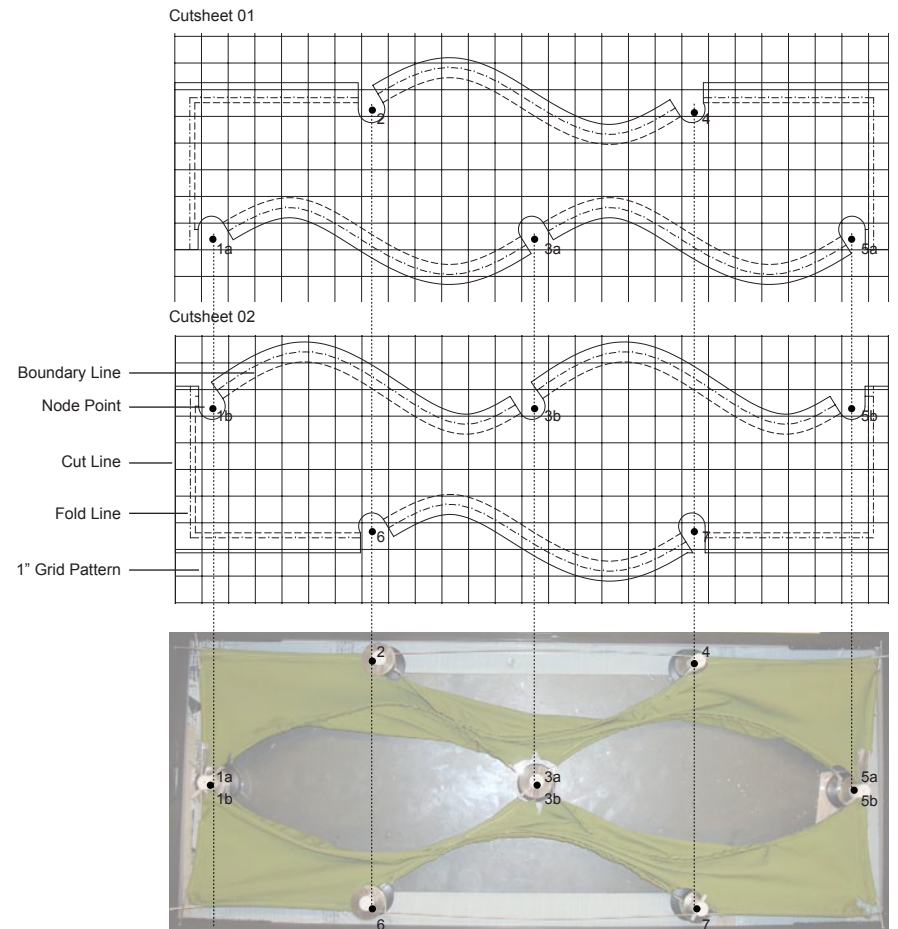


Figure 8.12, Membrane Cut Sheets and Integration to Enclosure

8.6 Prototype 03

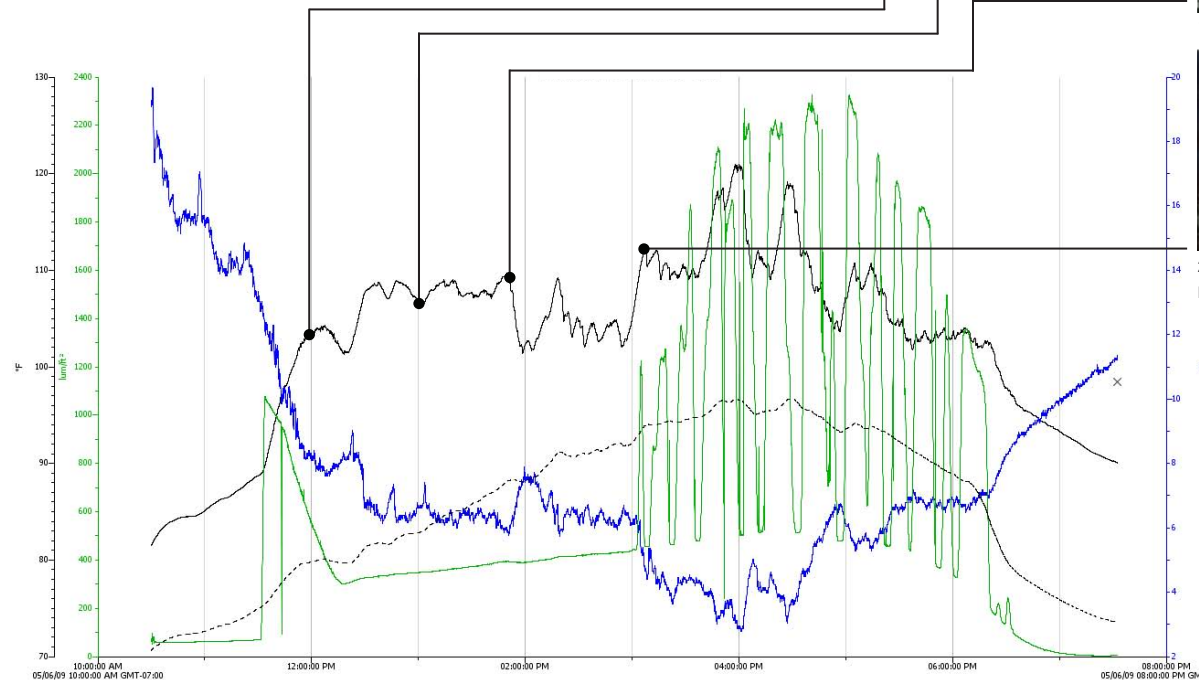
Prototype 03 was the result of the development process of the nodes, layout and membrane, utilizing a semi-nested design within the original enclosure box. Two apertures segmented the center-line of the box with two half apertures located above and below, creating an openness factor of 60%.

The enclosure box was updated with a more insulated and sealed edge condition and also allowed for a multi-functional HOBO sensor to record interior temperature (F), exterior temperature (F), relative humidity (%), and light intensity (lum/ft²).

A variety of tests were conducted using the set up to measure, record and photograph the movement of the bistable system. The adjacent figures, 8.13 & Graph 8.1, represent the average data for the test.

In general, the system proved to be passively functional with an average time of just over one hour in direct sunlight exposure at temperatures between 80 and 90 degrees Fahrenheit to completely close and provide shade. The bi-stability of the system took over as the enclosures heat exposure seized and immediately opened back up and repeated daily.

The graph below a recorded an entire day with the enclosure placed in a cardinal west direction. Please notice the change in temperature between the interior and exterior (solid versus dashed black lines).



Graph 8.1, Environmental Data for Testing of Prototype 03 - West Facade / All Day



12:00pm / Enclosure 85 F



1:00pm / Enclosure 95 F



1:30pm / Enclosure 110 F



2:15pm / Enclosure 120 F

Figure 8.13, Sequence of Movement - Prototype 03

8.7 Final Prototype

The completion of the research development stages led to the design of a final prototype, the first instance, of a finished enclosure panel with the self regulating shading skin efficiently incorporated within, possessing the capability of being installed in a building facade.

The glass enclosure was designed with overall dimensions of 2'-0" width by 4'-0" length and an overall thickness just over 2-1/2" (Figure 8.14). A nested surface of twelve bistable mechanism was organized onto the surface with equal distance to the edges. Sixteen thermostat coils connected to the sixteen related nodes (eight inside coils, eight outside coils) with twenty-four spring steel strips holding a polyester membrane. The fabric membrane was further supported to the glass enclosure by utilizing four, 1/16" pre-tensioned stainless steel stranded cables at the edges.

In more detail, the glass enclosure was designed to be assembled in an organized process, allowing the installation of the shade mechanism to occur onto a separate piece of glass before finally being situated within the box enclosure and hermetically sealed. The final design incorporated a three-pane glass system of 1/8" tempered clear glass, with two air spaces, one at 2" thickness to accept the shade mechanism, and the second at 1/4" thickness to further reduce heat gain (Figure 8.15).

The enclosure was designed to maximize the efficiency of the system, reducing additional parts and members and focusing on the function of the system as a productive shading enclosure.

Glaz-Tech Industries, a glass distributor in Tucson, Arizona generously donated all glass materials and services for the final prototype.

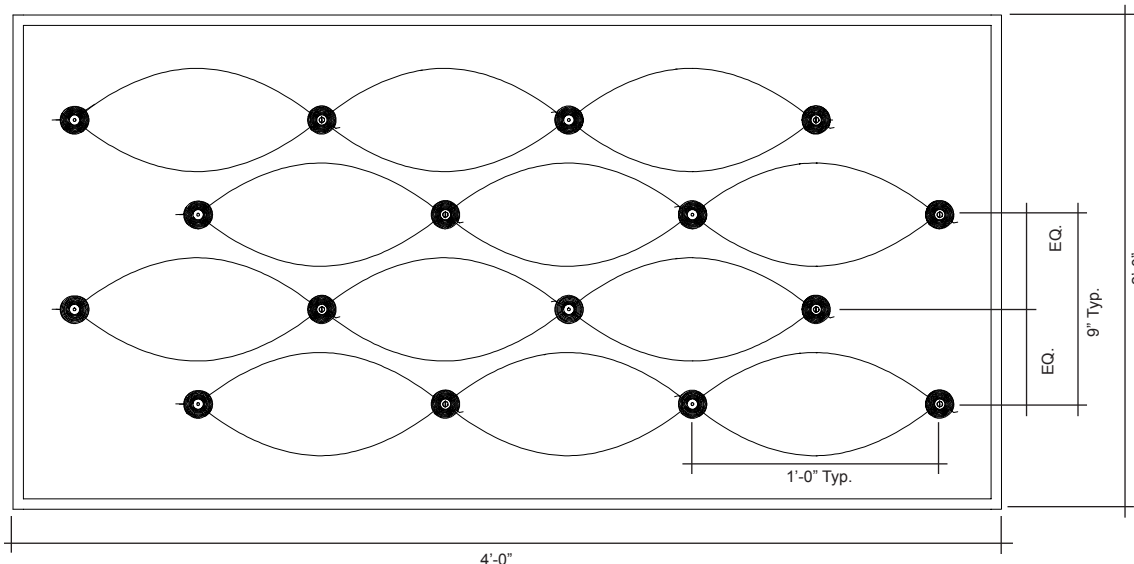


Figure 8.14, Front Elevation - Nested Array / Openness Factor = 42%

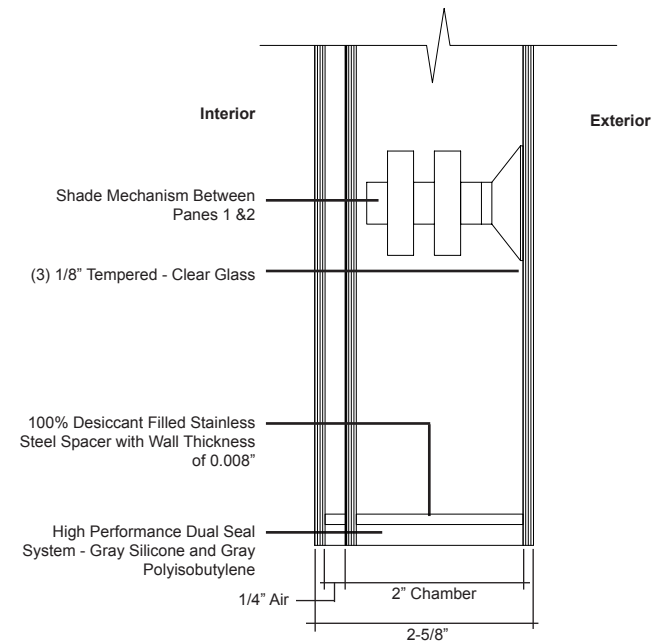


Figure 8.15, Section - Sill Detail

The resultant physical model represents the largest assembly of the internal shade mechanism to date. The adjacent photographs document the overall movement of the enclosure from an open condition to close condition, (Figure 8.16 & 8.17) and the details associated with the enclosure, nodes and membrane.

The model was tested over a two day period to record the movement of the shade device for both an East and West facade condition. In general, the model was effective in providing shade as the sun was exposed to its surface, however, at the end of the test, the suction cup seal had severely deteriorated and a few of the bistable units began to slip. The slippage of the units caused a disturbance in the force propagation throughout the system and limited its overall ability to close 100%. The problem was analyzed after the test and it was determined that during the assembly of the enclosure at the glass distributor, a minimal amount of dust particles had accumulated on the inside glass surface, decreasing the bond strength of the suction cup. To alleviate this problem in further designs, an ultra-violet adhesive product is to be specified and coated onto the suction cup surface to permanently seal to the glass.

It was also determined that due to the change of the overall system from an initially exterior attached unit condition to an integral interior unit, suction cup connections were no longer an efficient connection. The three-dimensional printed plastic node could then be simply bonded to the glass using an identical ultra-violet adhesive. This move in the design would also allow for the overall thickness of the enclosure to be reduced, lowering the solar heat gain coefficient even more as the air gap between the glass panes decreased.

The final prototype was a necessary step in developing the design and construction of the entire system, identifying the advantages and disadvantages of a possible future marketable component for further analysis. The prototype was analyzed in terms of the solar, heat, air and shade properties and the results are represented in the following pages.



Figure 8.16, West Elevation / Exterior - 2:30pm



Figure 8.17, West Elevation / Interior - 12:00pm



Figure 8.18, Node - 01 Outside Coil

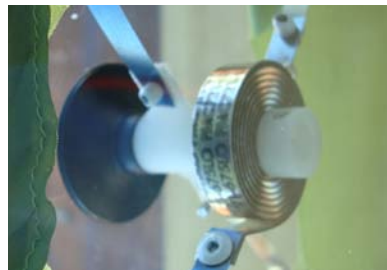


Figure 8.19, Node - 02 Inside Coil



Figure 8.20, All-Vac 138 - MS Suction Cup



Figure 8.21, Membrane Connection

8.8 Light Reflection Properties

The layout of the membrane within the system produced two sectional surface conditions for reflecting sunlight when closed, ground facing and sky facing (Figure 8.22 & 8.23).

The ground facing orientation of the fabric produced the best opportunity for reflecting diffused light through the closed surface by utilizing the lower side of the surface to reflect light down and then in to the interior. The upper end of this surface mainly reflected all light back out to the exterior.

The sky facing orientation reflects almost all light back to the exterior, while a small amount of light near the horizon line is capable of reflecting upwards to the inside.

Further development of these sectional variables would be required to justify when, where and why light may or may not want to be reflected through the surface, however, for now, this study was an attempt to understand the visual phenomena experienced by the surface from the exterior and interior in terms of light reflection and glare.

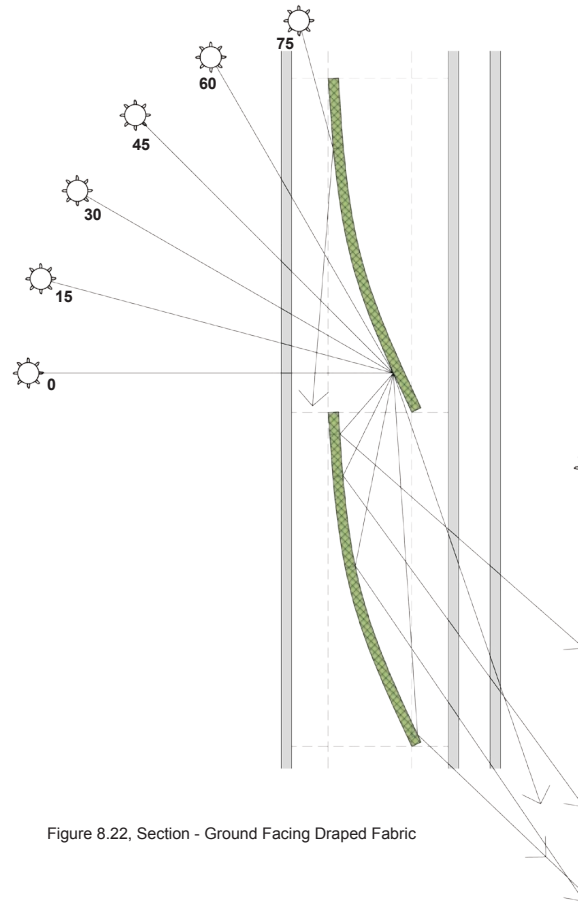


Figure 8.22, Section - Ground Facing Draped Fabric

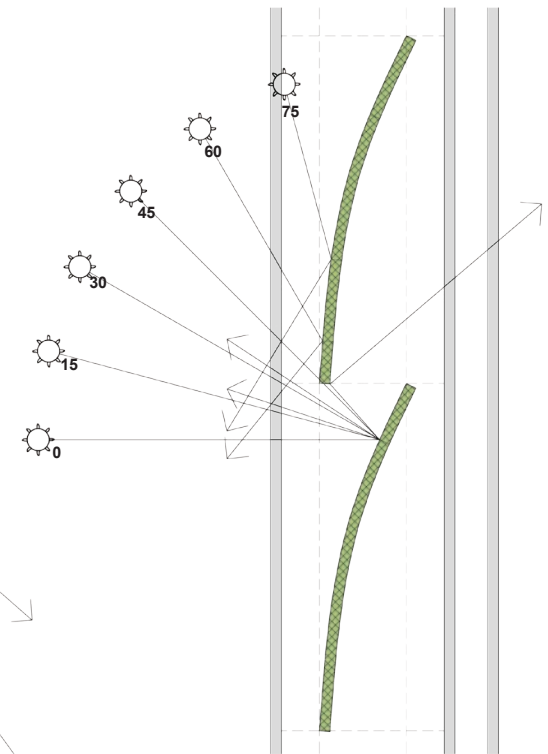


Figure 8.23, Section - Sky Facing Draped Fabric

8.9 Thermal Heat Properties

Utilizing a computational thermal analysis program, Square One Research - Ecotect, the closed surface of one of the units was analyzed to determine the levels of heat which the surface would be exposed to throughout the year. The importance of the analysis tool was to identify the area of surface subject to the highest levels of exposure, while also identify areas of the surface which provide self-shading performance.

It was concluded that through the overlapping nature of the membrane, areas of shade and shadow were produced along the seam line of the strip as well as around the open node as the surface was pulled taut, connecting to the offset adjacent surface (Figure 8.25). Throughout the seasons, the exposure was consistent with the movement of the sun, decreasing in value as the sunlight had less time exposed on the surface.

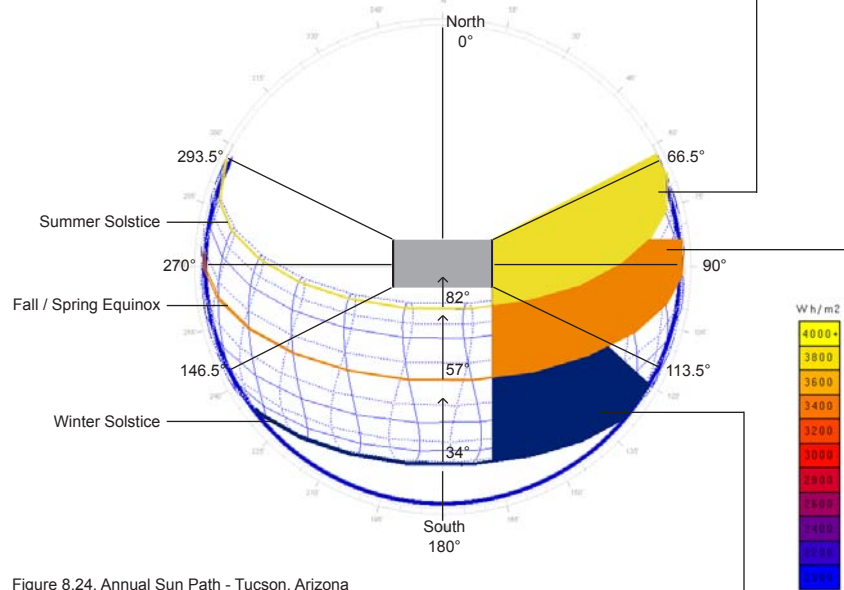


Figure 8.24, Annual Sun Path - Tucson, Arizona

This concludes the final prototype applications and research. The following section will identify the potential applications for the self-adjusting shade system in various forms, manipulating the scale, placement and performance functions to theorize on the optimal product.

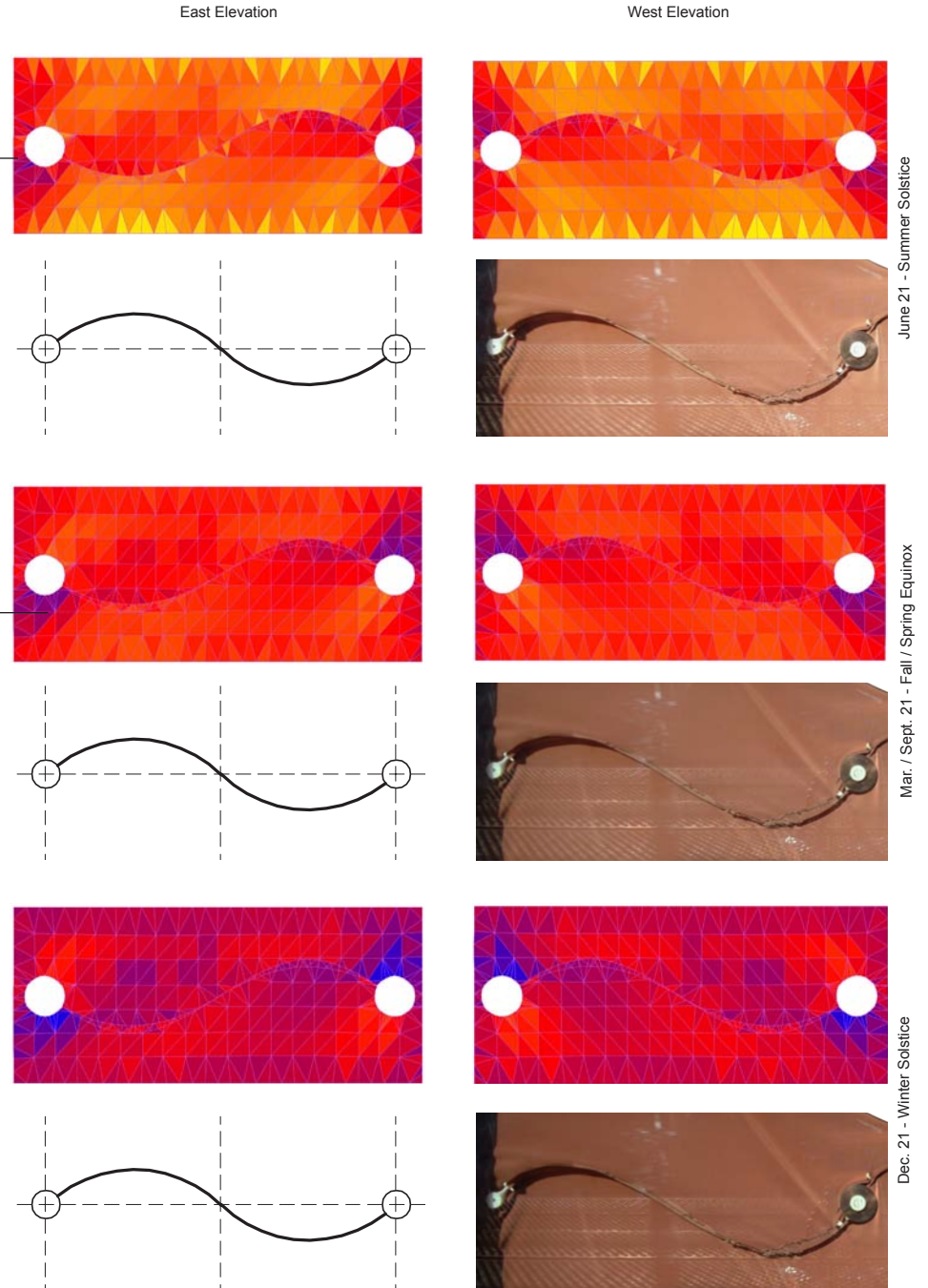


Figure 8.25, Incident Solar Radiation Exposure Related Diagrams / Photos

1.0 ABSTRACT

2.0 INTRODUCTION

3.0 PERFORMANCE CRITERIA

4.0 MATERIAL PROPERTIES

5.0 PRECEDENT STUDIES

6.0 PRELIMINARY EMPIRICAL INVESTIGATIONS

7.0 SYSTEM DEVELOPMENT

8.0 PROTOTYPE SYNTHESIS

9.0 POTENTIAL APPLICATIONS

10.0 APPENDIX

9.0 POTENTIAL APPLICATIONS

The potential application for the developed shading mechanism is focused on optimizing the function of the system while anticipating future technologies and applications. The first potential application lies in the 2009 U.S. Department of Energy Solar Decathlon Competition with The University of Arizona's School of Architecture's, application, entitled Seed POD. An ideal frame for the system was then theorized with calculated U-values and R-values and finally the scale and function is proposed for future industries.

9.1 University of Arizona, Solar Decathlon - Seed POD

The Seed POD was developed by the University of Arizona's School of Architecture for the entry into the 2009 competition in Washington D.C. In January of 2009, Professor Christopher Domin, principal for the team, asked for my participation in aiding in the research and development of the skin. From this point forward, a consultant relationship was formed, and through the iterations of the thesis work, the design and application of the self-adjusting shade system was clarified. Figure 9.1, identifies a sketch of the East facade, similar to the West facade, and the zones for applying a skin. Infill and framed areas were located for the facades based on known design strategies and the adjacent diagrams and sections show the focus of the system for the in-fill corner region. The placement was chosen for its visual and physical connection to the user, both from the inside and outside.

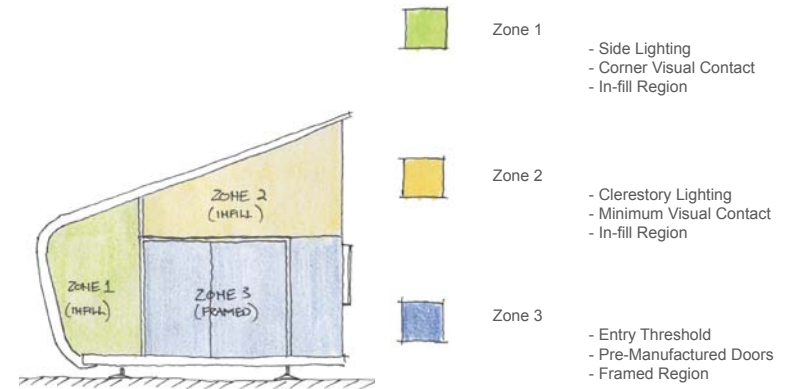


Figure 9.1, Placement Diagram

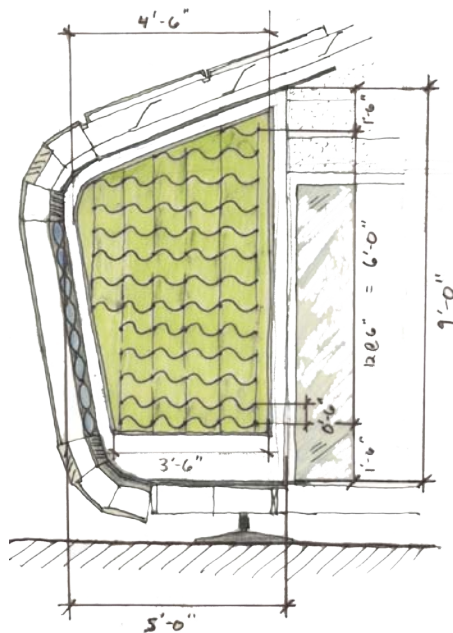


Figure 9.2, West Facade - Section / Closed

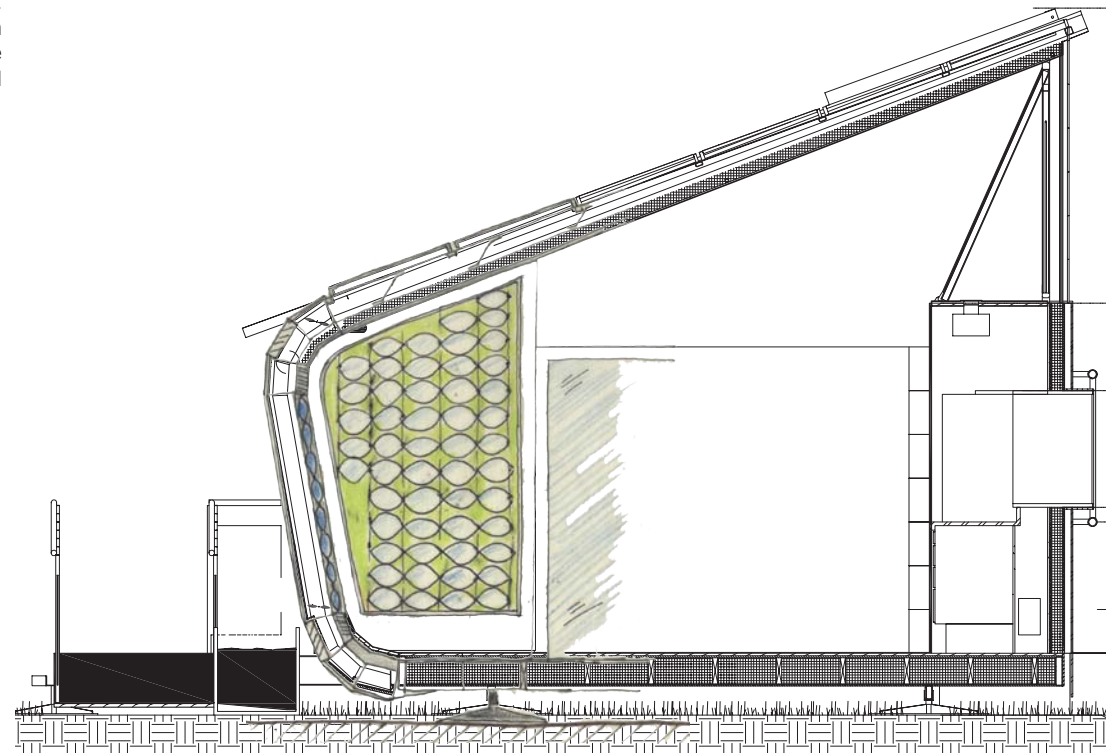


Figure 9.3, West Facade - Section / Open

After sequential iterations with both the design of the Seed POD building and the thesis work, it was realized that the most efficient application for the shade enclosure would be in the form of a rectangular glass enclosure on the East facade. The final construction documents for the Seed POD located a 4'-0" by 5'-0" opening on the East facade, within which the first application of the shade enclosure will be framed.

To accommodate to the thickness and framing of the proposed facade, a redesign of the enclosure and mechanism is currently in progress, reducing the overall thickness of the system by eliminating the suction cups, while optimizing shade cloth and node components. A simple wood or steel frame will secure the glass enclosure to the structure with all typical sealants and edges to protect against environmental conditions.

The ideal frame for the enclosure is identified next, and includes strategies for moving air through the chamber for both heating and cooling.

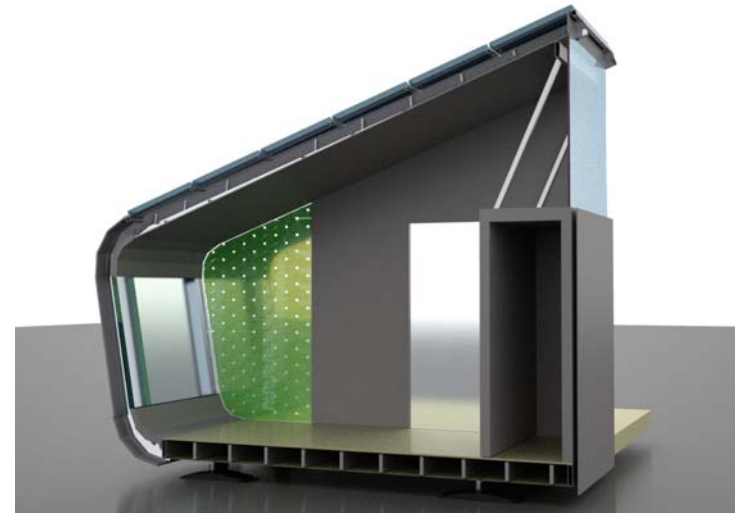


Figure 9.4, Rendering, West Facade - Closed

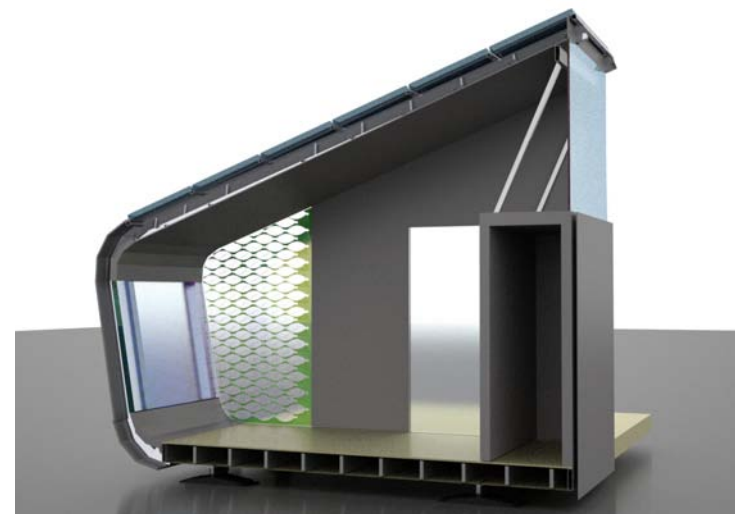


Figure 9.5, Rendering, West Facade - Open

9.2 Ideal Frame

With any interior to exterior component threshold, the seal and function of a frame system is as important as the function of the enclosure itself. With advancements in frame manufacturing, custom aluminum frames with vents can be designed for glass systems to take advantage of air movement through convective forces and infiltration.

For this study, the simple diagrams in Figure 9.6, identify the potential which a single frame with vents on the interior, exterior and within the shade mechanism chamber can be design for heating and cooling conditions.

First identified is the exhaust design. Given that the heat gain from the sun is inevitable and required to activate the shade mechanism, this design is intended for a post exposed condition, afternoon for an East facade or evening for a West facade, exhausting the heat out of the chamber and in turn opening the shade mechanism faster. The movement of the air in this design will reduce the thermal exchange on the facade, increasing its insulation value and overall performance.

The second design cycles the movement of air through the frame, from the bottom to the top, utilizing convection and heat gain from an exposed condition to heat the interior. This design is thus intended for a winter or heating day design and cycles warmer air passively and efficiently. Once again, the insulation value of the enclosure will be optimized with its function.

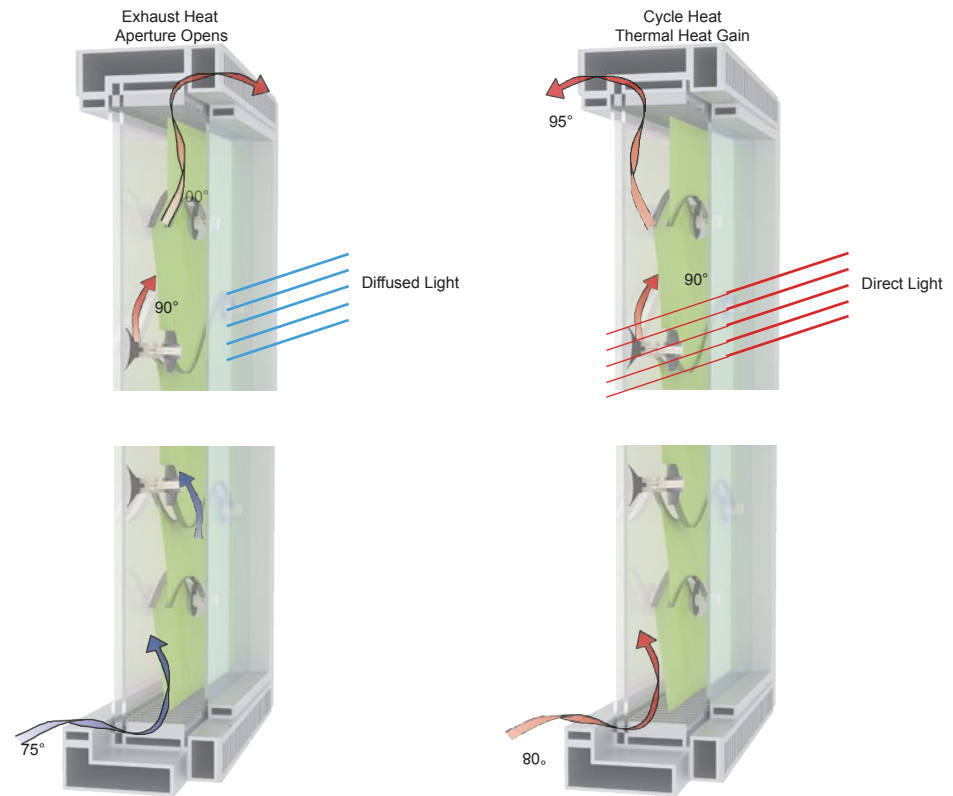


Figure 9.6 Ideal Frames / Exhaust Design (Left) and Cycle Design (Right)

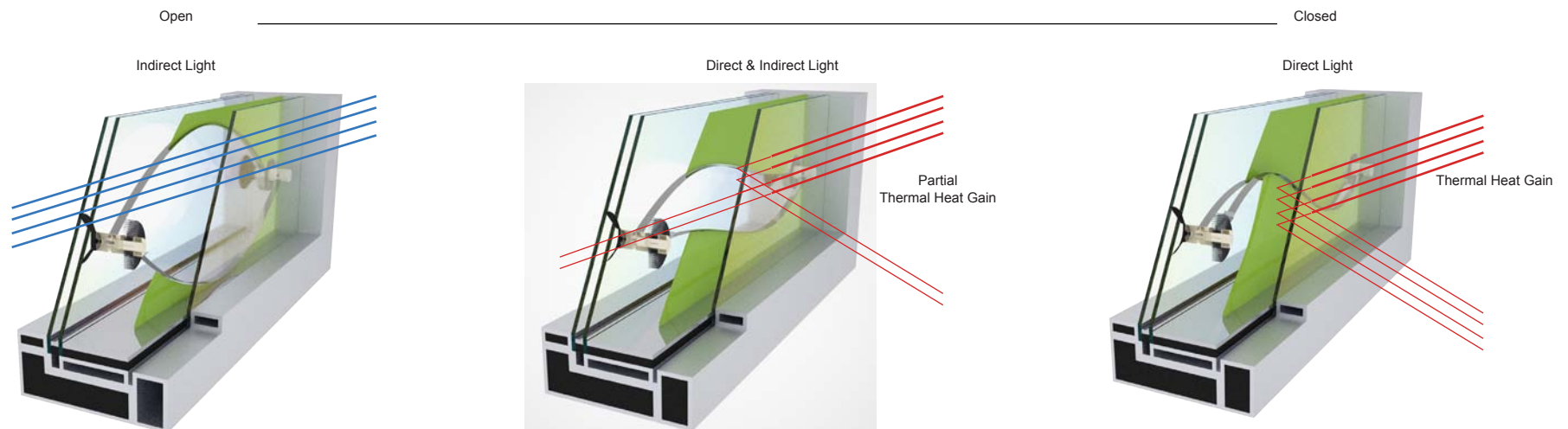


Figure 9.7, Open to Closed Light Conditions on Enclosure

9.3 SHGC / U - Value / R-Value Precedents and Properties

In response to the previous ideal frame application, the known performance values for the resistance (R-value) and conduction (U-value) of heat transfer was researched and analyzed for existing systems to estimate the overall value of the design. To preface, the R-value is the reciprocal of the U-value, and a low U-value identifies an enclosure's ability to effectively mitigate the heat transfer coefficient.

For example, in Table 9.1, a double glass window with a 1/4" air gap yields a U-value of 0.59 and an R-value of 1.69, and if we reference Table 9.2, and add a venetian blind between the two glass panes, we effectively reduce the U-value to 0.28 (a 0.31 difference) and in turn the R-value increases to 3.57 (a difference of 1.88). With the blinds between the glass, the amount of solar radiation which reaches the interior glass pane is reduced as the blinds reflect the light and radiation outwards, decreasing the heat transfer.

The venetian blinds between the glass enclosure system most accurately represents the potential data for comparison to the self-adjusting shade system. Both utilize materials and mechanisms which reflect and reduce heat gain, the only difference being no input is required to adjust the latter.

In addition to heat transfer values, a Solar Heat Gain Coefficient (SHGC) value is established for various enclosure systems identifying the ability to both shade and reduce heat transfer effectively. The lower the SHGC value the more effective the enclosure system is at reducing the transfer of heat. For the previous example, Table 9.2, shows the venetian blind system to yield a SHGC between 0.33 and 0.36, dependent upon the color of the blinds, light to medium. Appendix 10.3 further identifies the strategies for lowering the SHGC between interior, exterior and in-between enclosure design strategies.

It is thus proposed that with a framed and installed triple pane glass enclosure, including the self-adjusting shade mechanism between the two outermost panes, the resultant performance values are estimated to be such:

- R-Value = 4.00 - 5.00
- U-Value = 0.20 - 0.25
- SHGC = 0.25 - 0.30

The variations being a result of membrane color, air gap distance and triple pane glass enclosure design.

Table 9.1, Typical Window R- Values

Window Type	U-Value	R-Value
Single Glass	1.10	0.91
Double Glass - 3/16" Air	0.62	1.61
- 1/4" Air	0.59	1.69
- 1/2" Air	0.49	2.04
- 3/4" Air	0.42	2.38
- 1/2" Air w/ Low E	0.32	3.13
Triple Glass - 1/4" Air	0.39	2.56
- 1/2" Air	0.31	3.23
Air Spaces - 1/2" - 4"	1.00	1.00

<http://www.coloradoenergy.org/procorner/stuff/r-values.htm>

Figure 9.2, Shading Coefficient for Double Glazing with Internal and Between Glass Shading

Construction Type	Solar Heat Gain Coefficient	U-Value	R-Value
1/8" Clear Glass			
Venetian Blinds Between (light / medium)	0.33 / 0.36	0.28	3.57
Venetian Blinds Inside (light / medium)	0.58 / 0.62		
Louvered Sun Screen Between	0.42	0.30	3.33
Louvered Mirrors Between	0.34 - 0.52	0.25	4.00
Opaque Roller Shade Inside (white / translucent / dark)	0.35 / 0.40 / 0.71		
Draperies Inside			
- open weave / dark color	0.62		
- semi-open weave / medium color	0.52		
- closed weave / light color	0.42		

Sun, Wind & Light, Architectural Design Strategies, 2nd Ed.

9.4 Other Applications

The design and execution of the final prototype was performed at a scale which related to the human body, with adequate sizing of materials and parts, in relationship to mechanical properties, for the assembly and testing of the performance characteristics with ease. Now that the system holds validity as a functional mechanism, branches of other applications have grown out of the prototypes and are differentiated from the original by scale, function and performance.

First, it must be said that the sun is not the only source capable of moving the system from an open to close position. The key to the movement is the thermostat actuator, which when heated by any external means: exhaust, hot air or gas, heated appliances, fire, etc; the coil will produce a specific amount of rotation and force dependent on the maximum change in temperature and coil specifications.

Given this, alternate systems can be designed to comply with thermal performance loads for various products which radiate heat. Products such as: electrical devices, mechanical units, heat pumps and pipes, etc; all radiate heat through use, and a secondary system involving the thermostat coils and capacitors could store and release the thermal energy gained during use and later convert the energy for reducing electrical loads, heat loads or moving a related system for secondary or tertiary applications.

The coils could also be designed in conjunction with heat conductive materials which could transfer heat directly to the coil and move a capacitor system to shade (or not shade), not only glass enclosures, but additional facade elements as well, including but not limited to: metal sidings, rain-screens, stucco, wood panels, plastics, concrete and masonry units. Each application would individually involve calculated material specifications for transferring heat to the coil, and the coils resultant size, length, thickness and width would be the result of what is intended to move and how much it shall move.

Lightweight elements are critical for these design situations as the force to actuate, and actuator force, is limited to the coil dimensions and change in temperature, but, with new manufacturing technologies, nano-scaled and mega-scaled elements are possible of being arranged for applications requiring extremely low or high loads.

With these known strategies, an alternate hypothesis is formulated.

If the actuators (coils) ultimate force and maximum rotation is restricted by the overall change in temperature and actuator dimension properties, then by miniaturization of the actuator system, the change in temperature would be reduced as will the force and a micro-surface with a thickness no greater than the membrane could act as an adjustable shade skin.

The future goal then is to develop a self adjusting skin, in its purest sense, which changes opacity in relationship to solar exposure. Further air ventilation and thermal properties can then be propositioned and a new system of materials would be created.

It must also be said that extensive research of existing technologies and products for adjusting to heat and solar exposure was conducted for comparison. Electrochromic Windows, Liquid Crystal technologies, Thermo-chromic, Thermotropic and Photochromic materials and products were researched overall.

In general, these products involve advanced chemical relationships of light and heat compliant cells to provide adjustment, and each is being further developed in numerous material science programs around the world. The thin-film technology has systematically increased the use of these materials in building products, with advantageous performance characteristics but detrimental price and warranty protection.

The developed system in this report differentiates itself from the above products through its mechanical material relationships for actuation, versus the chemical actuation and with this, the price of the entire system is reduced in comparison, but the maintenance and performance longevity is in question.

For example, the final prototype was valued at costing \$20.00 per square foot, including all glass, frame, shade products as well as manufacturing and assembly costs. A similar performance product, by SAGEGlass®, utilizes electrochromic films within windows at a price of \$50.00 per square feet, for large area buildings, and a price of \$100.00 per square foot for a prototype size window, not including assembly costs. As the quantity of manufacturing and assembly is improved over time, the cost will most likely diminish, however, the true use of this research and future research is to look at additional material and systems that can compete with existing industries and even improve the future of passive actuating systems.

Final thoughts on this work and personal beliefs are presented next and conclude this report.

9.5 Final Thoughts

Building systems for architecture and engineering industries have already begun to show, and will inevitably involve globally, a delicate correlation between designing against the depleting environment and maintaining a homeostatic state demanded by humans. Exponential population growth, finite fossil fuel depletion, limited agriculture subsistence, and the globalization of all products and industries within the last century has exhausted the Earth of its own ability to achieve equilibrium without dramatic change. These effects are non-reversible, yet, are able to be edited with appropriate reconsideration, aimed towards a homeostatic goal.

The goal then must be a holistic design system formulated to accommodate reducing, reusing, recycling and regulating; The four R's, as written by William McDonough in "Cradle to Cradle".

For this thesis, the work and research falls primarily into the method of reducing design elements and regulating the functional performance of an enclosure to achieve a state of homeostasis between the sun and a building. The ability to recycle and reuse the system over time was a secondary thought of the work, but each hold valid arguments for equilibrium if particular materials and assemblies of the system are to be reconsidered. For example, based on the systems assembly of individual parts: spring steel strips, thermostat coils, membrane, glass, etc.; If broken or out-lasted beyond repair, each element only contains its own embodied energy and thus, each is capable of being recycled or reused appropriately.

The four R's are often only the beginning, or afterthought of most design elements and products however, where as sciences such as: Biomimicry, Multi-scale Regenerative Technologies, Bio-Instrumentation, and Robotics and Artificial Intelligence; are forced to adhere to inherent organic growth and development strategies, as simple as an amoebae, to programmatically grow new functional design elements.

If the past shall teach us about the present and in turn promote theories for the future then, the transfer of technology between modern sciences, to existing and original design industries, holds the key to regulating the Earth's environment with humans, much like the theory of relativity was based on classical mechanics, but once refined promoted new discoveries for understanding optics, astronomy, mechanics, color, time and more.

I promote then to everyone who reads this that we always look to the future as well as to the pasts of both technology and the environment, in terms of one's personal position, and the position of others, to create new ideas and new assemblies aimed towards a greater good.

"If everyone did it, would it work?"

Bill Richardson - An Influential High School Teacher

1.0 ABSTRACT

2.0 INTRODUCTION

3.0 PERFORMANCE CRITERIA

4.0 MATERIAL PROPERTIES

5.0 PRECEDENT STUDIES

6.0 PRELIMINARY EMPIRICAL INVESTIGATIONS

7.0 SYSTEM DEVELOPMENT

8.0 PROTOTYPE SYNTHESIS

9.0 POTENTIAL APPLICATIONS

10.0 APPENDIX

10.0 APPENDIX

10.1 Location - Tucson

Tucson, Arizona, USA

University of Arizona
School of Architecture

Hot and Arid Region
Elevation: 2.438' Above Sea Level
Lat./Long.: 32°11' N / 110°55' W

Tucson, Arizona was chosen as the location point due to its location in a hot and arid region within the Horse Latitudes (30° +/- from the equator) with a high percentage of clear sunny days, large diurnal temperature swings and high solar radiation exposure.

The following tables and charts quantify and analyze recorded weather data for Tucson in terms of solar radiation and temperature. Of interest in these diagrams are the temperature differential measurements, directional movement of the sun / heat and the interrelated phenomenon's which cause the temperature to fluctuate, i.e. rain, humidity, wind, night, day, etc.

Tucson Weather History									
	Temp. (F)	Relative Humidity (Percentage)		Extreme Temp. (Days Per Month)		Rain (Inches)	Cloudiness (Days Per Month)		
		A.M.	P.M.	Below 32	Above 90		Average	Clear	Partly Cloudy
January	51.3	62%	32%	6	0	0.9	14	7	10
February	54.4	59%	27%	4	0	0.7	13	7	9
March	58.7	53%	23%	1	0	0.7	15	7	9
April	65.8	42%	16%	0	5	0.3	17	7	6
May	74.0	35%	13%	0	18	0.2	20	7	4
June	83.8	32%	13%	0	28	0.2	21	6	3
July	86.6	56%	28%	0	29	2.4	10	12	9
August	84.5	65%	33%	0	29	2.2	12	12	7
September	80.4	56%	27%	0	24	1.7	19	7	4
October	70.4	52%	25%	0	9	1.1	20	6	5
November	59.2	54%	28%	1	0	0.7	18	6	6
December	52.0	61%	34%	5	0	1.1	15	6	10
Annual	68.4	52%	25%	17	143	12.0	193	91	81

Chart 10.1, Source: Cityrating.com

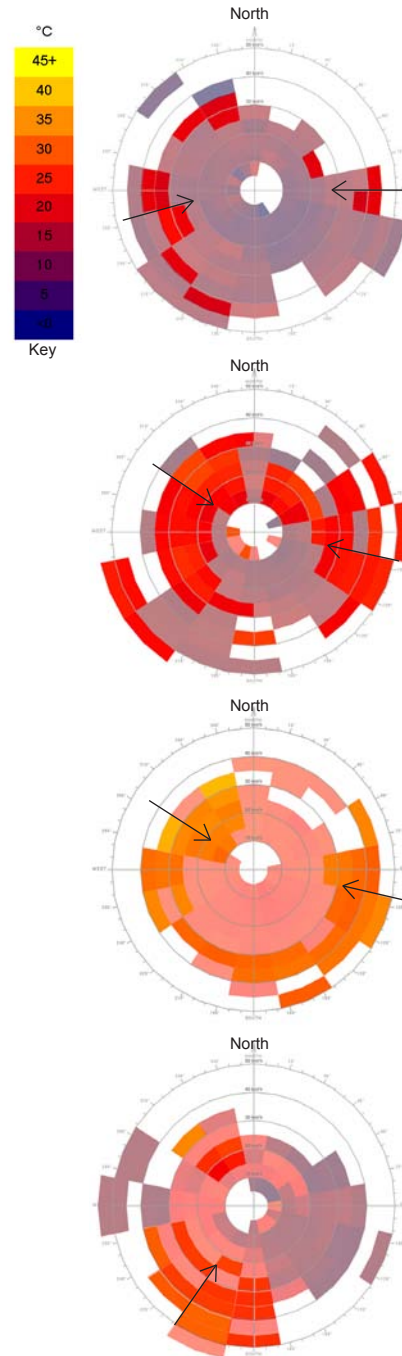


Figure 10.1, Maximum Wind Temperature, Velocity & Direction (Ecotect)

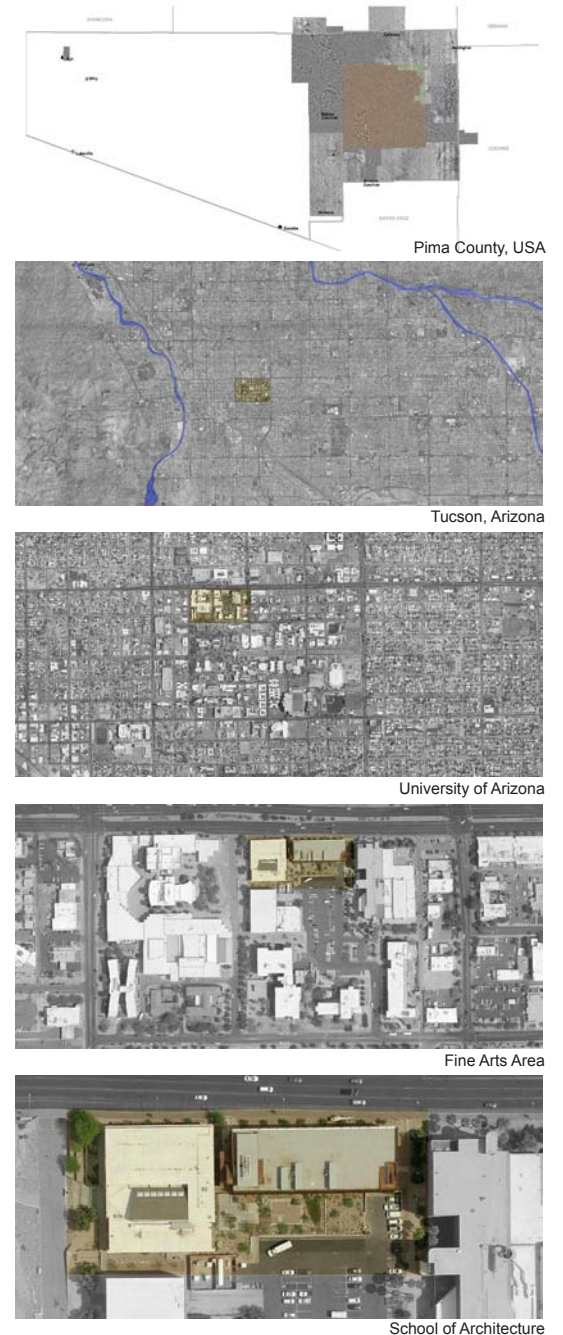


Figure 10.2, Aerial Map - Tucson, Arizona

10.1.1 Temperature Differential

The adjacent charts were derived using the program Ecotect. The weather data includes a summary of the year 2008 recorded information from the National Weather Service.

The charts have been analyzed to display the maximum, minimum and mean temperature differential for the winter, spring, summer and fall seasons. The data was separated into seasons for identification of time based on the declination angle of earth and its location to the sun, which directly affects the weather shifts of wind, temperature and humidity in desert regions.

Winter:
 Maximum = 24°C = 43.2°F
 Minimum = 5°C = 9.0°F
 Average = 15°C = 27.0°F

Spring:
 Maximum = 20°C = 36.0°F
 Minimum = 5°C = 9.0°F
 Average = 14°C = 24.2°F

Summer:
 Maximum = 23°C = 43.2°F
 Minimum = 5°C = 9.0°F
 Average = 13°C = 23.4°F

Fall:
 Maximum = 20°C = 36.0°F
 Minimum = 7°C = 12.6°F
 Average = 13°C = 23.4°F

Averages:
Maximum = 21°C = 37.8°F
Minimum = 5.5°C = 10.0°F
Mean = 14°C = 24.2°F

The next page identifies and analyzes the average solar radiation exposure for the first day of each season and the average radiation cycle for the entire season.

The time period of solar exposure for the East and West facades is depicted in relationship to maximum achieved radiation levels. The seasonal radiation charts identify the diurnal fluctuation and the consistent levels of radiation exposure throughout the year.

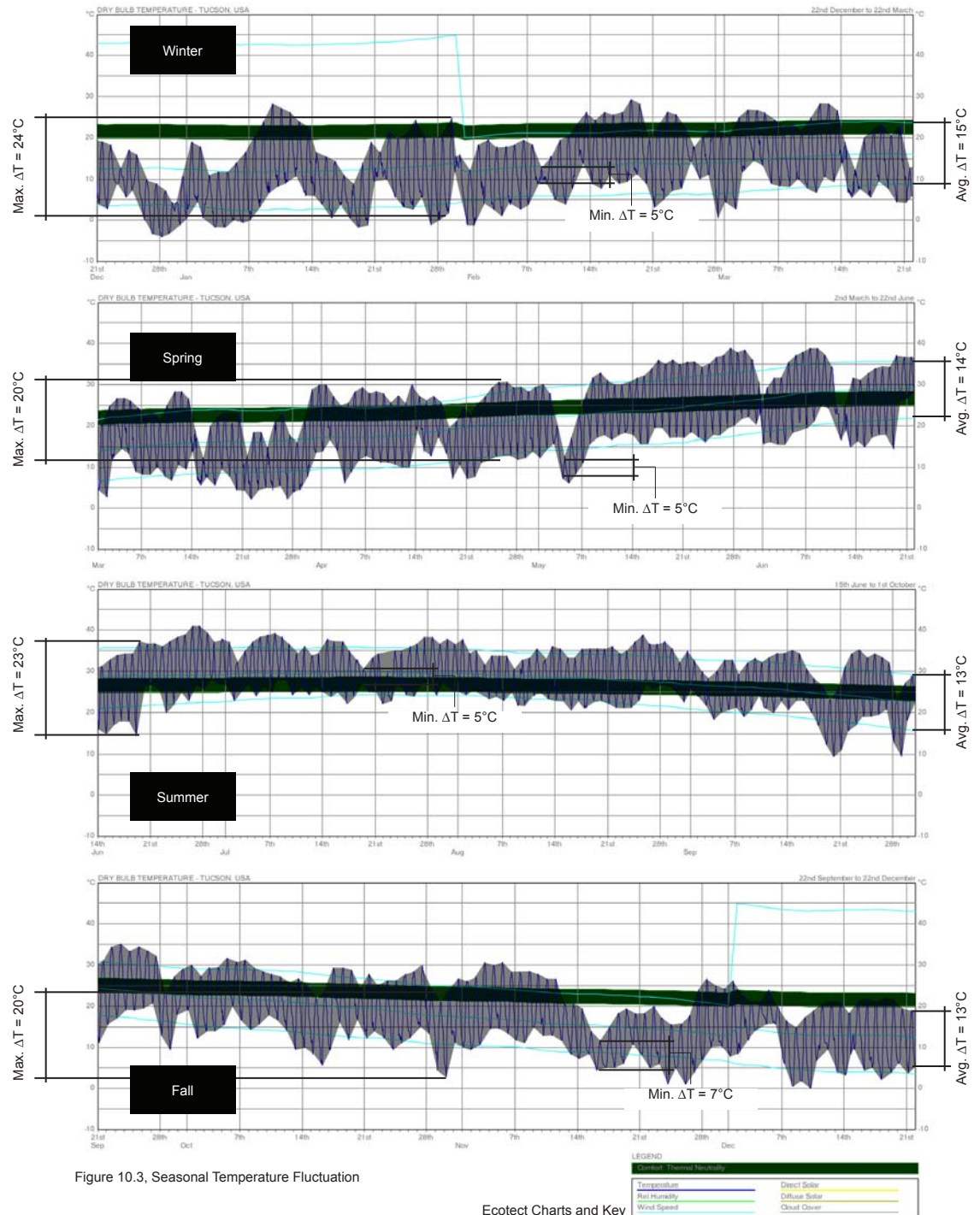
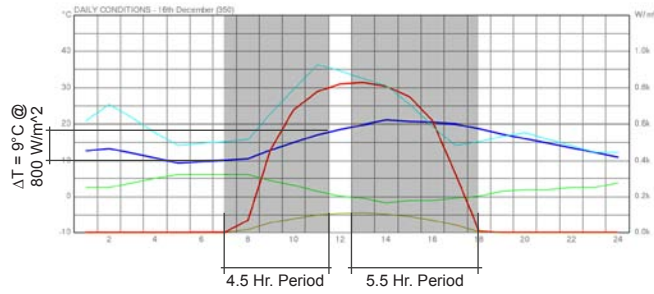


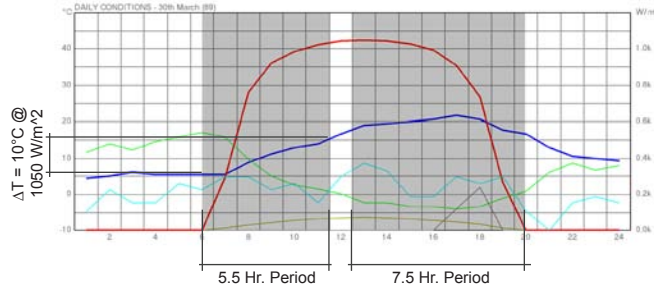
Figure 10.3. Seasonal Temperature Fluctuation

10.1.2 Solar Radiation Exposure

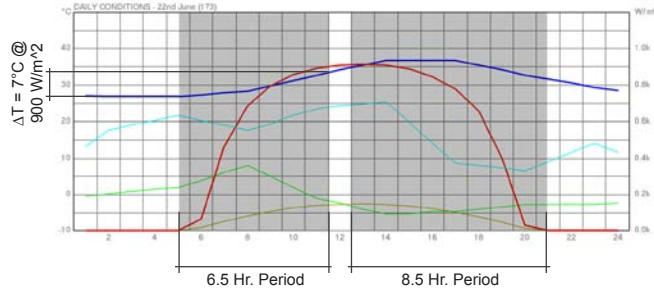
Winter Solstice - March 21st



Spring Equinox - March 21st



Summer Solstice - June 22nd



Fall Equinox - September 22nd

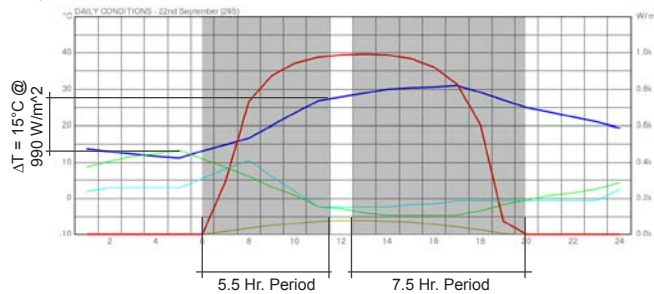


Figure 10.4, Diurnal Solar Radiation Exposure Diagrams

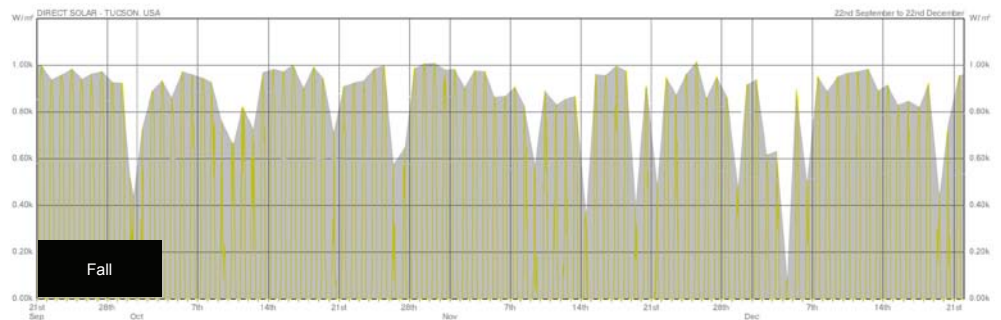
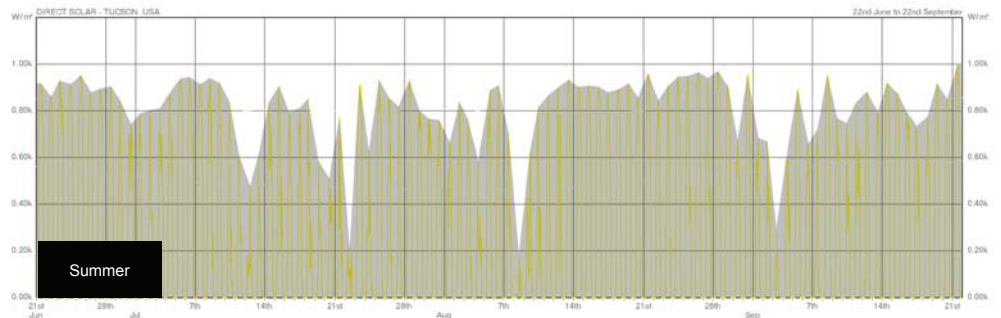
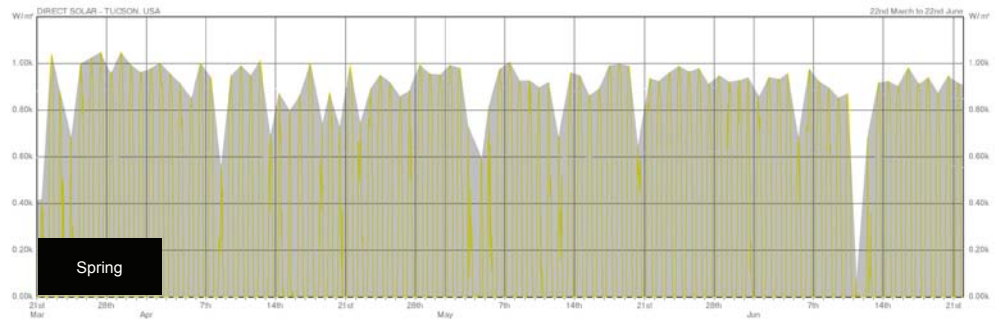
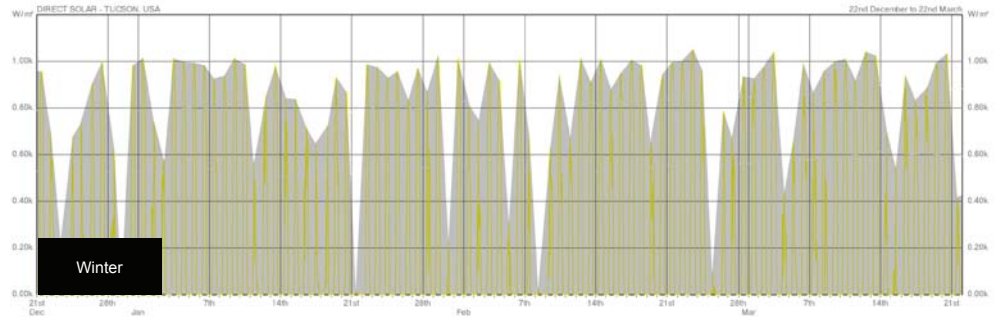


Figure 10.5, Seasonal Solar Radiation Exposure Diagrams



Ecotect Charts and Key

10.1.3 Placement

“If they looked toward the midi or the occident would not be salubrious because, during the summer, the necidional section of the sky grows warm at sunrise, and burning in the middle of the day; on the same account, those which look towards the occident grow warm in the middle of the day and burning in the evening. Also, bodies deteriorate in such places because of this alternating heat and cold”.

Vitruvius, *On Architecture*

In the desert, the East and West facades experience the most intense solar radiation exposure for vertical enclosures. The direct and parallel rays of light in the early morning and late afternoon penetrate deep through apertures in the building facades creating intense areas of glare, reflection, luminance and thermal absorption.

In the winter, the heating sun is often desired to warm the interior, however throughout the spring, summer and autumn seasons, the heat and light is typically undesirable and specific external and internal devices have been developed to regulate the sun and heat. The following pages identify existing shading functions and the related solar heat gain coefficient factors.

For this study, the placement of an enclosure on the E/W facades of a building is analyzed in terms of providing shade and regulating thermal radiation absorption for the hours in which the sun is directly exposed to the vertical plane.

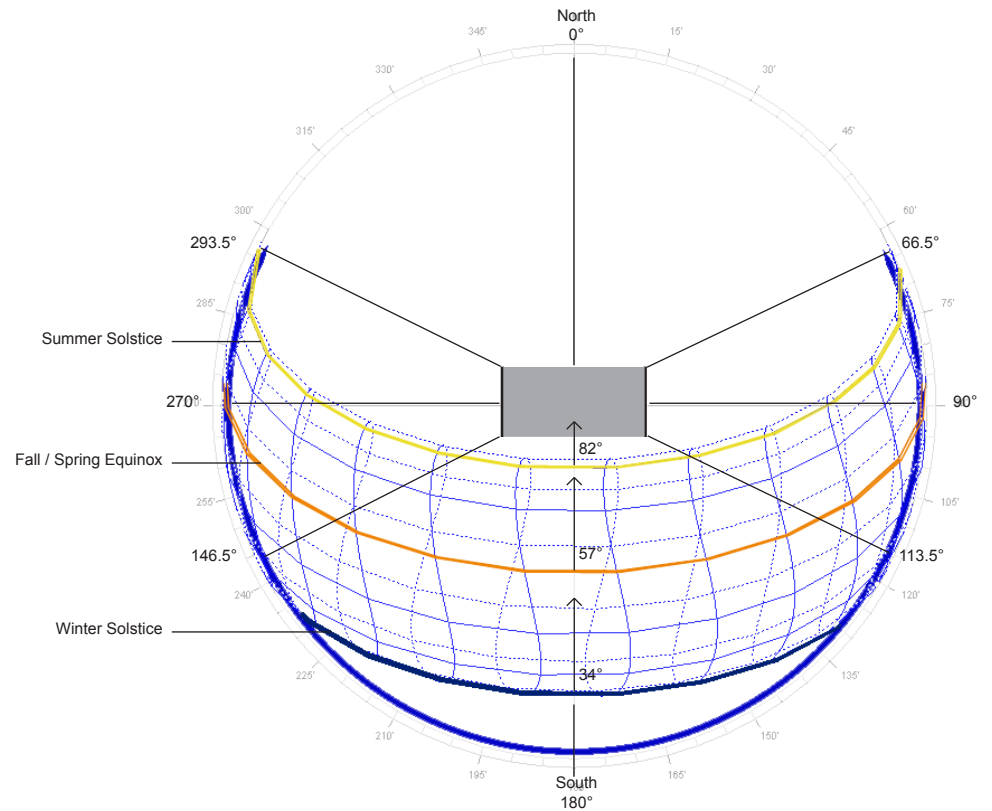


Figure 10.6, Annual Sun Path - Tucson, Arizona (Ecotect)

10.2 Location - Washington D.C

Washington D.C., USA
Solar Decathlon Project - Seed Pod

Region
Elevation: 409' Above Sea Level
Lat./Long.: 38°53' N / 077°01' W

Washington D.C. is the location for the 2009 Solar Decathlon Competition. The Seed POD Project is to be erected on the National Mall over a three week period in the month of October. The contrasting climate between Tucson and Washington D.C. is analyzed in terms of seasonal weather fluctuation in regards to temperature and solar radiation.

The following tables and charts quantify and analyze recorded weather data for Washington D.C. in terms of solar radiation and temperature. Of interest in these diagrams are the temperature differential measurements, directional movement of the sun and heat and the interrelated phenomenon's which cause the temperature to fluctuate, i.e. rain, humidity, wind, night, day, etc. Washington D.C. is unique, in that, depending on the weather systems that flow through the region the high temperature can vary upwards of 40 degrees Fahrenheit between two days with absolutely no radiation to a day of extreme radiation. Weather systems highly influence the region and bring over 40 inches of rain annually, with over 150 days per year of cloudy, overcast sky.

Washington D.C. Weather History									
	Temp. (F)	Relative Humidity (Percentage)		Extreme Temp. (Days Per Month)		Rain (Inches)	Cloudiness (Days Per Month)		
		A.M.	P.M.	Below 32	Above 90		Average	Clear	Partly Cloudy
January	30.6	77%	59%	26	0	2.7	7	7	17
February	33.6	78%	54%	22	0	2.8	7	6	15
March	43.2	78%	52%	17	0	3.2	7	8	16
April	52.7	76%	48%	5	0	3.1	7	9	14
May	62.2	83%	55%	0	1	4.0	7	10	14
June	71.0	84%	56%	0	5	3.9	6	12	12
July	75.6	86%	55%	0	12	3.5	8	11	12
August	74.2	89%	55%	0	8	3.9	8	11	12
September	67.1	90%	56%	0	3	3.4	9	9	12
October	55.1	89%	54%	5	0	3.2	11	8	12
November	45.4	82%	55%	15	0	3.3	7	8	15
December	35.4	79%	58%	23	0	3.2	7	7	17
Annual	53.8	83%	55%	113	29	40.2	92	105	168

Chart 10.2, Source: Cityrating.com

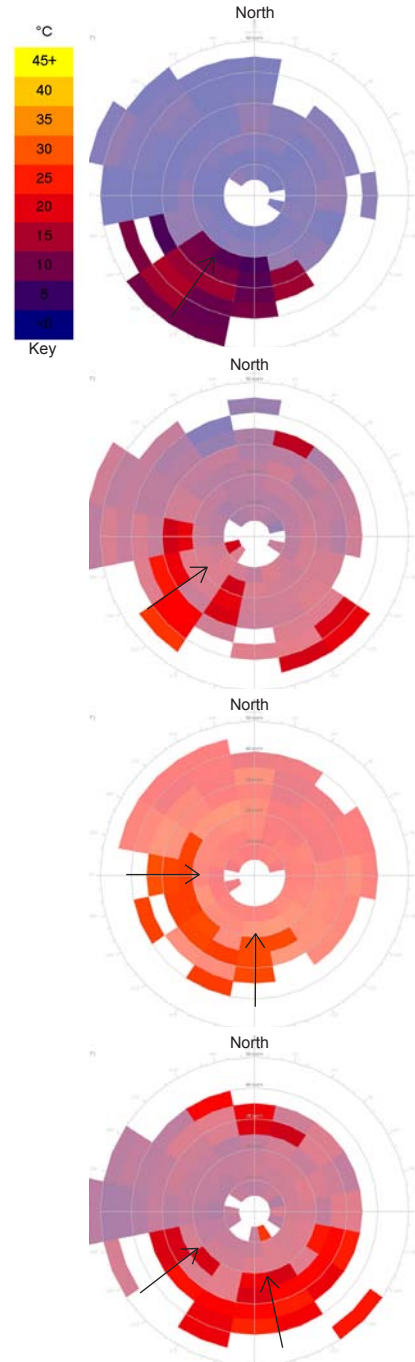


Figure 10.7, Maximum Wind Temperature - Velocity / Direction (Ecotect)

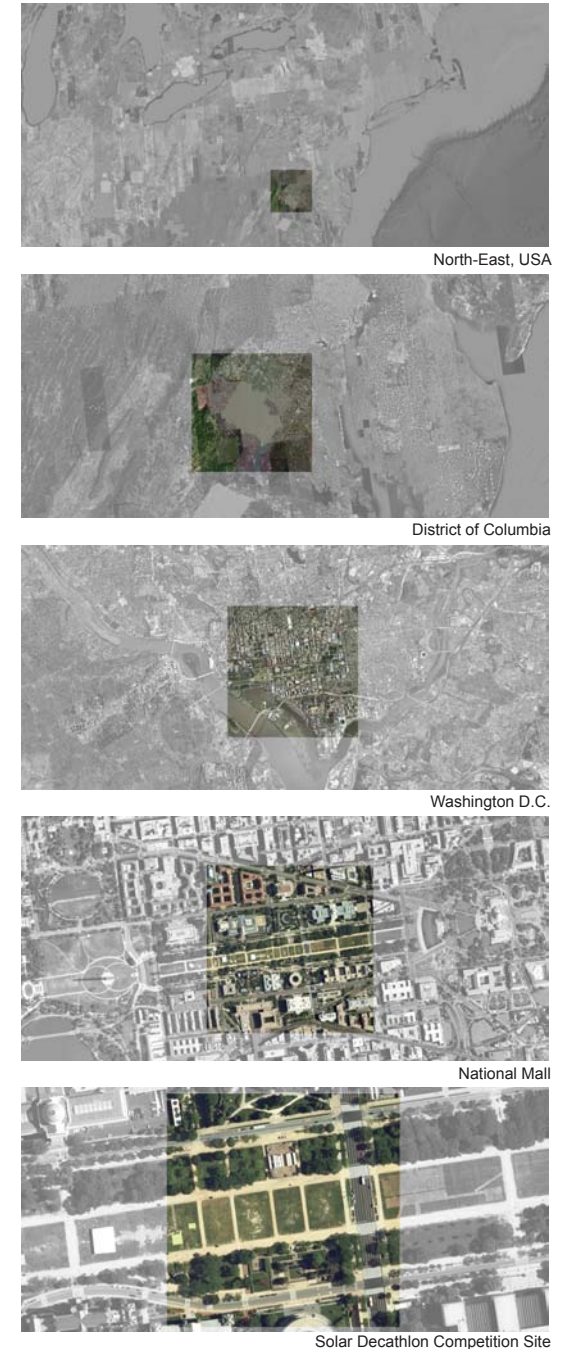


Figure 10.8, Aerial Map - Washington, D.C.

10.2.1 Temperature Differential

The adjacent charts were derived using the program Ecotect. The weather data includes a summary of the last years of recorded information from the National Weather Service.

The charts have been analyzed to display the maximum, minimum and mean temperature differential for the winter, spring, summer and fall seasons. The data was separated into seasons for identification of time based on the declination angle of earth and its location to the sun, which directly affects the weather shifts of wind, temperature and humidity for the region.

Winter:	Maximum	= 20°C	= 36.0°F
	Minimum	= 5°C	= 9.0°F
	Average	= 11°C	= 19.2°F
Spring:	Maximum	= 18°C	= 32.4°F
	Minimum	= 3°C	= 5.4°F
	Average	= 14°C	= 24.2°F
Summer:	Maximum	= 14°C	= 24.2°F
	Minimum	= 3°C	= 5.4°F
	Average	= 10°C	= 18.0°F
Fall:	Maximum	= 14°C	= 24.2°F
	Minimum	= 3°C	= 5.4°F
	Average	= 10°C	= 18.0°F
Averages:	Maximum	= 17°C	= 30.6°F
	Minimum	= 3.5°C	= 6.3°F
	Mean	= 11°C	= 19.2°F

The next page identifies and analyzes the average solar radiation exposure for the first day of each season and the average radiation cycle for the entire season.

The time period of solar exposure for the East and West facades is depicted in relationship to maximum achieved radiation levels. The seasonal charts identify the diurnal fluctuation and consistent levels of radiation exposure throughout the year.

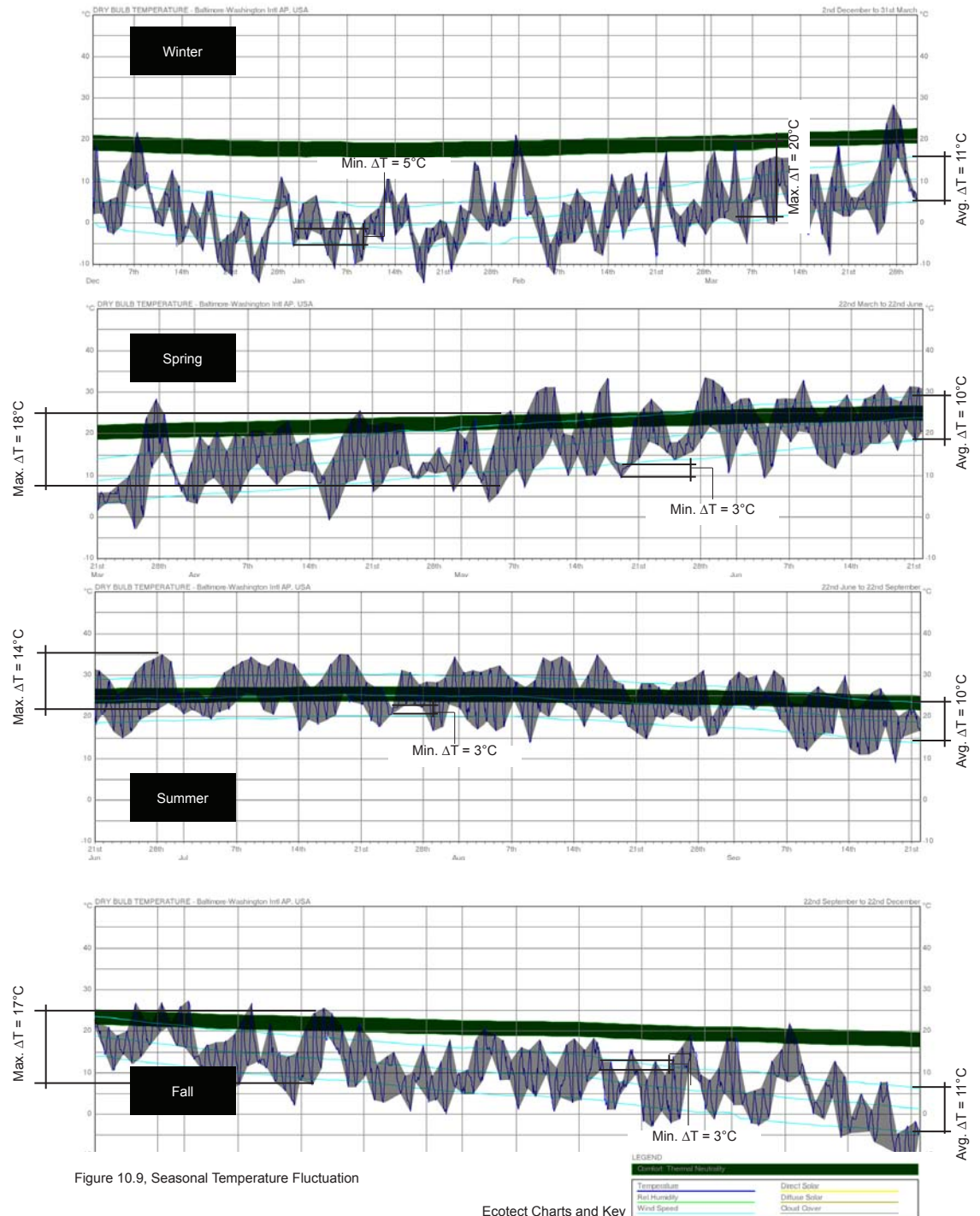
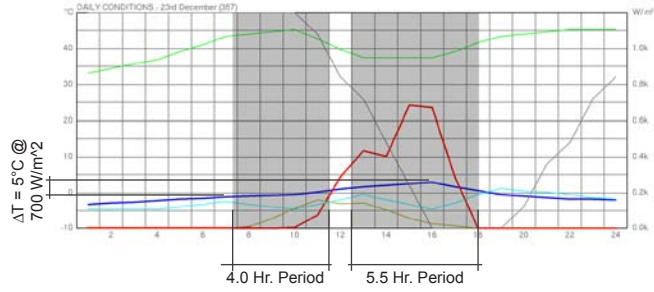


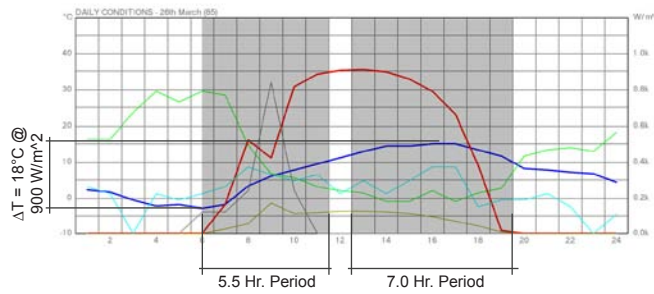
Figure 10.9, Seasonal Temperature Fluctuation

10.2.2 Solar Radiation Exposure

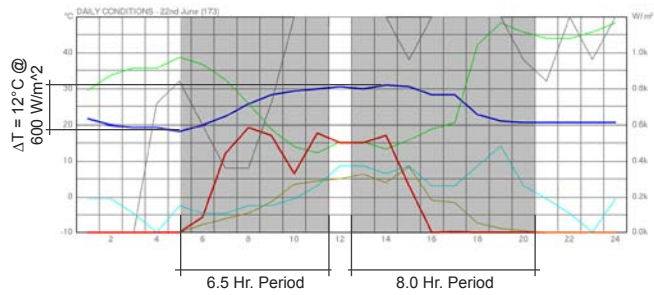
Winter Solstice - March 21st



Spring Equinox - March 21st



Summer Solstice - June 22nd



Fall Equinox - September 22nd

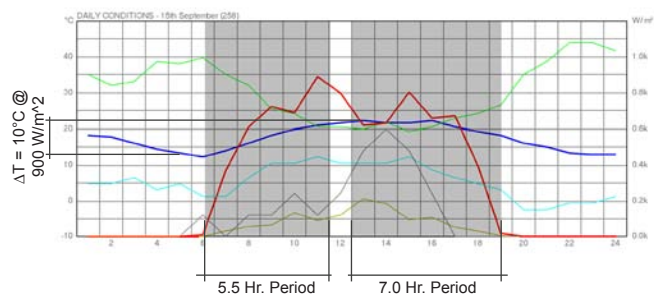


Figure 10.10, Diurnal Solar Radiation Exposure Diagrams

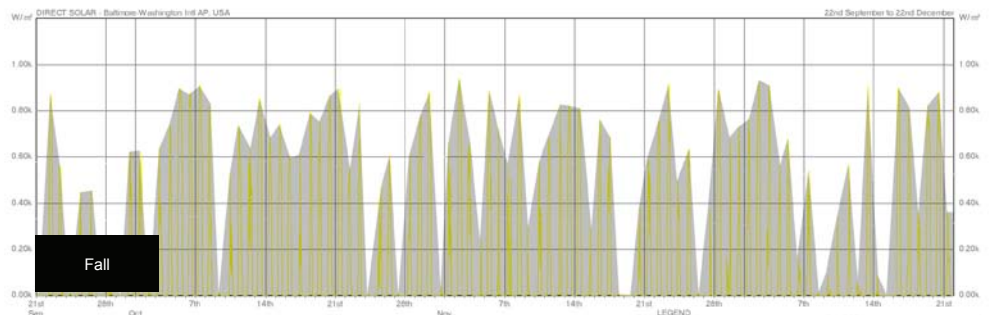
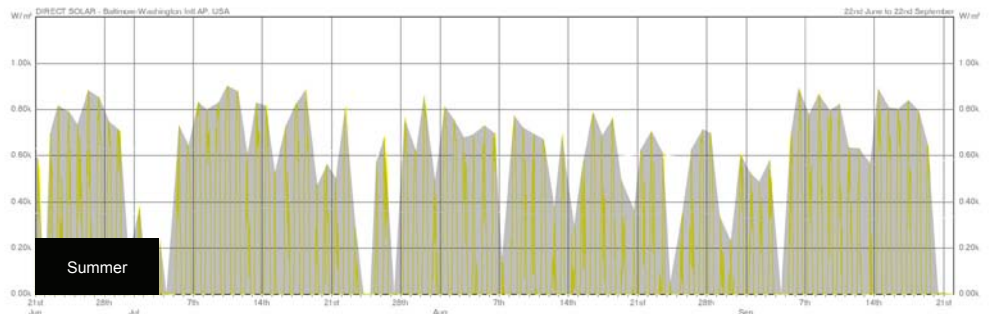
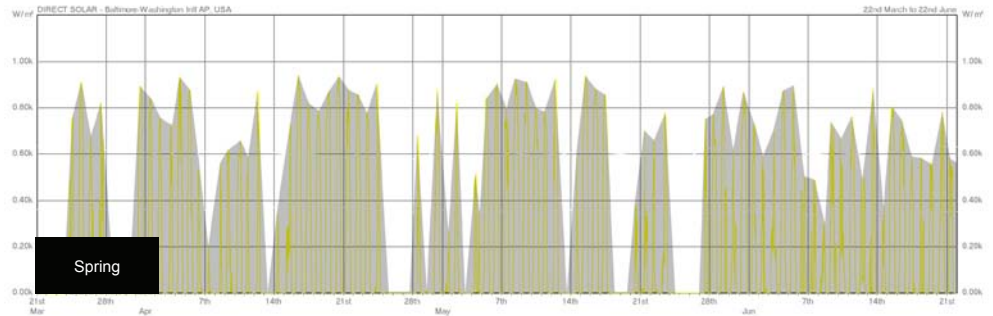
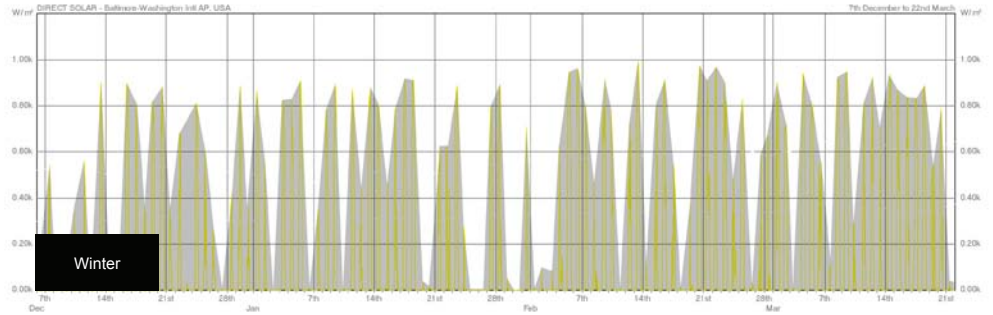


Figure 10.11, Seasonal Solar Radiation Exposure Diagrams

Ecotect Charts and Key

10.3 Existing Shading / Thermal Techniques

Solar Heat Gain Coefficient (SHGC) -

The Solar Heat Gain Coefficient is represented as numerical number between 0.00 - 0.87 to identify the amount of heat gain which is absorbed or transferred through an enclosure. A low number refers to a low amount of heat transmitted through the enclosure and the greater its shading ability.

Interior - 1. Venetian Blinds

2. Roller Blinds

3. Draperies

Exterior - 1. Venetian Blinds

2. Canvas Awning

3. Overhang

4. Horizontal (Adjustable)

5. Trees

6. Vertical Fins (Adjustable)

7. Eggcrate

8. Sunscreens

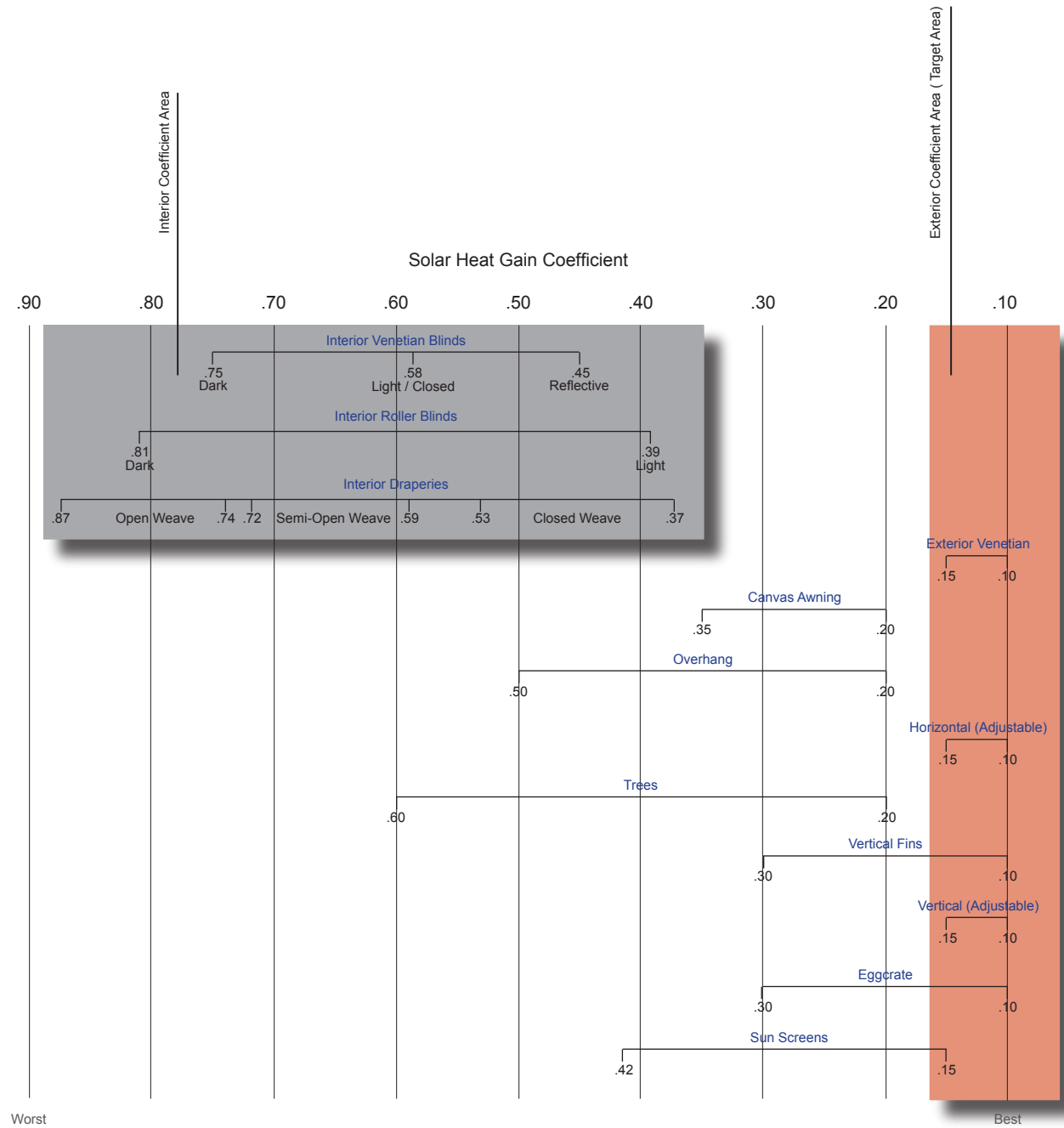


Figure 10.12, SHGC of Existing Shading Techniques - Source: G.Z. Brown, *Sun, Wind & Light*, 2001

10.4 Overview of Existing Light - Deflecting Systems

The following chart and diagrams identify existing enclosure techniques for deflecting light by means of reflection, refraction and absorption and the related light properties, i.e. glare, heat, ability to reduce artificial lighting, etc.

The chart was used as a reference guide for what properties are required for light enclosure systems and in particular to the chart are the highlighted tabs, including: Shading, and Visual Contact. These two properties are important as they are often the first properties required of an enclosure and yet are rarely satisfied together.

The design of a system which takes advantage of shading and visual contact characteristics is the ultimate goal and only through an adaptable or dynamic system can both be appropriately regulated, together, as well as in coordination with glare protection, directing light, even distribution of light in room, reducing artificial light and its application of night.

Type	System	Installation	Considerations For Installations						
			Shading	Glare Protection	Visual Contact	Directing Light	Even Distribution of Light in Room	Reducing Artificial Light	Application at Night
Diffuse light deflection	1.1 Light strut	Window	Marginal	Marginal	Yes	Marginal	Marginal	Marginal	No
Shading w/ diffuse light transmittance	2.1 Prismatic panels	Window Skylight	Yes	Yes	Marginal	Marginal	Marginal	Marginal	Yes/No
	2.2 Prisms & alum louvers	Window	Yes	Yes	No	Yes	Yes	Yes	Yes
	2.3 Shading mirror profiles	Skylight	Yes	Yes	No		Yes	No	No
Sunlight deflection	3.1 Laser-cut panels	Window Skylight	No	No	Yes	Yes	Yes	Yes	No
	3.2 Light deflecting glass	Window Skylight		Yes	Marginal	Yes	Yes		No
	3.3 Light strut for direct light deflection	Window Skylight	Marginal	Marginal	Yes	Yes	Yes	Yes	No
	3.4 Pivoting louvers	Window Skylight	Yes	Yes/Marginal	Marginal	Yes	Yes/Marginal	Yes	Yes
	3.5 Venetian blinds for light deflection	Window	Yes	Yes	Marginal	Yes	Yes	Yes	Yes
	3.6 Heliostat	Window				Yes		Yes	Yes

Chart 10.3, Existing Light Deflecting Systems - Source: Daniels, Klaus, *Advanced Building Systems: A Technical Guide for Architects and Engineers*. 2002

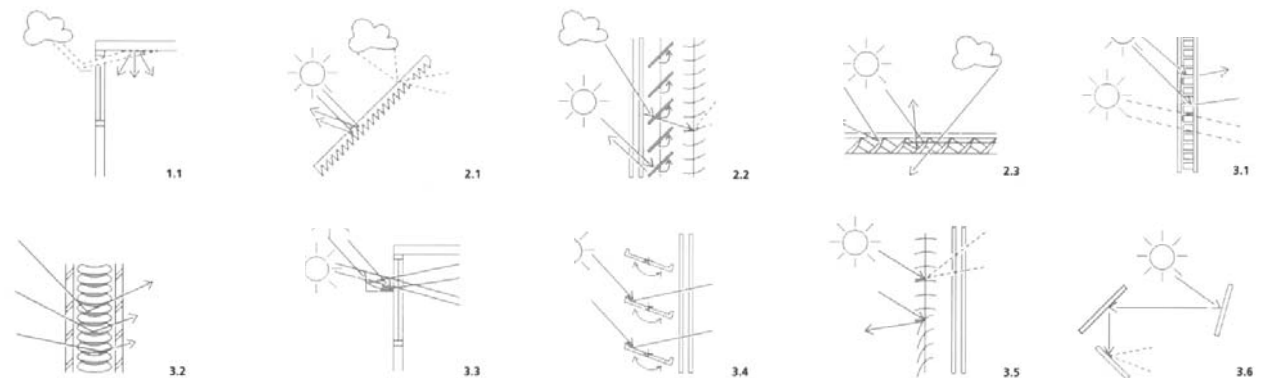


Figure 10.13, Source: Daniels, Klaus, *Advanced Building Systems: A Technical Guide for Architects and Engineers*. 2002

10.5 Glossary

Anisotropic:	Unequal physical properties along different axes.	Kinetic Energy:	Energy an object possesses due to motion.
Automorphic:	Movement of an object based on a reactive or trigger response.	Membrane:	Tautly stretched skin within a structural assembly of tensile and compressive forces in equilibrium.
Bistable Mechanism:	Elastic stressed mechanical device which demonstrates bi-stability.	Penumbra:	Property of shadows with partial light based on an extended light source with variable light tangency.
Bi-stability:	Mode of deformation for a mechanism between stable and unstable states. Energy transfer from maximum stress (unstable deformation form) to minimum stress (stabilized deformation form).	Potential Energy:	Energy stored within a physical system which can be transferred to other energies, i.e.: kinetic energy, rotational energy.
Bi-Laminates:	Forming of two different materials with similar molecular composition and bonding energy into one material with unique mechanical properties. Metals, polymers and elastomers are often bonded through heat and cold work processes for lamination.	Recoil:	From the law of conservation of momentum, an component or material which conveys an action with an equal and opposite reaction.
Bimetals:	Two different metals joined together for unique mechanical properties. Often used for increasing performance of metals while decreasing weight and corrosive properties. Metals with different C.T.E. are bonded for thermal expansion characteristics used in industrial applications.	Seed Pod:	University of Arizona's Solar Decathlon Building.
Coefficient of Thermal Expansion (C.T.E.):	Mechanical property by which the dimension of a material changes when bonding energy and molecular composition is altered by temperature. Typical measurement is recorded per micro-millimeter / millimeter degree Celsius ($\mu\text{m}/\text{m}^\circ\text{C}$).	Slenderness Ratio:	Ratio of a columns material properties and shape to determine structural strength limit and elastic stability limit, given: a materials Modulus of Elasticity, area moment of inertia, overall length, length factor, and force.
Corrosion:	Reaction of a materials appearance and mechanical properties when subject to corrosive chemicals in the environment, i.e.: gases, liquids, oxygen, etc.	Shade:	Spatial volume between an object, which intercepts a light source, and a surface which captures the absence of light or shadow.
Dynamic Frames:	Movement of a two-dimensional or three-dimensional framed structure consisting of elements and nodes from one stable position to a secondary stable position. Rigidization of structure through placement of elements through polygonal instability to triangulated stability with pinned nodes.	Shadow:	The projection of the absence of light on a surface. Two types of shadows exist, Umbra (total shade) and Penumbra (partial shade).
Elastic:	The reversible deformation of a material.	Smart Material:	An engineered material which exhibits dynamic mechanical properties based on the influence of external stimulus, including: temperature, electricity, light, impact force, magnetism, adhesion and absorption.
Ecotect:	Building analysis program utilized for solar placement.	Solar Decathlon Competition:	The U.S. Department of Energy's Building Competition of Universities which participate in designing and building a sustainable house which utilizes solar energy products for electrical, water and thermal regulation. The competition is held in Washington D.C each year and displays the most recent solar technology and newly engineered building materials.
Endurance Ratio:	Ratio between the cyclical stress and the maximum tensile strength of a material to determine the fatigue life of a stressed component system.	Solar Radiation:	Heat which is converted from electromagnetic light from the sun when penetrating the earth's atmosphere. Measured in watts per meter squared (W/m^2). Solar constant is approximately $1300 \text{ W}/\text{m}^2$ with a variation of 7% throughout the year due to the declination angle of the earth.
Euler's Buckling Modes:	Buckling principles to correlate stress, load and deformation sequences of slender columns based on columns material properties (Young's Modulus) and type of node (pin, rigid, Free - Roller).	Solar Heat Gain Coefficient (SHGC):	Amount of heat gain which is absorbed or transferred through an enclosure based on a numerical representation between 0 - 0.87. A low number refers to a low amount of heat transmitted through the enclosure and the greater its shading ability.
Fatigue:	Lowering of strength or failure of a material due to repetitive stress in the form of tension, compression, bending, vibration, thermal expansion, contraction and other stresses which may be above or below the yield strength.	Static Structural Frames:	Two dimensional and three dimensional framed structures which restrict tensile, compressive and bending forces based on nodal connections and shear plane relationships.
Isotropic:	Equal physical properties along axes.	Strain:	In mechanics, the deformation of a material or component with a change in shape or size between an initial state and stress induced state.

Stress: In mechanics, the average amount of force exerted per unit area of an object

Thermal Regulation: Maintenance of a constant temperature independent of the environmental fluctuating temperature.

Umbra: Property of shadows with no light, total shadow, projected on a surface.

Visual Contact: Degree of perception from one space to an adjacent space, in particular from an interior space to an exterior space.

Young's Modulus: Stiffness of an isotropic elastic material. Hooke's Law determines the ratio of the uniaxial stress over the uniaxial strain in the range of stress.

10.6 Bibliography

- Addington, Michelle. Smart Materials and New Technologies [Electronic Resource] : For the Architecture and Design Professions / D. Michelle Addington, Daniel L. Schodek. Ed. Daniel L. Schodek and Inc NetLibrary. Oxford : Architectural, 2005.
- Alexander, R. McNeill. Elastic Mechanisms in Animal Movement / R. McNeill Alexander. Cambridge ; New York : Cambridge University Press, 1988.
- Aranda, Benjamin. Tooling [Electronic Resource] / Edited by Benjamin Aranda, Chris Lasch. Ed. Chris Lasch and SpringerLink (Online service). New York : Princeton Architectural Press, 2006.
- Aronin, Jeffrey Ellis, 1927-. Climate & Architecture. New York,: Reinhold, [1953].
- Ashby, M. F. Materials and Design : The Art and Science of Material Selection in Product Design / Mike Ashby and Kara Johnson. Ed. Kara Johnson. Oxford ; Boston : Butterworth-Heinemann, 2002.
- Askeland, Donald R. The Science and Engineering of Materials / Donald R. Askeland, Pradeep P. Phulé. Ed. Pradeep Prabhakar Phulé . 5th ed. ed. Southbank, Victoria, Australia : Thomson, c2006.
- Bateson, Gregory. Steps to an Ecology of Mind: Collected Essays in Anthropology, Psychiatry, Evolution, and Epistemology. San Francisco,: Chandler Pub. Co., [1972].
- Brown, G. Z. Sun, Wind & Light : Architectural Design Strategies / G.Z. Brown, Mark DeKay ; Illustrations, Virginia Cartwright ... [Et Al.]. Ed. Mark DeKay. 2nd ed ed. New York : Wiley, c2001.
- Building Skins / Christian Schittich, Editor. Ed. Christian Schittich. Rev. ed. ed. Basel : London : Birkhäuser ; Springer [distributor], 2006.
- Calatrava, Santiago, 1951-. Santiago Calatrava's Creative Process / [Translation of the Dissertation Text into English: John Dennis Gartrell]. Ed. Alexander Tzonis and Liane Lefavre. Basel : Birkhäuser, 2001.
- Daniels, Klaus. Advanced Building Systems : A Technical Guide for Architects and Engineers / Klaus Daniels. Basel : London : Birkhäuser ; Momenta, 2002.
- . Technologie Des Ökologischen Bauens. English.: the Technology of Ecological Building : Basic Principles and Measures, Examples and Ideas / Klaus Daniels ; English Translation by Elizabeth Schwaiger. Basel ; Boston : Birkhäuser Verlag, c1997.
- Deleuze, Gilles. Mille Plateaux. English; A Thousand Plateaus : Capitalism and Schizophrenia / Gilles Deleuze, Félix Guattari ; Translation and Foreword by Brian Massumi. Ed. Félix Guattari. Minneapolis : University of Minnesota Press, c1987.
- Engineering Polymers / Edited by R.W. Dyson. Ed. R. W. (Robert William) Dyson. Glasgow : New York : Blackie ; Distributed in USA by Chapman and Hall, 1990.
- Engineering with Rubber : How to Design Rubber Components / Edited by Alan N. Gent ; with Contributions by R.P. Campion ... [Et Al.]. Ed. Alan N. Gent and R. P. Campion. Munich ; New York : New York : Hanser Publishers ; Distributed in the United States of America and in Canada by Oxford University Press, c1992.
- Frisch, Karl von, 1886-. Tiere Als Baumeister. English: Animal Architecture [by] Karl Von Frisch, with the Collaboration of Otto Von Frisch. Translated by Lisbeth Gombich. Ed. Otto von Frisch. [1st ed.] ed. New York,: Harcourt Brace Jovanovich, c1974.
- Gantes, C. J. (Charis J.). Deployable Structures : Analysis and Design / C.J. Gantes. Southampton: WIT Press, c2001.
- Horden, Richard. Light Tech : Towards a Light Architecture = Ausblick Auf Eine Leichte Architektur / Edited by Werner Blaser. Ed. Werner Blaser . Basel ; Boston : Birkhäuser Verlag, c1995.
- Howell, Larry L. Compliant Mechanisms / Larry L. Howell. New York ; Chichester [England] : Wiley, c2001.
- Jenski, Wayne A. "Thermostatic Composites and Systems for A Self-Regulating Architecture." Masters Of Architecture University Of Arizona, 2007.
- Materials: a Scientific American Book. San Francisco,: W. H. Freeman, [1967].
- "MatWeb, Material Property Data." Automations Creations, Inc. 2007. <www.matweb.com/index.asp>.
- McDonough, William. Cradle to Cradle : Remaking the Way we make Things / William McDonough & Michael Braungart. Ed. Michael Braungart . 1st ed ed. New York : North Point Press, 2002.
- McQuaid, Matilda. Extreme Textiles : Designing for High Performance / Matilda McQuaid ; with Essays by Philip Beesley ... [Et Al.] ; with Contributions by Alyssa Becker, John W. S. Hearle. Ed. Philip Beesley and CooperHewitt Museum. New York : Smithsonian Cooper-Hewitt, National Design Museum : Princeton Architectural Press, c2005.

Minnaert, M. G. J. (Marcel Gilles Jozef), 1893-. Natuurkinde Van't Vrije Veld. English.: the Nature of Light & Colour in the Open Air. Translation [by] H. M. Kremer-Priest. Revision [by] K. E. Brian Jay. [New York]: Dover Publications, [1954].

Ritter, Axel. Smart Materials in Architecture. Interior Architecture and Design / Axel Ritter. Basel ; Boston : Birkhäuser, c2007.

Schodek, Daniel L., 1941-. Structures / Daniel L. Schodek. 3rd ed. ed. Upper Saddle River, N.J. : Prentice Hall, c1998.

Thermostat Metals Designer.s Guide. Texas Instruments, 1991.

Thompson, D'Arcy Wentworth, 1860-1948. On Growth and Form / by D'Arcy Wentworth Thompson. Ed. John Tyler Bonner. An abridged ed. edited by John Tyler Bonner. ed. Cambridge : Cambridge University Press, 1971.

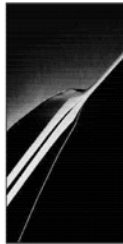
"University of Cambridge, Material Selection And Processing." 25/02/2002 2002. <<http://www-materials.eng.cam.ac.uk.ezproxy1.library.arizona.edu/mpsite/default.html>>.

Valéry, Paul, 1871-1945. Introduction to the Method of Leonardo Da Vinci. Translated from the French of Paul Valéry; by Thomas McGreevy. Ed. Thomas MacGreevy. London,: J. Rodker, 1929.

10.7 Company Profiles

10.7.1 Engineered Material Solutions (EMS)
 39 Perry Avenue
 Attleboro, MA 02703
 USA

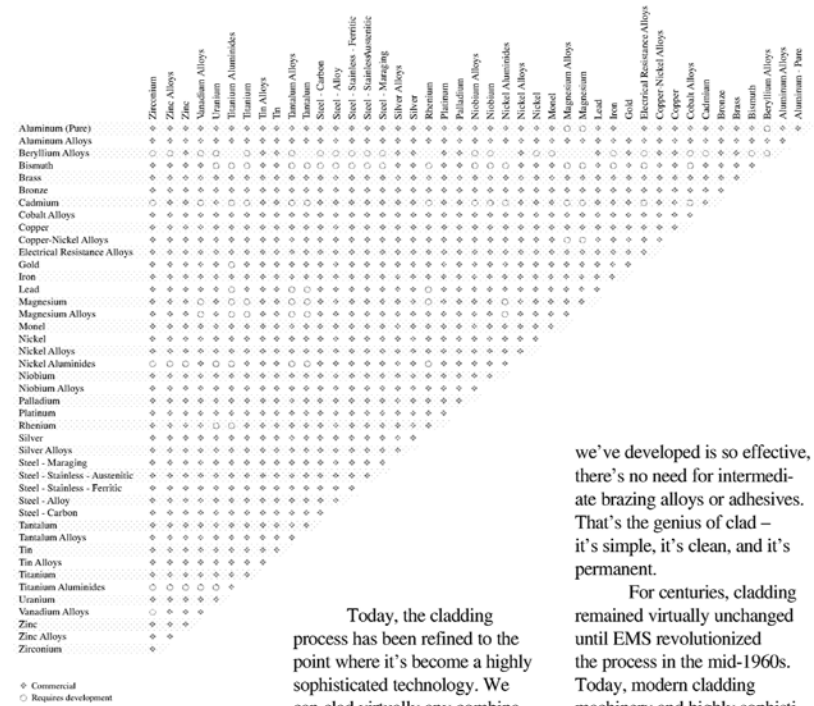
Clad It.



CLAD METAL: What it is. How it's made.
 What it can do for you.



METALS THAT CAN BE CLAD.



Basic cladding has been around for centuries. It originally served as a way to bond decorative gold or silver surfaces onto base metals. Perhaps the most famous example of an early clad metal "product" is the Damascus sword – crafted from layers of steel and valued for its ability to take and keep an edge.

Today, the cladding process has been refined to the point where it's become a highly sophisticated technology. We can clad virtually any combination of ductile metals and create a remarkably broad range of characteristics to fit an extensive and expanding range of applications.

At EMS, we've bonded well over a thousand different combinations of metals and alloys, in all shapes and sizes, including some with fifteen different metal layers in a single strip. The bonding technique

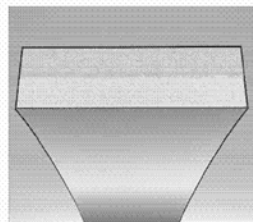
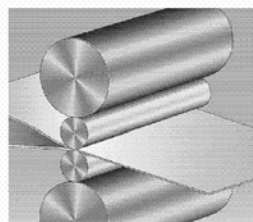
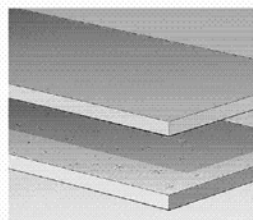
we've developed is so effective, there's no need for intermediate brazing alloys or adhesives. That's the genius of clad – it's simple, it's clean, and it's permanent.

For centuries, cladding remained virtually unchanged until EMS revolutionized the process in the mid-1960s. Today, modern cladding machinery and highly sophisticated heat-treating, rolling, and finishing techniques produce materials that provide singular performance characteristics for hundreds of products – from tiny electrical contacts to truck bumpers, from cookware to engine oil coolers, from electronic components to automobile parts, plus residential and aircraft circuit breakers as well as appliance and industrial thermal controls.

HOW CLAD BECOMES CLAD.

Anatomy of a metallurgical bond.

Clad metals are joined by a roll bonding and thermal treatment process that produces a metallurgical bond as the lattice structures of the metals are forced into conformance with each other. High pressure, producing massive deformation of the metals, causes a sharing of electrons at the interface, which produces a bond on the atomic level. No intermediate layers such as adhesives or braze metal are involved.

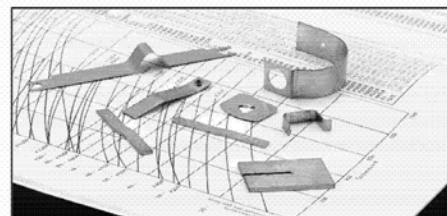


Roll bonding starts with two or more coils of cold finished strips of different metals or alloys. The metals are cleaned chemically, then abraded by a brushing operation to eliminate oxides and other surface impurities.

The cleaned metals are rolled under very high pressure, which reduces their thickness and bonds the metals together. As their surfaces are extended, typically by more than five times that of their original area, the atomic lattices of the metals merge, sharing electrons between mating surfaces.

Coils of bonded strip are heat treated to "relax" the materials and to extend diffusion of the electrons of one material into the other at the bond interface. Impurities that become gaseous when heated diffuse into the metals; nondiffusible impurities consolidate by spheroidization.

EMS THERMOSTAT METALS



Over 100 thermostat metals are always in stock.

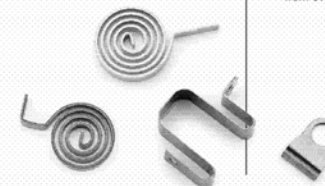
Wherever there's a need to sense, control or protect.

Thermostat metals comprise one of the most widely applied families of clad metals. Typically processed in strip form, they are combinations of metals that are selected and joined to best take advantage of the "bimetal effect" – movement caused by their different coefficients of expansion, as they respond to temperature changes. At work, at home, in an airplane, boat or car – virtually anywhere on earth – you are almost always within reach of a thermostat metal device.

At Engineered Materials Solutions we are a start-to-finish resource for materials and parts made from thermostat metals. We have produced more of these materials for more

different applications than anyone else in the world. And we've done it using a greater number of component metals yielding a higher number of materials combinations offering a wider range of performance parameters. It's given us an immense amount of knowledge about all aspects of the technology, from input material selection to measuring end product performance.

We invite you to take advantage of what we've learned and put this knowledge to work to maximize the performance and minimize the cost of your products.



Some of the things clad thermostat metal devices do:

- Regulate and control temperature on clothes irons, toasters, toaster ovens, coffee makers, ovens, clothes dryers, hair dryers, deep fat fryers, electric blankets, electric frying pans and tea kettles, rice cookers, griddles, grills and waffle irons, and others
- Protect fluorescent light ballasts from overheating
- Regulate room temperature
- Turn automotive fans on or off
- Record the temperature of food in transport to assure it has not varied from the safe frozen or not frozen range
- Protect home, office, factory electrical circuits
- Protect aircraft electrical circuits
- Open/close vent doors on furnaces and heating systems
- Open/close crawl space and attic vents
- Regulate electric range burner temperatures
- Protect electric motors from overloading
- Protect circuitry in computer and peripheral surge protectors
- Provide anti-scald protection in hospital and nursing home showerheads
- Protect tractor trailer self-adjusting brakes from over-adjusting
- Compensate for ambient temperature variations in car and SUV hatch and hood struts
- Compensate for viscosity variations due to temperature changes in automatic transmissions
- Assure correct readings by gas meters
- Protect circuits in large transformers
- Protect refrigerator motors and compressors from overload

10.7.2 Polymetallurgical Corporation (PMC)
 262 Broad Street
 North Attleboro, MA 02760
 USA



Home
 About Us
 Products
 Sales
 Quality
 Tech Info
 Whats New
 Directions
 Other Links
 Contact Us

Polymetallurgical Corporation
PRECISION CLAD METALS
Thermostat Metal Parts & Assemblies
Shaped Materials

PMC produces clad metal strip in the broadest range of metal combinations, configurations, and dimensions in the industry. Virtually any ductile metal can be metallurgically bonded to produce a material system with the exact characteristics your application requires. By combining the appropriate metals, we produce composites that effectively enhance strength, conductivity, appearance, heat dissipation, expansion coefficient, thermal deflection rate, welding characteristics, spring properties, wear, contact resistance, other mechanical and physical properties, in a cost effective manner.

Please explore our products and feel free to contact us for your clad metal needs.



[Home | Contact Us | Directions]
 Copyright 2008 - Polymetallurgical Corporation - All Rights Reserved

THERMOSTAT METAL

ENGINEERING DESIGN FORMULAS
DEFINITIONS

MECHANICAL FORCE (F_m): The force required to bend a mechanical member, without regard to heat.

THERMAL FORCE (F_t): The force developed by thermostat metal over the temperature range normally used, if completely restrained from movement.

THERMAL DEFLECTION (D_t): The amount of movement of a thermostat metal member, over the operating temperature range.

Symbols:
 t = Thickness in inches
 w = Width in inches
 F = Flexivity value °F
 M = Modulus of elasticity lbs/in²
 L = Active Length in inches
 A = Angular rotation in degrees
 D_t = Deflection in inches
 r = Radius in inches at point load applied
 ϕ = Disc Diameter in inches
 d = Diameter of hole in disc in inches
 ΔT = Temperature change °F
 W = Force in ounces

Thermal Deflection $D_t = \frac{0.53F_t \Delta T L^2}{t}$
Mechanical Force $W = \frac{4MD_t w t^2}{L^3}$
Thermal Force $W = \frac{2.12MF_t \Delta T w t^2}{L^3}$

Thermal Deflection $D_t = \frac{0.133F_t \Delta T L^2}{t}$
Mechanical Force $W = \frac{64MD_t w t^2}{L^3}$
Thermal Force $W = \frac{8.51MF_t \Delta T w t^2}{L^3}$

Thermal Deflection $D_t = \frac{0.265F_t \Delta T L^2}{t}$
Mechanical Force $W = \frac{1.6MD_t w t^2}{L^3}$
Thermal Force $W = \frac{4.24MF_t \Delta T w t^2}{L^3}$

Thermal Deflection $A = \frac{67F_t \Delta T L}{r}$
Mechanical Force $W = \frac{0.0232MAw t^2}{Lr}$
Thermal Force $W = \frac{1.55MF_t \Delta T w t^2}{r}$

Thermal Deflection $A = \frac{67F_t \Delta T L}{r}$
Mechanical Force $W = \frac{0.0232MAw t^2}{Lr}$
Thermal Force $W = \frac{1.55MF_t \Delta T w t^2}{r}$

Thermal Deflection $D_t = \frac{0.106F_t \Delta T (\phi^2 - d^2)}{t}$
Mechanical Force $W = \frac{64MD_t \phi^2 (\phi^2 - d^2)}{L^3}$
Thermal Force $W = \frac{6.78MF_t \Delta T \phi^2 (\phi^2 - d^2)}{L^3}$

CANTILIVER



SIMPLE BEAM



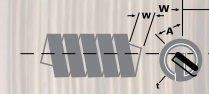
U-SHAPE



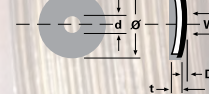
SPIRAL COIL



HELIX COIL

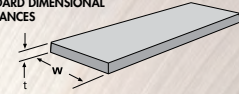


DISC

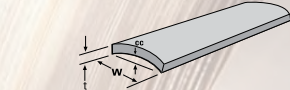


TOLERANCES

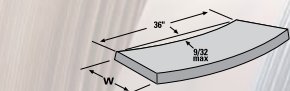
STANDARD DIMENSIONAL TOLERANCES



Thickness Tolerances (in.)
 .005 to .010 ± .0004
 .011 to .020 ± .0005
 .020 and over ± 2 1/2%
Width Tolerances (in.)
 Up to .500 ± .003
 .500 to .999 ± .004
 1.00 and over ± .005
 Premium Process tolerances available at extra charge, consult factory.



Cross Curvature (ASTM Test B478)
 $cc = 10\%$ of thickness + $cc =$ cross curvature in inches
 (.00025W²) or 1/16"
 $t =$ Thickness in inches
 $W =$ Width in inches
 Whichever is smaller where:
 Direction of cross curvature is High Expansion Side concave. Consult factory for special requirements.



Edgewise Camber
 9/32" max. in 3 feet when measured by placing a 3-foot straightedge on the concave edge of material. Camber is measured from the center of the straight-edge to the strip edge.



Lengthwise Flatness (Coil Set)
 Lengthwise Flatness = .0005/t in inches
 Maximum in 3 inches at 7.5°F, where t is thickness in inches. Coil set may be High Expansion Side or Low Expansion Side concave.

Standard Etch Patterns
 PMC Type number and LO indicating low expansion side is standard unless otherwise specified by customer. A wide variety of other etch patterns are available to meet your requirements.

THERMOSTAT METAL

THERMOSTAT METAL - MECHANICAL & PHYSICAL PROPERTIES

COMPOSITIONS

ALLOY	EQUIVALENCY TABLE				HIGH EXPANSION SIDE		INTERMEDIATE		LOW EXPANSION SIDE		ELECTRICAL RESISTIVITY		RESISTANCE
	PMC	ASTM	EMS	CHACE	HOOD	ALLOY	%	ALLOY	%	ALLOY	%	ohms c.mil/ft	
N-1	TM22	Ni	3000	36-100	Ni	50							
27-1	---	BPI	---	---	223	5	721	45	1	50	650	4	7
27-560	TM7	BP560R	---	HR360	223	25	721	29	1	50	560	4	7
181-1	TM20	G1	2100	36-18	181	50			1	50	472	4	7
181-3	TM21	G3	2300	---	181	50			3	50	420	4	7
192-1	---	C1	2450	36-19	192	50			1	50	483	4	7
192-3	TM18	C3	3650	42-19	192	50			3	50	415	4	7
192-11	TM19	C11	3950	39-19	192	50			11	50	456	4	7
223-1	TM1	B1	2400	36-22	223	50			1	50	475	4	7
223-2	TM6	B2	3700	40-22	223	50			2	50	424	4	7
223-3	---	B3	3600	42-22	223	50			3	50	415	4	7
223-11	---	B11	3900	39-22	223	50			11	50	452	4	7
223-N	---	BN	4800	---	223	50			Ni	50	95	6	10
223-100	TM9	R100R	6100	R22-100	223	25	Ni	50	1	25	100	5	9
223-125	TM10	R125R	6125	R22-125	223	31	Ni	38	1	31	125	5.5	9
223-150	TM11	R150R	6150	R22-150	223	35	Ni	30	1	35	150	5.5	9
223-175	TM12	R175R	6175	R22-175	223	39	Ni	23	1	38	175	5.5	9
223-200	TM13	R200R	6200	R22-200	223	40	Ni	20	1	40	200	5.5	9
223-250	TM14	R250R	6250	R22-250	223	44	Ni	12	1	44	250	5.5	9
223-300	TM15	R300R	6300	R22-300	223	46	Ni	8	1	46	300	5.5	9
223-350	TM16	R350R	6350	R22-350	223	48	Ni	4	1	48	350	5.5	9
223-400	TM17	R400R	6400	R22-400	223	49	Ni	2	1	49	400	5.5	9
258-1	---	E1	2600	36-25	258	50			1	50	500	4	7
258-3	TM3	E3	2800	42-25	258	50			3	50	440	4	7
258-4	TM4	E4	3500	45-25	258	50			4	50	406	4	7
258-5	TM5	E5	2500	50-25	258	50			5	50	360	5	7
703-1	---	A1	---	36-62	703	55			1	45	74	15	20
721-3	TM23	P3	7000	42-10	721	55			3	45	565	4	8
721-30	---	P30R	9030	R72-30	721	26	982	38	1	36	30	10	14
721-35	---	P35R	9035	R72-35	721	36	982	32	1	32	35	8	12
721-40	---	P40R	9040	R72-40	721	38	982	27	1	35	40	7.5	11.5
721-50	---	P50R	9050	R72-50	721	41	982	22	1	37	50	7.5	11.5
721-60	---	P60R	9060	R72-60	721	44	982	18	1	38	60	7.5	11.5
721-70	---	P70R	9070	R72-70	721	45	982	15	1	40	70	7.5	11.5
721-90	---	P90R	9090	R72-90	721	47	982	11	1	42	90	6	10
721-100	---	P100R	9100	R72-100	721	49	982	9	1	42	100	6	10
721-125	---	P125R	9125	R72-125	721	49	982	8	1	43	125	6	10
721-150	---	P150R	9150	R72-150	721	50	982	6	1	44	150	6	10
721-175	---	P175R	9175	R72-175	721	50.5	982	5	1	44.5	175	6	10
721-200	---	P200R	9200	R72-200	721	51	982	4	1	45	200	6	10
721-250	---	P250R	9250	R72-250	721	51.5	982	3	1	45.5	250	6	10
721-300	---	P300R	9300	R72-300	721	44	LCS	17	1	39	300	5	9
721-350	---	P350R	9350	R72-350	721	46	LCS	13	1	41	350	5	9
721-400	---	P400R	9400	R72-400	721	48	LCS	10	1	42	400	5	9
721-675	TM2	P675R	6650	36-10	721	55			1	45	675	4	7
721-850	TM8	P850R	6850	R72-850	721	80			1	20	850	4	7
925-1	---	J1	---	---	925	55			1	45	110	15	20
925-17	---	J7	---	---	925	55			17	45	95	15	20
982-15	---	F15R	---	HR15	223	17	982	70	1	13	15	10	14
982-20	TM24	F20R	1020	HR20	223	8	982	54	1	38	20	10	14
982-25	---	F25R	1025	HR25	223	14	982	46	1	40	25	10	14
982-30	TM25	F30R	1030	HR30	223	20	982	36	1	44	30	7.5	11.5
982-35	---	F35R	1035	HR35	223	23	982	30	1	47	35	7.5	11.5
982-40	---	F40R	1040	HR40	223	26	982	27	1	47	40	7.5	11.5
982-50	TM26	F50R	1050	HR50	223	31	982	21	1	48	50	7.5	11.5
982-60	---	F60R	1060	HR60	223	39	982	17	1	44	60	7.5	11.5
982-70	TM27	F70R	1070	HR70	223	41	982	14	1	45	70	7.5	11.5
982-90	TM28	F90R	1090	HR90	223	42	982	11	1	47	90	5	9
982-100	---	F100R	1100	HR100	223	43	982	9	1	48	100	5	9
982-125	---	F125R	1125	---	223	44	982	7	1	49	125	5	9

PMC TYPE	ASTM FLEXIVITY		MAXIMUM SENSITIVITY TEMPERATURE RANGE °F	USEFUL DEFLECTION TEMPERATURE RANGE °F	RECOMMENDED MAXIMUM TEMPERATURE °F	MODULUS OF ELASTICITY lbs./sq. in. (X 10 ³)	ELECTRICAL RESISTIVITY AT 75°F		RECOMMENDED STABILIZING ONE HOUR AT °F	DENSITY lbs./cu. in
	50° TO 200°F TEMPERATURE RANGE F ₁ (X 10 ⁻⁷)	100° TO 300°F TEMPERATURE RANGE F ₂ (X 10 ⁻⁷)					ohms c. mil/ft	ohms mil ² /ft		
N-1	102	101	0 to 300	-100 to 200	900	26.0	95	75	700	0.31
27-1	185	185	0 to 300	-100 to 500	500	20.0	650	510	500	0.28
27-560	145	145	0 to 300	-100 to 700	900	24.0	560	440	700	0.28
181-1	139	139	0 to 300	-100 to 700	900	25.0	472	371	700	0.29
181-3	106	109	200 to 600	-100 to 1000	900	25.0	430	338	700	0.29
192-1	154	151	0 to 300	-100 to 700	900	25.0	483	380	700	0.29
192-3	120	120	200 to 600	-100 to 800	900	25.0	420	330	700	0.29
192-11	143	141	150 to 450	-100 to 900	900	25.0	472	371	700	0.29
223-1	150	146	0 to 300	-100 to 700	1000	25.0	475	373	700	0.29
223-2	129	125	100 to 550	-100 to 1000	1000	25.0	440	346	700	0.29
223-3	172	172	200 to 600	-100 to 1000	1000	25.0	415	327	700	0.29
223-11	140	141	150 to 450	-100 to 1000	900	25.0	452	355	700	0.30
223-N	46	47	0 to 300	-100 to 700	700	28.5	95	75	700	0.31
223-100	112	105	0 to 300	-100 to 700	900	26.0	100	78.5	700	0.30
223-125	124	127	0 to 300	-100 to 700	900	26.0	125	98	700	0.30
223-150	135	133	0 to 300	-100 to 700	900	26.0	150	118	700	0.30
223-175	138	137	0 to 300	-100 to 700	900	25.5	175	137	700	0.30
223-200	140	140	0 to 300	-100 to 700	900	25.5	200	157	700	0.30
223-250	147	143	0 to 300	-100 to 700	900	25.5	250	196	700	0.30
223-300	149	144	0 to 300	-100 to 700	900	25.5	300	236	700	0.30
223-350	150	145	0 to 300	-100 to 700	900	25.0	350	275	700	0.29
223-400	150	146	0 to 300	-100 to 700	900	25.0	400	314	700	0.29
258-1	138	136	0 to 300	-100 to 700	1000	25.0	500	393	700	0.29
258-3	104	106	200 to 600	-100 to 1000	1000	25.0	440	346	700	0.29
258-4	84	86	250 to 700	-100 to 1000	1000	25.0	400	314	700	0.29
258-5	63	64	300 to 800	-100 to 1000	1000	25.5	350	275	700	0.29
703-1	150	150	0 to 300	-100 to 350	850	18.0	74	58	300	0.30
721-3	180	180	200 to 600	-100 to 600	500	20.0	565	447	500	0.28
721-30	188	188	0 to 400	-100 to 500	500	20.0	30	23.6	500	0.30
721-35	198	190	0 to 400	-100 to 500	500	20.0	35	27.5	500	0.30
721-40	201	196	0 to 400	-100 to 500	500	20.0	40	31.4	500	0.30
721-50	207	250	0 to 400	-100 to 500	500	20.0	50	39.3	500	0.30
721-60	210	200	0 to 400	-100 to 500	500	20.0	60	47.1	500	0.29
721-70	211	202	0 to 400	-100 to 500	500	20.0	70	55.0	500	0.29
721-90	213	204	0 to 400	-100 to 500	500</					

THERMOSTAT METAL - INSTANTANEOUS FLEXIVITY VALUES $F_f \times 10^7$

PMC TYPE	TEMPERATURE °F																			
	-100	-50	0	50	100	150	200	250	300	350	400	450	500	550	600	650	700	800	900	1000
N-1	95	93	98	101	102	102	101	100	96	86	66	43	26	20	14	8				
27-1	150	168	189	185	185	185	186	186	186	185	183	165	139	129	126					
27-560	128	135	143	145	145	143	142	139	137	125	112	109	69	57	48	43	40	35	34	32
181-1	124	130	137	138	139	139	138	135	132	120	99	75	60	47	37	30	24	15	9	5
181-3	83	89	95	97	101	107	110	116	119	121	121	121	121	120	115	95	68	52	39	32
192-1	136	142	149	153	154	154	153	149	144	117	102	85	65	49	39	31	25	15	14	12
192-3	97	104	110	116	118	121	123	126	129	134	135	137	142	144	144	128	113	60	25	15
192-11	118	129	136	140	143	145	149	151	152	152	152	149	125	95	73	57	45	31	19	15
223-1	126	135	144	150	150	150	150	146	139	130	116	92	68	47	38	35	31	28	24	22
223-2	108	114	118	123	126	129	130	132	134	135	137	138	135	124	92	69	55	47	44	38
223-3	81	90	98	105	111	113	117	119	122	123	124	124	126	126	120	100	75	48	44	37
223-11	113	120	125	135	137	142	146	146	146	146	146	146	142	120	98	83	65	57	33	30
223-N	35	38	44	44	45	47	48	47	47				38	36	32	30	24	23	15	
223-100	102	110	112	113	113	114	114	113	106	100	86	65	42	32	25	22	17	16	16	16
223-125	110	119	124	125	126	126	124	122	121	115	96	75	54	45	31	27	24	22	16	16
223-150	118	126	135	136	137	138	136	135	130	121	105	76	53	42	37	31	26	19	17	16
223-175	122	129	141	142	142	143	142	141	135	125	109	78	54	45	38	31	28	21	18	16
223-200	124	134	143	143	144	145	145	140	134	126	112	81	50	40	31	30	26	25	22	18
223-250	130	140	142	147	147	147	147	144	139	125	112	82	67	53	44	38	30	28	25	22
223-300	132	142	145	149	149	150	149	146	141	128	112	83	67	53	44	38	30	28	25	22
223-350	135	140	147	149	150	150	148	144	140	129	111	81	64	48	33	31	29	25	23	21
223-400	135	140	147	149	150	150	148	144	140	129	111	81	64	48	33	31	29	25	23	21
258-1	125	129	136	138	139	138	135	134	133	118	100	73	54	39	33	26	25	22	19	17
258-3	77	83	90	93	99	105	108	112	116	120	121	121	121	121	121	108	60	41	30	23
258-4	62	63	69	75	78	82	85	92	96	98	101	104	107	107	107	107	107	56	38	25
258-5	44	47	51	55	57	60	66	68	71	74	75	77	81	82	83	83	83	82	59	45
703-1	146	148	149	150	150	150	149	146	142	134										
721-3	148	155	164	171	176	182	189	195	202	210	216	222	224	220	210					
721-30	135	161	183	187	188	189	189	189	189	185	183	161	135	121	114					
721-35	139	168	192	194	198	198	198	198	198	193	190	169	140	126	118					
721-40	143	171	194	198	201	201	201	201	201	196	193	171	143	131	122					
721-50	146	176	198	202	207	207	207	207	207	201	198	176	146	132	121					
721-60	150	179	203	207	210	210	210	210	210	206	203	179	150	136	129					
721-70	150	180	203	207	211	211	211	211	211	206	203	180	150	136	129					
721-90	151	182	205	210	214	214	214	214	214	209	206	182	151	138	128					
721-100	153	184	207	211	215	215	215	215	215	210	207	184	153	138	129					
721-125	156	185	209	213	216	216	216	216	216	212	209	185	155	139	129					
721-150	155	184	209	213	216	216	217	217	216	211	208	184	154	138	129					
721-175	155	184	209	213	216	216	217	217	216	211	208	184	154	138	129					
721-200	155	184	209	213	216	216	217	217	216	211	208	184	154	138	129					
721-250	154	184	208	213	216	216	217	217	216	211	208	184	153	140	130					
721-300	154	185	208	212	216	216	216	216	216	211	208	185	154	138	130					
721-350	155	184	209	213	216	216	216	216	215	211	209	184	154	140	129					
721-400	155	184	209	213	216	216	216	216	215	211	209	184	154	140	129					
721-675	174	196	208	215	215	215	216	216	216	215	213	191	162	150	146					
721-850	133	145	148	149	149	150	150	150	148	142	136	132	120	108	90					
925-1	124	129	132	134	135	135	134	131	130	115	89	63	48	39	29					
925-17	54	56	56	56	56	56	56	56	56	56	56	56	56	56	56					
982-15	63	70	72	73	72	71	67	66	63	52	47	43	38	31	28	22	13			
982-20	114	121	124	127	128	129	127	126	118	109	93	68	48	38	28	22	15			
982-25	119	130	133	134	135	135	134	129	125	118	97	72	52	41	31	25	19			
982-30	129	134	137	139	139	139	137	132	127	118	97	72	52	42	33	26	19			
982-35	130	137	141	143	143	141	140	137	130	121	96	72	53	44	36	29	21			
982-40	131	139	142	144	144	144	142	139	135	123	100	72	56	46	39	32	23			
982-50	134	141	144	146	146	145	145	142	136	124	101	75	58	47	39	32	24			
982-60	133	139	145	146	146	146	144	140	134	123	100	74	58	46	40	32	25			
982-70	135	140	147	147	147	147	144	141	135	123	100	75	59	46	40	32	25			
982-90	137	143	145	147	149	149	146	143	137	128	107	75	60	47	41	34	27			
982-100	137	143	145	148	149	149	147	143	138	128	110	77	65	49	41	34	29			
982-125	137	143	145	148	149	149	147	143	138	128	110	77	65	49	41	34	29			

PROPERTIES OF COMMON BASE METALS

METAL	NOMINAL COMPOSITION	DENSITY (lbs./in. ³)	ELECT. CONDUCT. (% IACS)	MELTING TEMP SOLIDUS (°F)	ANNEALING TEMP (°F)	TENSILE STRENGTH KSI ANNEALED HARD	% ELONGATION IN 2" ANNEALED HARD
Aluminum Alloy 1100	99.0 min Al	.098	57.0	1215	650-775	13 24	35 5
C10200 Copper	99.95 min Cu	.323	101.0	1981	700-1200	32 50	45 6
C19400	97.4Cu, 2.4Fe, 1.3Zn, 0.4P	.322	65.0	1980	700-1200	45 67	32 4
C21000 Gilding Metal	95Cu, 5Zn	.320	56.0	1920	800-1450	34 56	45 5
C22000 Commercial Bronze	90Cu, 10Zn	.318	44.0	1870	800-1450	37 61	45 5
C23000 Red Brass	85Cu, 15Zn	.316	37.0	1810	800-1350	39 70	48 5
C24000 Low Brass	80Cu, 20Zn	.313	32.0	1770	800-1300	42 74	52 7
C26000 Cartridge Brass	70Cu, 30Zn	.308	28.0	1680	800-1400	44 76	66 8
C51000 Phosphor Bronze A	94.8Cu, 5Sn, 2P	.320	15.0	1750	900-1250	47 81	64 10
C52100 Phosphor Bronze C	91.8Cu, 8Sn, 2P	.318	13.0	1620	900-1250	55 93	70 10
C68800	73.5Cu, 22.7Zn, 3.4Al, 4Co	.296	18.0	1740	750-1100	82 109	36 6
C71500 Cupro-Nickel	69.5Cu, 30Ni, 5Fe	.323	4.6	2140	1200-1500	55 78	45 5
C72500	88.2Cu, 9.5Ni, 2.3Sn	.321	11.0	1940	1200-1475	55 83	35 3
C75200 Nickel-Silver	65Cu, 18Ni, 17Zn	.318	6.0	1960	1100-1400	58 85	40 3
C7025 High Performance Alloy	Bal. Cu, 3.0Ni, 6.5Si, 1.5Mg	.318	40.0	1967	Proprietary	90 125	10 5
BERYLLIUM COPPER ALLOYS (T=Precipitation Heat Treated)							
C17000	98.3Cu, 1.7Be, Ni, Co, Fe	.304	22.0	1590	1425-1475	70 110	45 5
C17000 T						165 190	7 3
C17200	98.1Cu, 1.9Be, Ni, Co, Fe	.298	22.0	1590	1425-1475	70 110	45 5
C17200 T						175 200	6 2
C17500	96.9Cu, 2.55Co, 5.3Be	.311	45.0	1885	1675-1725	45 78	28 5
C17500 T						110 115	12 8
Nickel 201	99.5Ni, 20Mn, 1.5Fe, 0.1C	.321	22.5	2615	1300-1500	55 115	55 5
Nickel 270	99.97Ni	.321	23.5	2650	700-1200	50 90	50 5
Monel 400	Bal. Ni, 31.5Cu, 1.1Fe, 1Mn, 2.5Si, 2C	.319	3.3	2460	1400-1600	80 105	48 5
Alloy 42	58.5Fe, 41.5Ni	.293	2.5	2597	1400-1500	68 100	45 8

10.7.3 Diversified Silicone Products, Inc.
 13937 Rosecrans Ave.
 Santa Fe Springs, CA 90670
 USA

Diversified Silicone Products, Inc.

13937 Rosecrans Ave.
 Santa Fe Springs, CA 90670
 Tel: (562) 404-8942 Fax: (562) 404-1323

Other Data Sheets Are Available On Our Website
www.diversifiedsilicone.com



SILICONE SHEETING

“DSP5008”
 TRANSLUCENT GRADE
 50 Shore “A”

Diversified Silicone Products, Inc.

13937 Rosecrans Ave.
 Santa Fe Springs, CA 90670
 Tel: (562) 404-8942 Fax: (562) 404-1323

Other Data Sheets Are Available On Our Website
www.diversifiedsilicone.com



SILICONE SHEETING

“DSP5008”
 TRANSLUCENT GRADE
 50 Shore “A”

DESCRIPTION:

This translucent grade silicone sheeting is used in many different types of applications. This material is low volatile, peroxide free and does not discolor over time. The ingredients used to make this product are listed in CFR 177.2600. This FDA regulation deals with rubber articles intended for repeated use in contact with food. This material is ozone and UV resistant.

FEATURES:

- Excellent Gasketing Material
- Extreme High & Low Temperature Resistant
- UV / Ozone Resistant
- Non-Toxic, Peroxide Free,
- Non-Yellowing, Will not Discolor
- All FDA approved Ingredients
- Low Compression Set
- Fungus Resistant

PHYSICAL PROPERTIES

PROPERTIES	Test Method	Typical Properties
Specific Gravity, G/CC	ASTM D297	1.15
Durometer, Shore “A”	ASTM D2240	50 +/-5
Tensile Strength, ppi	ASTM D412	1000
Elongation, %	ASTM D412	500
Tear, ppi Die “B”	ASTM D624	150
Temperature Range	(F)	-80 to +450

The above values are typical properties and are provided for information only. They should not be used to set specification requirements. It is up to the end user to determine whether the material is suitable for the intended application.

DESCRIPTION:

This translucent grade silicone sheeting is used in many different types of applications. This material is low volatile, peroxide free and does not discolor over time. The ingredients used to make this product are listed in CFR 177.2600. This FDA regulation deals with rubber articles intended for repeated use in contact with food. This material is ozone and UV resistant.

FEATURES:

- Excellent Gasketing Material
- Extreme High & Low Temperature Resistant
- UV / Ozone Resistant
- Non-Toxic, Peroxide Free,
- Non-Yellowing, Will not Discolor
- All FDA approved Ingredients
- Low Compression Set
- Fungus Resistant

PHYSICAL PROPERTIES

PROPERTIES	Test Method	Typical Properties
Specific Gravity, G/CC	ASTM D297	1.15
Durometer, Shore “A”	ASTM D2240	50 +/-5
Tensile Strength, ppi	ASTM D412	1000
Elongation, %	ASTM D412	500
Tear, ppi Die “B”	ASTM D624	150
Temperature Range	(F)	-80 to +450

The above values are typical properties and are provided for information only. They should not be used to set specification requirements. It is up to the end user to determine whether the material is suitable for the intended application.

10.7.4 Green-Belting Industries
381 Ambassador Drive
Mississauga, ON L5T 2J3
Canada



Green Belting Industries FABRICS DATA SHEET

FLUOROFAB® FABRICS

Our Fluorofab® Fabrics are woven fiberglass cloth substrates coated with PTFE.

<p>FEATURES:</p> <ul style="list-style-type: none"> ■ Excellent release properties, low surface friction ■ High chemical and abrasion resistance ■ Dimensionally stable from -100°F to +550°F. ■ FDA compliant for food processing, packaging and handling 	<p>APPLICATIONS:</p> <ul style="list-style-type: none"> ■ Heat sealing plastic films ■ Reusable laminating press release sheets ■ Tray lining for non-stick baking and drying ■ Blister pack die covers ■ Covering the sealing surface on polyethylene bag-making equipment ■ Release liner in bonding processes ■ Chemically inert diaphragms/gaskets
---	--

SILICONE-GLASS FABRICS

Our Silicone-Glass fabrics are woven fiberglass cloth substrates coated on one or both sides with silicone rubber.

<p>FEATURES:</p> <ul style="list-style-type: none"> ■ Excellent release properties. ■ High strength and tear resistance ■ High dielectric strength ■ High resistance to wear and flexing ■ High chemical resistance, impervious to mild alkalies, non-oxidizing acids, most salts, mineral and lubricating oils, air, moisture and sunlight ■ Operating temperature range from -100°F to +500°F. ■ Non-toxic, odorless and tasteless 	<p>APPLICATIONS:</p> <ul style="list-style-type: none"> ■ Many food handling operations ■ Shrink tunnel curtains ■ Gasketing ■ Release sheet/separator material
--	--

SPECIALTY FABRICS

Green Belting Industries will cost-effectively custom coat Kevlar®, Nomex® and laminate substrates with PTFE or silicone to your exact specifications.

Kevlar® and Nomex® are registered trademarks of DuPont Company.
Fluorofab® is a registered trademark of Green Belting Industries Ltd.
PTFE is a generic name for the resin polytetrafluoroethylene.
Fluorofab DXL™ is a trademark of Green Belting Industries.

FLUOROFAB® FABRICS					
Code#	Maximum Width	Nominal Mil Thickness	Nominal Weight oz./sq. yd.	Breaking Strength lbs./in. of width Warp Direction	Breaking Strength lbs./in. of width Fill Direction
Premium Grade					
100-3 PR	50"	3	4.3	70	50
100-6 PR	60"	6	9.1	120	120
100-10 PR	60"	10	15.2	240	190
100-10 PR 28	60"	10	15.2	240	190
100-14 PR	89"	14	21.6	425	270
100-27 SP50 PR	89"	27	37.5	450	390
Standard Grade					
100-3	50"	3	4.0	70	50
100-5	60"	5	7.6	120	120
100-6	60"	6	8.8	120	120
100-8	60"	8	12.3	240	190
100-8 SW	41"	8	9.8	240	190
100-10	89"	10	14.4	240	190
100-10 SW	40"	9	9.8	240	190
100-14	89"	14	17.0	425	270
100-20	36"	20	28.6	475	400
100-22	60"	22	20.8	400	400
100-27	89"	27	31.2	450	390
100-27 SP50	89"	27	31.4	450	390
Fluorofab DXL™					
DXL 4	36"	4	5.6	70	50
DXL 5	60"	5	7.6	120	120
DXL 5 TR	60"	5	7.6	120	120
DXL 6	60"	6	8.8	120	120
DXL 10	50"	10	15.4	240	190
DXL 12	50"	12	18.0	240	190
SP 85-5	36"	5	7.6	120	120
SP 86-4	36"	5	7.6	120	120
Mechanical Grade					
100-3	50"	3	3.2	70	50
100-5	60"	5	6.0	120	120
Porous Grade					
100-3	50"	3	1.8	70	50
100-5	60"	5	3.2	120	120
100-10	60"	8	7.0	240	190
100-14	89"	12	10.2	425	270
100-32	60"	32	30.5	800	740
Tear Resistant					
100-3 TR	36"	3	4.1	70	50
100-4 TR	36"	4	5.8	155	75
100-5 TR	60"	5	7.5	120	120
100-6 TR	60"	6	8.8	120	120
100-10 TR	40"	10	14.4	240	190
Enhanced Grade					
100-3 SP 40	36"	4	5.0	70	50
100-5 SP 05	36"	5	4.5	120	120
100-10 SP 10	50"	10	14.4	240	190
Black					
100-3	50"	3	4.0	70	50
100-5	60"	5	7.6	120	120
100-6	60"	6	8.8	120	120
100-10	60"	10	14.4	240	190
100-14	44"	14	18.0	425	270
Anti-Static Black					
100-3 SP 30	36"	3	4.0	70	50
100-5 SP 30	36"	5	7.6	120	120
100-10 SP 30	89"	10	14.4	240	190
100-14 SP 30	89"	14	20.8	425	270
All Premium and Standard fabrics are available etched one or both sides.					
Open Mesh					
30-89 Brown	130"	35	13.3	235	290
30-89 Brown	84"	35	13.3	235	290
30-90 Brown	80"	25	15.5	280	250
SILICONE-GLASS FABRICS					
Code#	Maximum Width	Color	Mil Thickness	Weight oz./sq. yd.	Breaking Strength lbs./in. of width
S/W-7	38"	white	6	5.9	125
S/W-10	38"	white	10	10.08	150
S/W-23 CO50*	38"	white	23	19.9	500
S/R-23 CO50*	38"	red	23	19.9	500
S/W-25	38"	white	25	28.8	500
S/R-25	38"	red	25	26.8	500
S/W-32	38"	white	32	30.4	800
S/W-35	38"	white	35	33.8	800

*COATED ONE SIDE ONLY



Green Belting Industries Limited
381 Ambassador Drive, Mississauga, Ontario L5T 2J3
TEL 905-564-6712 • FAX 905-564-6709

Greenbelt Industries Inc.
45 Comet Street, Buffalo, New York 14216
TEL 800-668-1114 • FAX 905-564-6709

www.greenbelting.com



DIA48.2 101503
DZA42.3 101503

10.7.5 All-Vac Industries
 7350 N. Central Park Ave.
 Skokie, IL 60076
 USA



- Home
- Vacuum Suction Cups
- Vacu-Lifters
- Raised Flooring Tools
- Suction Cup Lifters
- Safety Hand Tools
- Suction Cups
- Custom Molding
- Safety Guidelines
- About All-Vac
- Contact Us

Suction Cups

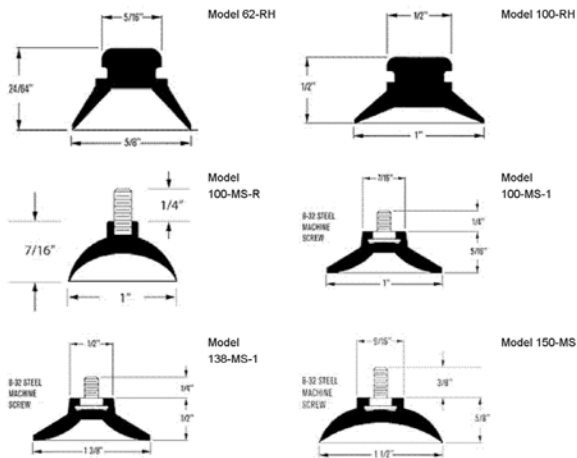
What can we tell you about suction cups? When they stick, they're good. All-Vac's superior line of industrial suction cups stick and hold, and they also release when you need them to. The most typical application of suction cups is for footings. But, our customers have used suction cups in varied applications, making them one of the most popular types of suction products we carry.



Most of our suction cups are molded in a general all purpose rubber. A few of our suction cups are molded in EPDM rubber, which is specifically formulated for outdoor use and is rated well to resistant weather aging. Some of our suction cups molded in EPDM are used as footings for commercial poultry cutters because they rate well for use when subjected to animal oils and fats.

If you don't see the style of suction cup that you are looking for, please call us at 847-675-2290 and ask for customer service. We may have other suction cups available not currently on our website. Also, for larger quantities, All-Vac can easily make a custom suction cup to meet your specific needs.

Below are mechanical drawings with specifications of the suction cups we stock.



10.7.4 McMaster-Carr
 9630 Norwalk Blvd.
 Santa Fe Springs, CA 90670
 USA

McMASTER-CARR
 OVER 480,000 PRODUCTS

Need help finding a product?
 E-mail or call (562) 463-4277.

[CONTACT US](#)

[BOOKMARKS](#)

[ORDER HISTORY](#)

06/14/09 - 0 lines

[CURRENT ORDER](#)

[FIND PRODUCTS](#) [BUILD ORDER](#)

PRINT HOW CAN WE IMPROVE?

9075K19

Blue-Finished and
 Polished 1095 Spring Steel
 .007" Thick, 1/4" Width, 25'
 Coil

In stock at \$25.96 Each

Each

[Bookmark this Product](#)

[Catalog Page](#)

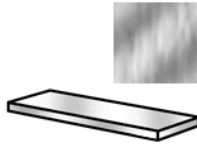
[Product Specifications](#)

[More About Steel Alloys](#)

[Current Order - 0 lines](#)

Steel

This product matches all of your selections.



Part Number: [9075K19](#)

\$25.96 Each

Alloy	1095
Material	Tough Wear-Resistant 1095 Spring Steel
Finish/Coating	Polished (Blue Finish)
Shape	Sheets, Bars, and Strips
Sheets, Bars, and Strips Type	Plain
Thickness	.007"
Thickness Tolerance	±.00075"
Length	25'
Length Tolerance	+12", -1"
Width	1/4"
Width Tolerance	±.005"
Flatness Tolerance	Not Rated
Tolerance	Standard
Temper/Condition	Spring Tempered (Hardened)
Hardness	Rockwell C53-C59
Yield Strength	Not Rated
Specifications Met	Not Rated
WARNING	Hardness is not guaranteed and is intended only as a basis for comparison.

Thank You

University of Arizona

Álvaro Malo, Architecture

3 years of continual guidance and support

Dr. William Bickel, Physics

For keeping me grounded

Larry Medlin, Architecture

Always willing to talk

Jason Vollen, Architecture

Early development and focus

Dale Clifford, Architecture

Continual aid and support

Christopher Domin, Architecture

Solar decathlon integration

Mike Nofziger, Optical Science

Light, shade and shadow assistance

Paulus Musters, Architecture Material Laboratory Manager

Shop help and instruction

Individuals

My Family: Mom, Dad, Brian and Drew

Thank you for your continual support and unconditional love. I would not be the person or student that I am today without you all.

Ben Hall

Thank you for your inspiration and your occasional lies throughout our short time living together. I wholeheartedly look forward to a long-lasting friendship for years to come.

Ryan White

I know I told you I only needed a place to stay for six months...which later was drawn out to over a year, but I truly thank you for your enduring friendship and splendid accommodations.

Kevin, Eric and Gabe

UofA was never the same without you, but your interest and support of my educational endeavors throughout the years kept me focused and driven to finish. Thank you!

Paulina Carvallo

Thank you for keeping me focused, and distracted until the end. Our talks, discussions and metalogues about the theory of the universe to nanotechnology to the color of time was inspiring and refreshing beyond words. Your love and friendship during these times will never be forgotten.

Businesses

Alex Miramontez, Glaz-Tech Industries

Carl Pallister, Polymetallurgical Corporation

Joel Allegrezza, Engineered Material Solutions

All-Vac Industries

Diversified Silicone Products, Inc.

Green-Belting Industries